STRUCTURAL ANALYSIS OF POLY ETHYLENE TEREPHTHALATE BOTTLES USING THE FINITE ELEMENT METHOD

By

ROHIT VAIDYA

Bachelor of Technology in Aeronautical Engineering

Jawahar lal Nehru Technological University

Hyderabad, Andhra Pradesh

2009

Submitted to the Faculty of the
Graduate College of the
Oklahoma State University
in partial fulfillment of
the requirements for
the Degree of
MASTER OF SCIENCE
May, 2012

STRUCTURAL ANALYSIS OF POLY ETHYLENE TEREPHTHALATE BOTTLES USING FINITE ELEMENT METHOD

Thesis Approved:

Dr. Jay C. Hanan

Thesis Adviser

Dr. Ranji Vaidyanathan

Dr. Raman P. Singh

Dr. Sheryl A. Tucker

Dean of the Graduate College

.

TABLE OF CONTENTS

LIST OF TABLES

LIST OF FIGURES

SUMMARY

Packaging is an important step of the production process that involves delivery of the final product to end users. In particular, materials used in beverage packaging that deals with carbonated and non-carbonated drinks has shifted from glass and Aluminum to high performance polymers such as poly-ethylene Teraphthalate (PET) owing to their superior mechanical properties, ease of manufacturing and low cost. For example, one can readily see the melt temperature is suggestive of the lower cost in manufacturing since glass has the highest of the three and polymers the lowest. Even with the lower cost to process PET, the industry has evolved to further expand the gap. One of the greatest pushes in this area is called "light weighting," where unnecessary material is designed out of the package, saving weight. Light weighting not only reduces the material usage but also minimizes impact on the environment; this has been a driving force behind substantial research in this area. For design optimization, it is critical to evaluate the structural performance of bottles under different loading conditions.

Injection stretch blow molding is a manufacturing process of PET that yields non-uniform thickness and material properties along the length of the bottle. Understanding the behavior of PET, observing the changes in non-uniform thickness and material distribution are also key factors in assessing the design and structural performance.

FEM was implemented to study the structural performance of PET bottle designs manufactured using ISBM under the conditions of bending and hoop stiffness (impacting hoop strength). The behavior of a PET bottle under a top loading condition was analyzed using a FE model and validated experimentally. The validated FE model was considered for bending tests and the effect of change in wall thickness on bending is reported. To further study the bending of PET

bottle designs and see the effect of designs on bending, CAD models of four different finished parts were built using a novel 3D scanning technology and were imported for FE analysis. The hoop strength tests were also performed on eight different designs with different processing histories using a specialized fixture. A correlation between the stretch ratio and the wall thickness were also established which lead to further understanding of the structural performance of light weight bottles.

The outcome of this work provides a procedure to study the mechanical behavior of PET bottles under conditions of bending and hoop deformation. The effect of wall thickness and design on the bottle behavior under bending was also analyzed. The 3D scanning technology that leads to a new way of CAD modeling is introduced and the imported designs were subjected to FE analysis.

CHAPTER I

1. INTRODUCTION

Packaging is an important part of production in delivering products to consumers [1]. Beverage packaging deals with packaging of liquid beverages such as water and flavored varieties, carbonated soft drinks, (CSD), juices, and milk. Aluminum, glass, and paperboard were common materials which were used in this industry and recently many products have moved to polymers. Now polymers are dominate packaging materials with PET leading that group. Light weight, tough, and ease of manufacturing are a few criteria for choosing polymers in the packaging industry [2]. Polymers have complex mechanical behavior and their properties are process dependent [3]. The strengthening of polymers with second phases is done to improve the structural performance of the final product. The properties of the polymers are being improved by reinforcing nano particles and other additives [4-6], optimizing the process parameters is also done to improve the performance [7]. To improve the structural performance, efficient design also plays a key role [1, 2]. Improving the structural performance by assessing the design, understanding the mechanical behavior and process parameters is ongoing research in packaging industry.

1.1 Polymers in Manufacturing and Packaging Industry

Polymers are considered as wonder materials in industry. Thousands of polymers have been made since the 18^{th} century. Polymers vary in strength, glass transition temperature and its repeating unit in its molecular chains. Today polymers have made an impact in all industries. In the packaging industry, polymers take up to 70 % volume of products [8]. Polymers have applications ranging from light weight structures, textile industry, and extend to heavy duty applications.

1.2 Mechanical Behavior of Polymers

Polymers are natural or organic materials consisting of large molecules in chains and the mechanical properties of polymers are determined by strength of the chains that is on the intermolecular bonds. These bonds depend on factors including chemical composition, Van der Waals force and hydrogen bonds. Different mechanical properties are a result of different strength of these intermolecular bonds. The properties of the polymer depend on type of polymer (structure related) which includes amorphous, semi crystalline, elastomers and duromers. Polymers exhibit elastic, plastic and viscous properties. Figure 1 shows the generalized stress strain curve of a typical polymer.

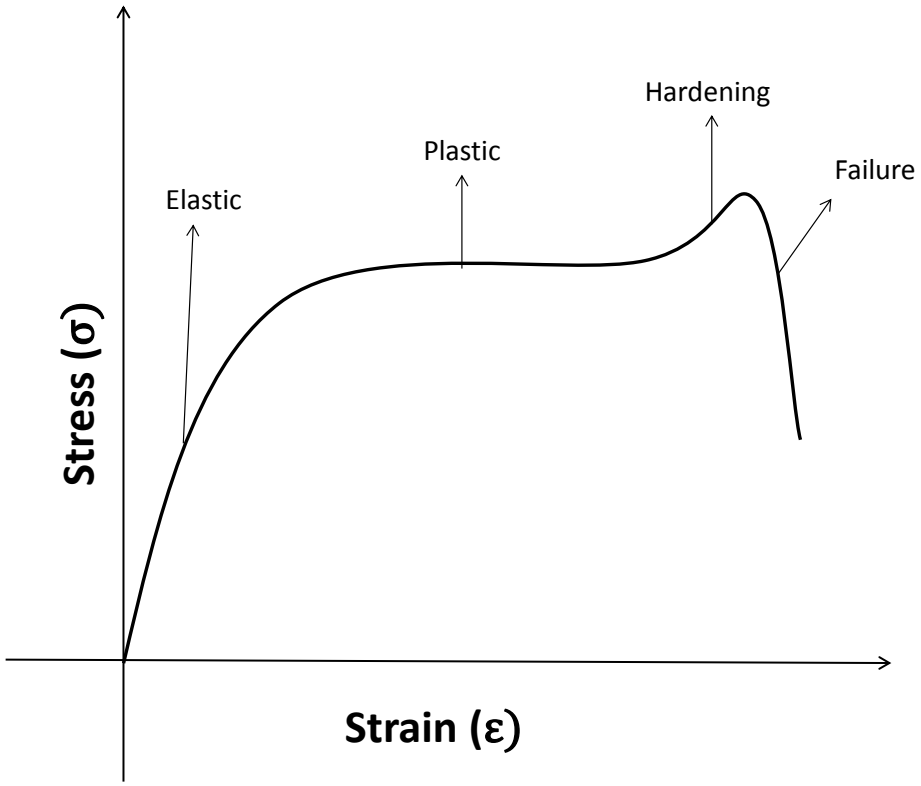

Figure 1: Generalized stress strain curve of a typical polymer.

Elastic behavior for amorphous thermoplastics is explained by the displacement of atoms from its equilibrium position, during loading and relaxation of atoms, during unloading. Young's modulus (E) depends on the glass transition temperature (T_g); a low T_g value explains the low Young's modulus of polymers when compared to other materials. Above the glass transition temperature, the Young's modulus decrease rapidly because sliding of the chains becomes easy. In semi-crystalline thermoplastics, the E values are slightly higher because of strong intermolecular bonding in the crystalline region. The decrease in E near the T_g is less as sliding of molecules is initially restricted to amorphous regions, crystalline regions remain elastic longer. In contrast to the above, the elastic properties of elastomers and duromers depend on the additional covalent cross links; these crosslinks play a major role beyond T_g, elastomers exhibit hyper elastic properties at higher temperatures. Duromers have high density cross linking; hence

they have high elastic properties compared to other polymers. Figure 2 shows the temperature dependence of Young's modulus for different polymers.

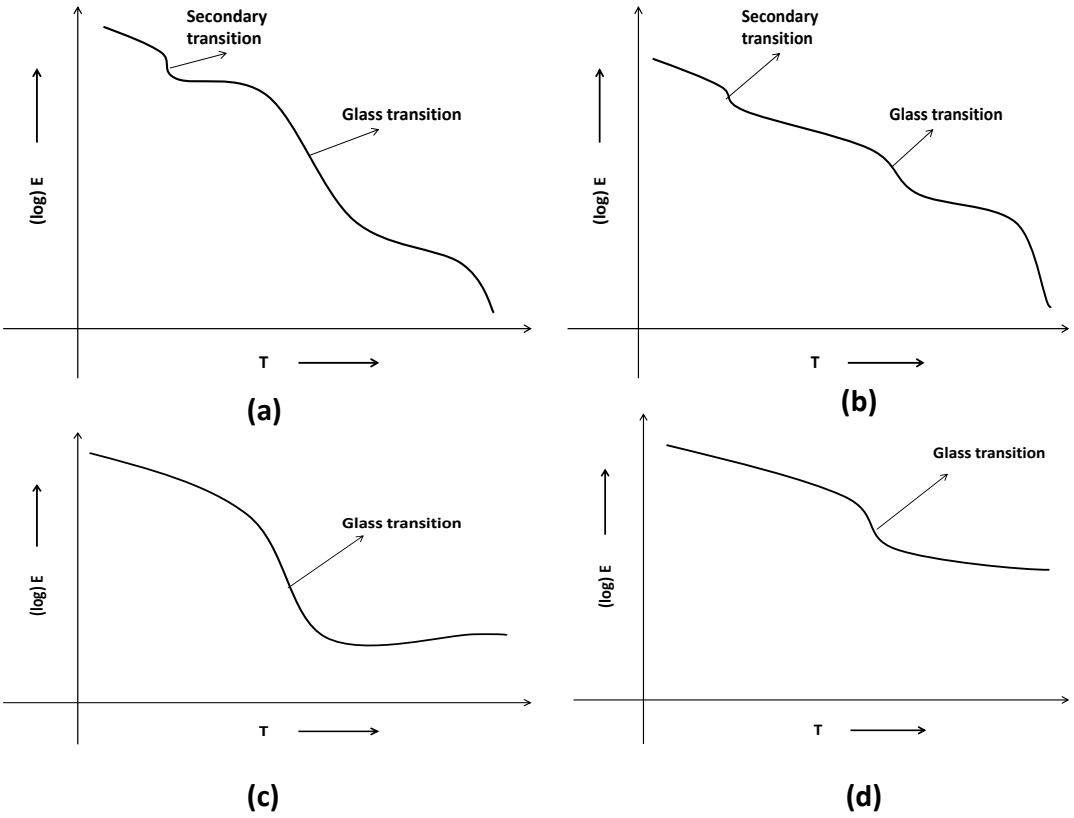

Figure 2: Temperature dependence of Young's modulus (a) Amorphous thermo plastic (b) Semi crystalline thermo plastic (c) Elastomers (d) Duromers [9].

Plastic deformations of polymers are explained by sliding of the chains along each other for long distances, in this process the molecules have to overcome thermal activation energy, hence temperature plays a key role. Polymers can deform by crazing and formation of shear bands created at an angle between 45^{o} and 60^{o} to the loading direction [10-13]. Crazes are generally initiated at surface defects like impurities and scratches. Stress concentration is slightly more in these regions upon loading; hence the plastic deformation starts in these regions and causes local

necking and formation of cavities. The material between these cavities is heavily loaded and undergoes plastic deformation and the fibrils between the cavities form crazes, the crazing by cavitation is mostly formed under hydrostatic tensile loading. Shear bands are formed under compressive load, within these bands are large plastic deformations. In semi-crystalline thermoplastics, the plastic deformation starts in the amorphous regions by lengthening. Later the crystalline regions rotate and molecules orient in the loading directions. Upon loading further, crystalline regions break into blocks and deform. Figure 3 shows the plastic behavior of semi-crystalline polymers. Elastomers and duromers undergo very small plastic deformations because the cross links on the chains prevent sliding motion.

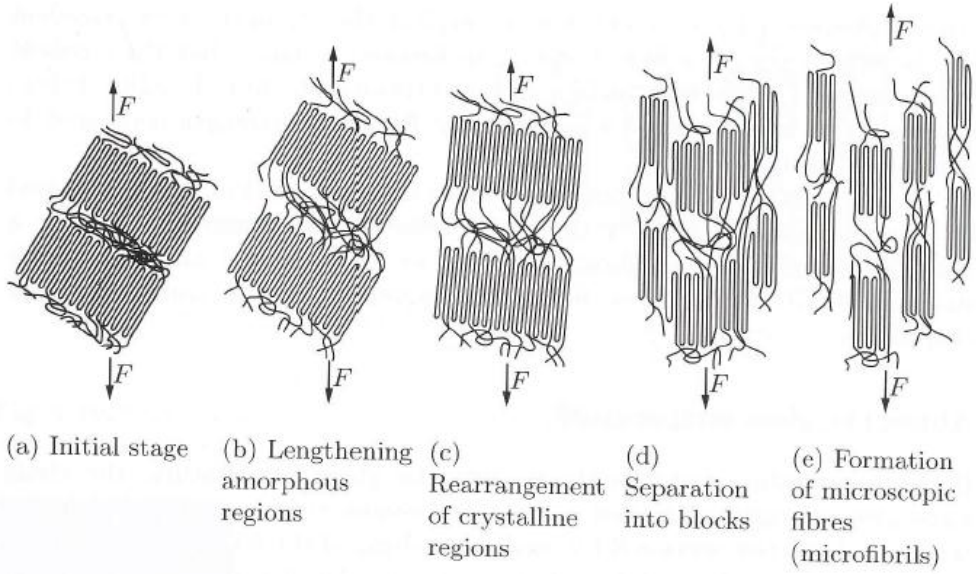

Figure 3: Plastic deformation of semi crystalline polymers [10].

The elastic and plastic behavior of polymers depend on time, their behavior is neither completely solid nor completely liquid. It is in the intermediate region. Hence, they are termed as viscoelastic and viscoplastic. Polymers when stressed below the yield strength, σ, strain

increasingly until a value ε_o, showing elastic material properties. As time increases, the polymer shows time dependent properties. Bond stretching is the cause of the elastic response. Uncoiling of the chains and slipping of the chains explains the time dependent response and viscous response. Polymers show the same behavior during unloading. Recovery is instantaneous initially and slow after prolonged time. At small strains (up to 0.3% strains and 100 seconds) polymers are generally linearly viscoelastic, and at high strains they behave as a nonlinear viscoelastic material [14]. Creep is the tendency of a material to deform slowly on the application of constant load over time and relaxation is opposite of creep behavior, it describes how the polymer relives stresses under constant strain [15]. Creep properties depend on microstructure [14, 16]. Crystalline polymers exhibit lower creep properties, and duromers and elastomers (because of large chain molecules) show higher creep properties.

1.3 Constitutive Models for Creep and Relaxation

To explain the physical behavior of any material in a mathematical way, constitutive models were developed. General mechanical models of elasticity cannot be used to describe the creep and relaxation behavior in a polymer; more complex models are emerging to explain this behavior. Maxwell, Kelvin Voigt, four parameter models and an empirical power law model are the renowned mechanical models to explain creep and relaxation behavior.

The Maxwel model has a Hookean spring and a Newtonian dashpot in series as shown in Figure 4. The Hookean spring explains the elastic behavior and the dashpot provides viscous behavior. In stress relaxation experiments, the system is subjected to axial loading during which the spring undergoes the initial deformation and the dashpot relaxes after a certain time, allowing spring to

contract. If E is the modules of spring, η is the viscosity of the dashpot, the equation of system is governed by

$$\frac{d\varepsilon}{dt} = \frac{1}{E}\frac{d\sigma}{dt} + \frac{\sigma}{\eta} = 0 \qquad 1.\ 1$$

$\varepsilon = \frac{\sigma}{E}$ for Spring and $\frac{d\varepsilon}{dt} = \frac{\sigma}{\eta}$ for dashpot. The solution for the above equation is

$$\frac{\sigma}{\sigma} = e^{\frac{-Et}{\eta}} \qquad 1.\ 2$$

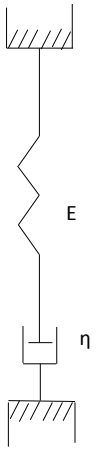

Figure 4: Maxwell model [17].

The Kelvin Voigt model also has a Hookean spring and a Newtonian dashpot, but configured in parallel as shown in Figure 5. Under constant load, the spring strains initially but the friction in the dashpot provides resistance to the strain and causes it to increase with time. The strains in two elements are equal and stress is the sum of the stresses in two elements.

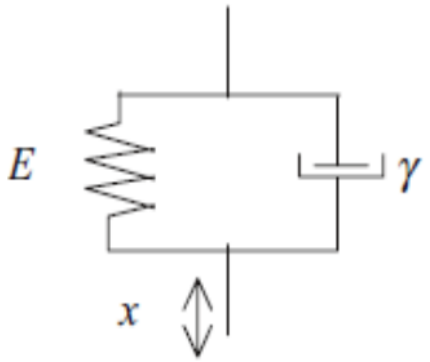

Figure 5: Kelvin Voigt model [13, 17, 18].

$$\frac{d\varepsilon}{dt} = E\varepsilon(t) + \gamma\frac{d\varepsilon(t)}{dt} \qquad 1.3$$

In the two models abovementioned, the viscoelastic behavior of the polymer can be explained but, polymers also exhibit viscoplasticity which cannot be explained by the Maxwell or Kelvin Voigt models. A four parameter model explains the behavior of time dependence of plasticity. Figure 6 explains the setup of a four parameter model. On loading, the spring of stiffness E_1 elongates, followed by spring with stiffness E_2, followed by dashpot with viscosity η_2 and then a dashpot with viscosity η_3 elongates. The total elongation is the summation of the elongation of three parts

$$\varepsilon = \frac{\sigma_0}{E_1} + \frac{\sigma_0}{E_2}\left(1 - e^{-\frac{t}{\tau}}\right) + \frac{\sigma_0}{\eta 3}t \qquad 1.4$$

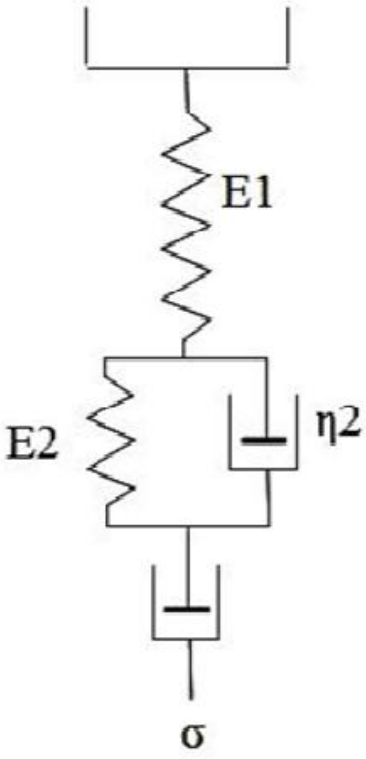

Figure 6: Four parameter model [19].

During recovery, the creep is recoverable, except for the dashpot η_3. The reduction on elongation is $(\frac{\sigma 0}{E1})$. The creep recovery equation is

$$\varepsilon = \varepsilon_2 e^{-(t-t_1)/\tau} + \frac{\sigma_0 t_1}{\eta 3} \qquad 1.5$$

The Power law Model, is an empirical model to model creep, the creep strain rate ε^{cr} depends on the uniaxial equivalent stress q and time t

$$\varepsilon^{cr} = A q^n t^m \qquad 1.6$$

Where A, n, m are dependent on temperature and need to be determined, limitations for these values are in table (1). If the material is isotropic or orthotropic, q corresponds to a misses equivalent stress and the Hills orthotropic deviatoric stress [20].

A	$>10^{-27}$
n	>0
m	-1 < m <0

Table 1: Limitations of power law parameters [21].

The Hills deviatoric stress function is

$$q(\sigma) = \sqrt{F(\sigma_{22}-\sigma_{33})^2 + G(\sigma_{33}-\sigma_{11})^2 + H(\sigma_{11}-\sigma_{22})^2 + 2L{\sigma_{23}}^2 + 2M{\sigma_{31}}^2 + 2N{\sigma_{12}}^2} \quad 1.7$$

where $q(\sigma)$ is the equivalent stress and F, G, H, L, M and N are constants extracted from experiments. For Equation 1.8

$$F = \frac{1}{2}\left(\frac{1}{{R_{22}}^2} + \frac{1}{{R_{33}}^2} - \frac{1}{{R_{11}}^2}\right)$$

$$G = \frac{1}{2}\left(\frac{1}{{R_{33}}^2} + \frac{1}{{R_{11}}^2} - \frac{1}{{R_{22}}^2}\right)$$

$$H = \frac{1}{2}\left(\frac{1}{{R_{33}}^2} + \frac{1}{{R_{11}}^2} - \frac{1}{{R_{22}}^2}\right)$$

$$L = \frac{3}{2{R_{23}}^2}$$

$$M = \frac{3}{2{R_{13}}^2}$$

$$N = \frac{3}{2{R_{12}}^2}$$

the variables R_{ij} are orthotropic stress ratios. These ratios must be defined in each direction [21]. However, the ratios have limitations, in a deviatoric stress plane the yield surface must be a closed surface which yields to a constraint

$$\frac{4}{{R_{11}}^2{R_{22}}^2} > \left(\frac{1}{{R_{33}}^2} - \left(\frac{1}{{R_{11}}^2} + \frac{1}{{R_{22}}^2}\right)\right)^2 \qquad 1.9$$

When creep strain rates are constant in all directions, R_{ij} describes the ratio of current stress and equivalent stress as in equation 1.10:

$$R_{13} = \frac{\sigma_{33}}{q}; \qquad R_{22} = \frac{\sigma_{22}}{q}; \qquad R_{33} = \frac{\sigma_{33}}{q}$$

$$R_{12} = \frac{\sigma_{312}}{q/\sqrt{3}}; \qquad R_{13} = \frac{\sigma_{13}}{q/\sqrt{3}}; \qquad R_{23} = \frac{\sigma_{23}}{q/\sqrt{3}}$$

1.4 Polyethylene Terephthalate [PET]

Polyethylene Terephthalate, a semi crystalline thermoplastic is made by a condensation reaction of ethylene glycol with terephthalic acid or dimethyl terephthalate [22]. The main criteria in determining the properties of PET are the molecular weight and crystalinity. PET can undergo strain induced crystallization and biaxial orientation on stretching which effects the properties.

A great deal of research has been carried out to study these affects using techniques ranging from tensile testing to X ray scattering [23-32]. General properties of semi-crystalline PET includes high stiffness, Young's modulus; good electrical properties, chemical resistance and transparency.

PET, because of its physical properties and chemical inertness is used for wide range of applications. Its applications are being increased over the last decade and expected to increase further. Figure 7 shows the consumption of PET over the decade. Of all the applications, PET has considerable significance in the water bottling industry, 92% of the water bottles are made of PET [33]

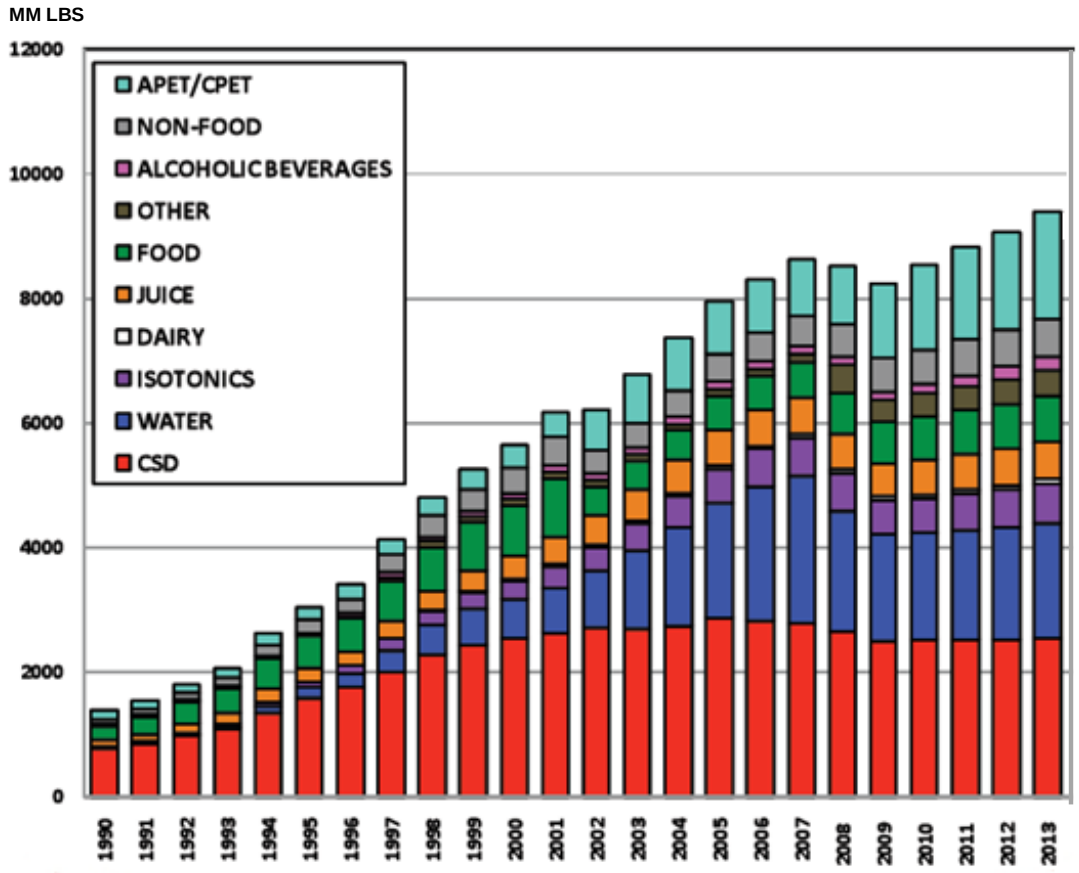

Figure 7: Consumption of PET from 1990 to 2013 [33].

1.5 Injection Stretch Blow Molding (ISBM)

Injection stretch blow molding is a manufacturing process which is used to produce hollow objects with bi axial molecular orientation like plastic bottles. PET resin pellets are dried at 165^{o}C to reduce the moisture content which reduces the molecular weight. The dried PET pellets are compressed and melted at about 290^{o}C in a rotating screw of an injection molding machine. The molten PET is injected by means of a hot runner into the mold, by using high cooling rates to get an amorphous preform. In one stage ISBM, the injection and blowing processes are performed on the same machine, the preform temperature is adjusted for an optimum blowing level which is about 95-120^{0}C at the condition station. At a blowing station, the hot preform is placed in the mold, a stretch rod is inserted through the neck of the preform, stretches the preform and simultaneously high pressure inflates the preform causing biaxial orientation. Finally the rigid bottle with an injection molded neck finish is obtained. In a two stage ISBM, injection and blowing processes are performed in two different machines; the preforms produced are cooled and stabilized before the blow molding stage. The preform is later heated above the recrystallization temperature and divided into different zones using lamps fixed in the blowing machine. Different zones are heated to different temperatures and the lamps control the temperature, the temperature control at different zones is an effective factor in determining the distribution of material during blowing. The heated preform undergoes stretching and blowing simultaneously to take the final shape of the mold. Figure 8 shows the ISBM process.

The performance of the final part depends on the intermediate processes which govern the molecular arrangements and microstructure, they change in each stage. During injection molding, the molecules are somewhat aligned in the direction of injection, the orientation

changes along the thickness of the preform. The molecular orientation and crystallization mainly depends on cooling time and mold temperature. During the stretch blow molding process the preform molecules undergo strain during stretching. During blowing, the molecules undergo biaxial strain. In making PET bottles, under biaxial strain, PET molecules change from amorphous to partially crystalline. This phenomenon is knows as strain induced crystallization. The orientation and crystallinity of the molecules changes along the length of the bottle. Figure 9 shows the orientation map along the length of the bottle.

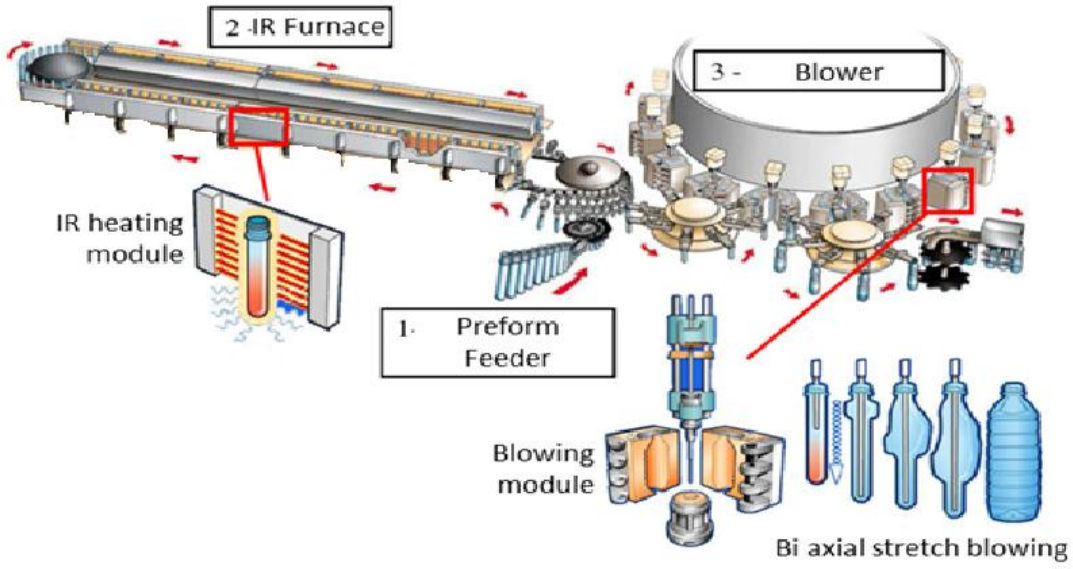

Figure 8: Stretch blow molding process [84].

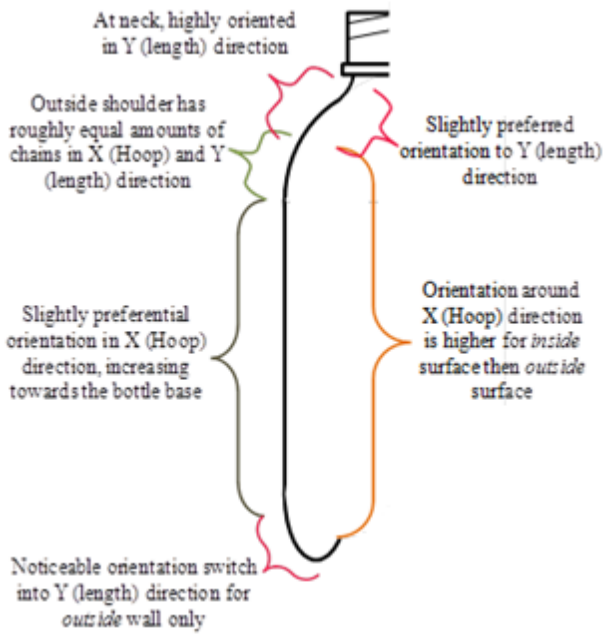

Figure 9: Orientation map along the length of bottle [34].

CHAPTER II

2. PROBLEM DEFINITION

2.1 Motivation

Plastics have a major role in the beverage packaging industry, of which PET takes the lead, mainly in liquid beverage packaging [3, 8] due to its chemical inertness and physical properties. It has major share in plastic bottles and is also used in other nonfood packaging [35].

Injection stretch blow molding is a commonly used manufacturing process for making plastic bottles, in which it yields non uniform thickness and material properties along the length of the bottle. In this process, typically 70-75% of total production costs of bottle are material costs [36-38]. Due to its dominant share, the packaging industry is focusing to reduce the material usage. Over the past decade, the bottling industry has moved from a 21 gram to 9.2 gram package which is about a 60% reduction in the amount of polymer [39], light weighting not only drives reduction in material usage but also reduces its impact on the environment. After production, bottles are stacked in layers (filled or empty), stored in ware houses and transported to different locations. During this process the bottle undergoes different loading conditions. Figure 10 shows how bottles are stored and subjected to bending, efficient design is required to overcome different loading conditions. The deformation behavior of plastic bottles in its useful life is a function of the shape, material characteristics, process parameters, geometry and loading conditions [40]. Hence we need to study the performance of the bottle design considering all the

above parameters. Apart from the structural performance, the hoop strength is one of the criteria. Considering the complications and requirements, a proper approach was needed to understand the various aspects of design. The finite element method was validated to solve complex engineering problems like crash simulations and many other complex problems like bio simulations [44-48]. It is applied even in beverage packaging industry

Figure 10: Bottles stored in warehouses.

2.2 Finite Element Method

The complex engineering problems are represented in a mathematical way, in the form of partial differential equations and integral equations. The finite element method is a numerical method of finding solutions to partial differential equations and integral equations. The primary idea of FEM is to break up the continuum problem to discrete problems. The primary criterion is to form the equations from the original problems reducing the numerical complexity and error. Creating the stiffness matrix, the application of loads considering the boundary condition from the equations developed is the next challenge. It is followed by solving the equations and getting the solutions. Several numerical models [41-43] have been developed to define the equations,

high technology in computer hard ware and commercial codes from software packages solve the complex equations with ease. Care must always be used in interpretation of solutions.

2.3Literature Review

Over a few decades, finite element analysis was used to solve problems in the beverage packaging industry. A review of FEM works in the bottling industry is presented in this study, focusing mainly on structural performance of bottles. After a thorough study, the FEM works in bottling industry are classified into four classes.

1. Modeling polymer behavior
2. Preform optimization
3. Stretch Molding simulation
4. Structural performance

2.3.1 Modeling polymer behavior and their mechanical properties

Polymers when subjected to loading undergo molecular orientation, which constitutes to complex mechanical behavior. This mechanical behavior which leads to material properties are the primary input to any complex finite element problem. Modeling this material behavior is a key factor. Over the past few decades, the behavior of polymers has been studied by several researchers.

Amoeedo and Lee, 1992 [49] assumed that the stress is dependent on strain rate, temperature and a set of internal variables and developed a constitutive model to study yielding, strain softening, hardening on amorphous polymers, and study the intial visco plastic and nonlinear hardening of semi crystalline polymers. Aruda and Boyce in 1993 [50] conducted tests on PC, PMMA and

developed a 3 D constitutive model to predict a flow strength and deformation behavior of anisotropic material. Vigney *et al.*, 1999 studied the visco plastic behavior of amorphous PET during the stretching process and developed a constitutive model to predict the stretching behavior of PET. Dommelan, *et al.*, 2003 [51] considered different models for different phases of semi crystalline polymers and developed a macro mechanical based constitutive model to model the elasto viscoplastic deformation, and texture evolution of semi-crystalline polymers. Colak and Dusunceli, 2006 [16] utilized visco plasticity theory based on over stress and developed a model to study visco elastic and visco plastic behavior of HDPE under uniaxial monotonic and cyclic loading. Hasanpour and Rad, 2008 [52] developed a model to predict time dependent material properties of polymers, the same model was implemented to study the friction in polymers during compression testing. Modeling the complex behaviors including rheological, residual stresses, microstructure, and viscous nature of polymer composites are also studied [53-59].

2.3.2 Preform optimization

The "preform" is an intermediate part in the bottle making process, the performance of bottle depends first on the quality of its preform. Optimization of preforms is also important in bottle making. Studies were performed by researchers to optimize preform shapes.

Lee and Soh, 1996, [60] developed a finite element optimization method to determine the optimal preform thickness to obtain a required blown part of particular thickness. The finite element was based on a thin membrane approximation. The results were validated with published experimental results and computer simulations. Thibaulte *et al.*, 2007 [61] , developed a new design approach to predict optimal preform geometry for the given processing parameters

and optimal processing parameters for a particular preform geometry. The gradient based optimization algorithm which iterates over predictive FE software automatically was used. Wei *et al.*, 2010 [3], performed a simulation study on reduction of preform weights using blow view software in terms of process ability and product quality. The weight of the preform was reduced by reducing the thickness. By reducing the preform weight, reduction in the end cap (end cap-injection gates in the preform) was observed and the end cap center was off centered. The effect on product quality was not justified.

2.3.3 Blow Molding

PET is process dependent; several attempts were made to study the process dependent parameters of PET. Thorough understanding of material behavior during blow molding is required for optimizing the bottle dimensions and material distribution. Hence equivalent finite element models for blow molding processes have been developed by researchers over the past two decades. The thorough understanding of material behavior of polymers is required while building the models for blow molding.

Mc.Evoy *et al.*, 1998 [62], used Germain material model (Germain, *et al.*, 1989) [63] simulated bottle molding process in ABAQUS. Wall thickness measurements were in correlation with experimental results, but the blowing rates considered and stretch rod displacements were lower when compared to experimental results. Venkateshwaran *et al.*, 1998 [64], worked on stretching experiments of PET films and could predict the mechanical behavior during the stretching process. The film data was extrapolated on actual blow molding process. Wang and Mackinouchi, 2000 [65], reduced computational time for blow molding simulation by developing a set of contact search algorithms; these are implemented in finite element codes used

to simulate the blow molding process. Marckmann *et al.*, 2001 [66], developed a dynamic finite element procedure to simulate blow molded and thermoforming of thermoplastic parts. Yang *et al.*, 2004 [7], performed a coupled temperature displacement finite element analysis using a Buckley glass rubber model [67] in ABAQUS to predict the thickness distribution and strain along the length of the bottle. The heat transfer between stretch rod, preform and mold were considered during the analysis and failed to impose strain induced crystallization. Sistala, 2010 [68], used a Dupiax-Krishnan [69] material model and performed simulations in ABAQUS to study the effect of the change in temperature, stretch rod displacement and rate, pre blow and full blow pressures on stress strain behavior and wall thickness distribution of the bottle.

2.3.4 Structural performance

Preform optimization and blow molding simulations yields an optimized bottle design. Assessing the structural performance when subjected to different loading conditions plays a key role after the bottle is obtained. Finite element analysis is being used by the researchers to study the structural performance.

Dijk *et al.*, 1998 [70], studied the lateral deformation of plastic bottles due to internal vacuum, a phenomenon called paneling. The performance was checked for both round and square bottles. Deformations were related to initial head space in the bottle. Finite element analysis was also used apart from numerical and experimental methods to determine the deformations. Paneling can occur until the deformation is unable to compensate the head space. The addition of ribs to symmetric round bottles can reduce paneling but, square bottles show better performance without ribs, it is easier to minimize paneling in square bottles than in round bottles.

Karalekas *et al.*, 2001[40], conducted numerical and experimental investigations to study the deformation behavior under columnar crush loading of plastic containers used to store agro based chemicals. A nonlinear elasto plastic analysis was carried out using ABAQUS to observe the stress concentration areas and deformations. The most stressed areas and the plastic deformation areas were found based on the yield stress values of PET material. The numerical, experimental results were correlated and finite element analysis could successfully evaluate the performance in its early phase of design.

Masood *et al.*, 2006 [71], developed a design of 15 L water cooler bottles. The main criteria were to develop recyclable and collapsible PET bottles to replace existing refillable polycarbonate bottles. They followed a finite element approach to perform the structural analysis of two bottles under different loading conditions and orientations. There was no predetermined method to solve the criteria, so a trial and error method was employed. The proposed design reduced the weight by 200 grams (24%) and improved the structural stability.

Demirel and Dever, 2009 [72], worked on carbonated bottles. Carbonated bottles due to high pressures inside are subjected to environmental stress cracking (ESC) mainly at the petaloid base. The experimental study based on numerical modeling and stress cracking as a function of key design parameters was employed to get an optimized geometry resisting ESC. The experimental study generated various geometric combinations and these geometries were incorporated in CATIA for simulating stress distributions and an optimized base with the least stress cracking was proposed.

Chittepu *et al.*, 2009 [73], used LS dyna as a finite element analysis tool to check the structural performance of plastic bottles during labeling. The labeling process is performed at high speeds

(in excess of 1000 bottles per minute) and hence high deformations were expected. Before dealing with the high speed labeling, the initial steps was to modeling water particles and understanding the physics associated with water, and validating the top load performance. Three approaches were evaluated and implemented in LS dyna to consider water (liquid physics). First was a control volume (CV) approach which takes a compressibility effect into account, no liquid particles are modeled and it is the least computationally expensive. The top load of filled bottles can be modeled using this approach. Second was a smoothed particles hydrodynamics (SPH) approach, this accounts for inertial effects between water and air but fails to determine the compressibility effect. The last one was an Arbitrary Legrangian Eularian(ALE) approach. Here liquid particles were modeled using Eulerian elements and computationally expensive drop impact testing can be modeled using this approach. The top load of empty and filled bottles was validated with experimental results using the CV approach. Both the CV and SPH approaches were combined to study the performance of bottles during labeling. Figure 11 shows the comparison of simulation and experiments.

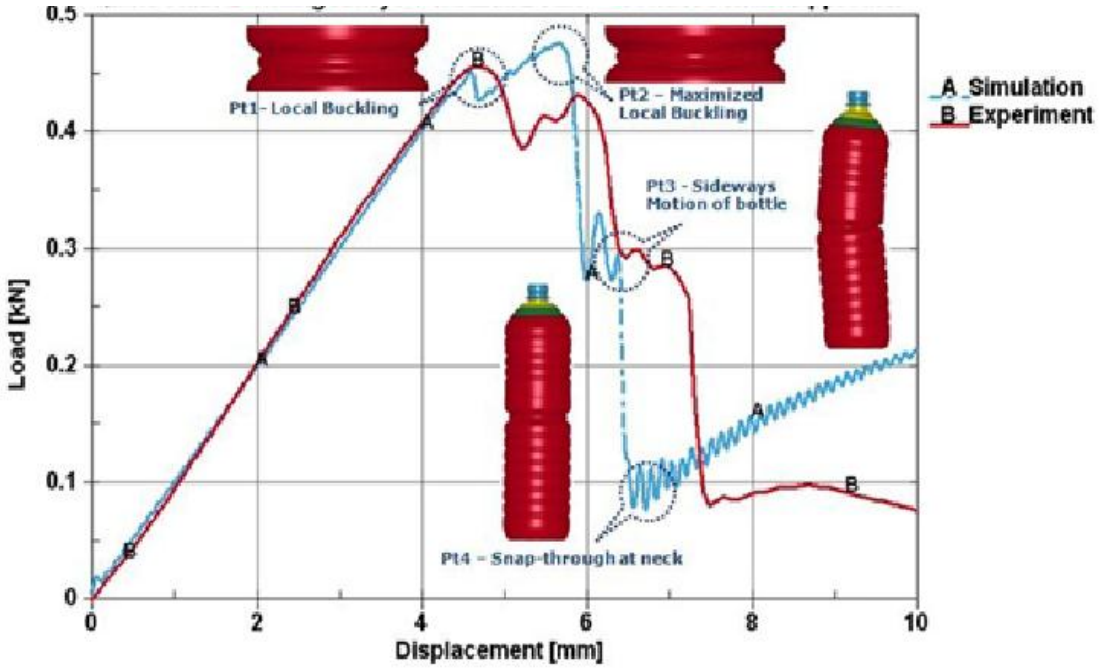

Figure 11: Top Load comparision of simulation and experiments [73].

Sumit Mukherjee, 2010 [74], developed an analytical approach to study top load and side load performance of oval containers. Virtual prototyping was used to implement the material properties and thickness distribution along the length of the bottle in FEA. The study proved that the containers which were preferentialy heated during molding (preferential heating- changing the lamp spacing in the molding process according to the asymmetric design and non-preferential heating is using the common lamp spacing for all designs) have uniform thickness distribution (0.3mm-0.4mm) and showed high empty and filled top load performance but less squeeze strength. Non-preferential heated containers have non-uniform thickness distribution (0.4mm-0.6mm) and showed low empty and filled top load performance and more squeeze strength.

Ing *et al.*, 2010 [75], developed an integrative approach to check the performance of injection stretch blow molded PET bottles. The stretch ratios were correlated with stretch ratio dependent material properties. The wall thickness and stretch ratios were determined by process simulation, these were used as input for the structural analysis. The developed integrative

approach (The approach in which process dependent material properties and wall thickness were used in the model) was compared with the conventional simulation approach. The results of the integrative approach were more comparable to the experimental results than the conventional approach results. The integrative approach was more accurate for empty bottles than filled bottles; filled bottles showed slight deviation but could predict the failure mode accurately. Figure 12 shows the results of conventional and integrative approach.

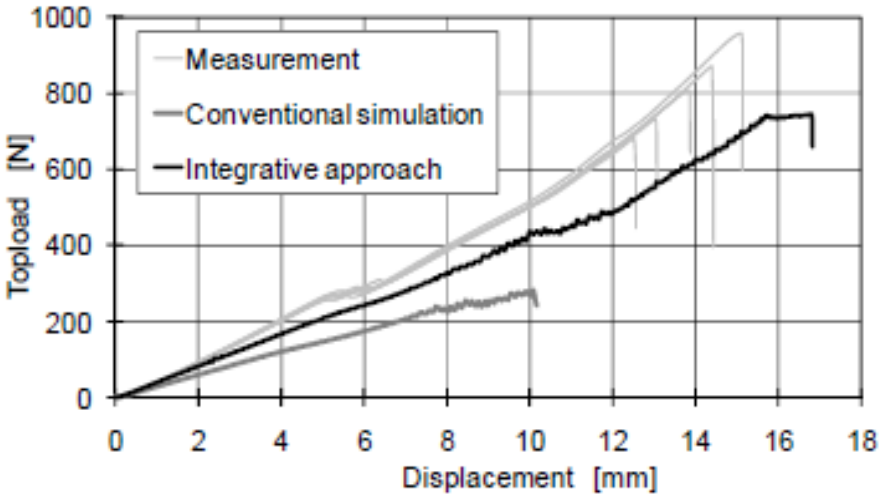

Figure 12: Top Load comparision of integrative approach,conventional simulation and experiments[75].

Overall, studies have been focused on material modeling, preform optimization, process simulations and structural performance. Assessing the structural design features of bottles under service loading has not received much focus. Moreover, bottles are even subjected to bending during transportation which is one of the problems in light-weight packaging, hoop strength, similar to squeeze strength, of the bottle was not generally studied by researchers.

Understanding the design features based on the deformation of the bottle helps to improve the features of the designs. Figure 13 shows the different features of the bottle.

Assessing the design features of the bottle; studying the bottle subjected to bending and its effect with change in wall thickness and designs; and studying the hoop stiffness of different bottle designs were the primary focus here. Apart from that, stability (structural performance) of light weighting of bottles by correlating stretch ratios and thickness values are discussed.

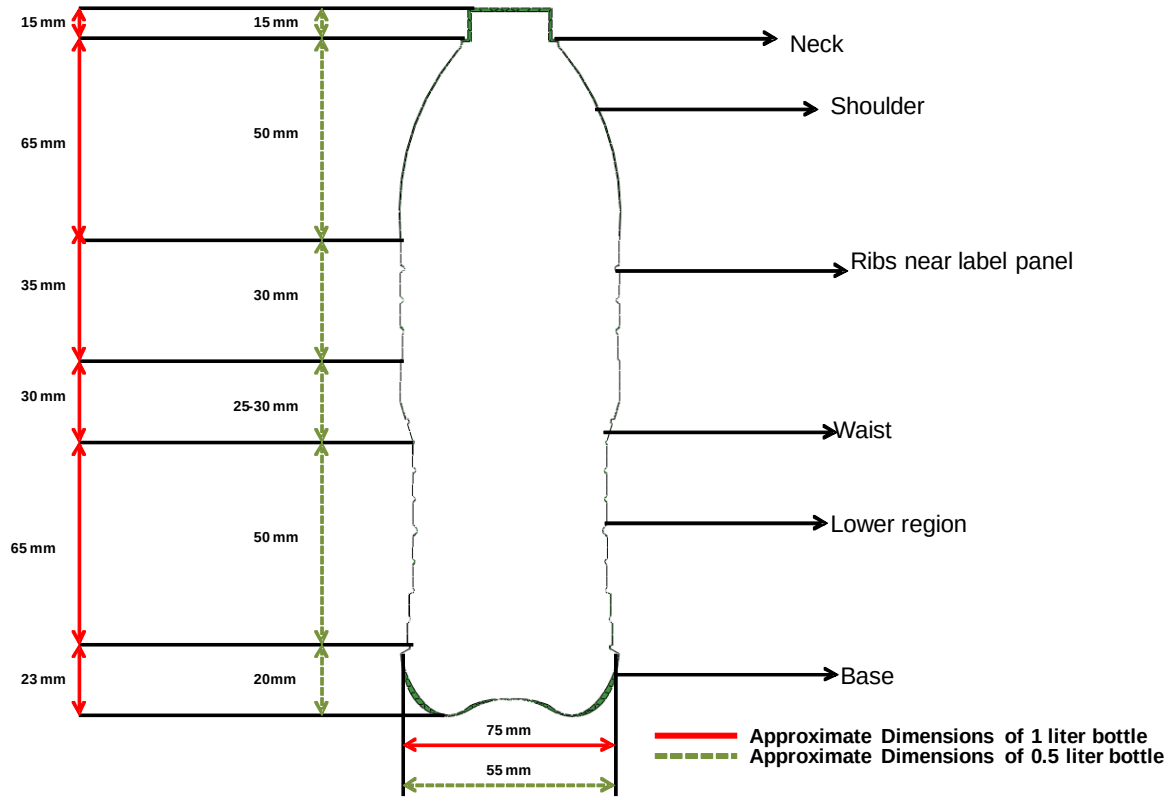

Figure 13: Features of a bottle and approximate dimensions of 1liter and 0.5 liter bottle.

CHAPTER III

3. MATERIALS AND METHODS

The importance of assessing the design features of the bottle as discussed in the previous sections motivates us to develop standard procedures in fulfilling the required aims. A lack of CAD models of all the designs provoked us to use 3D scanning technology and develop our own procedure to build CAD models from finished parts. The absence of equipment and test procedures to perform hoop strength measurements provoked us to build a test fixture to develop a procedure. In addition, uniaxial compression tests were also performed using an INSTRON machine in order to validate FEM results and a Magna Mike was used to measure thickness along the length of the bottle.

3.1 3D scanning Technique

3.1.1 Equipment:

3D scanning is a technique which analyzes the object with its color, shape, and size. The main principle behind this is the laser emits rays which identifies the object from reflection and couples the distance results with a color image. A range of techniques including laser triangulation and laser time of flight were used for 3D scanning. Research is being done to improve and provide algorithms [76-78]. A Next Engine 3D scanner was the equipment used in this research as a 3D scanning tool. This is a compact scanner of dimensions 229 X 101X

279mm (9X 4 X 11") weighting 15.4 kg (7 lbs) It has four lasers, two 3.0 mega pixel cameras and two lights to capture the image.

lectro optical architecture and refined algorithms were used to get an array of lasers to scan in parallel with 0.1 mm (0.005") accuracy. It has macro and wide precessions. Macro precession gives an accuracy of 0.1 mm (0.005") and the object should fit in 76 X 127 mm (3"X5") area [limitations of size of the object]; wide precession gives an accuracy of 0.3 mm (0.015") and the object should fit in the range of a 254 X 330 mm (10"X 13") area [limitations of size of the object]. Figure 14 shows the typical set up of 3D scanner.

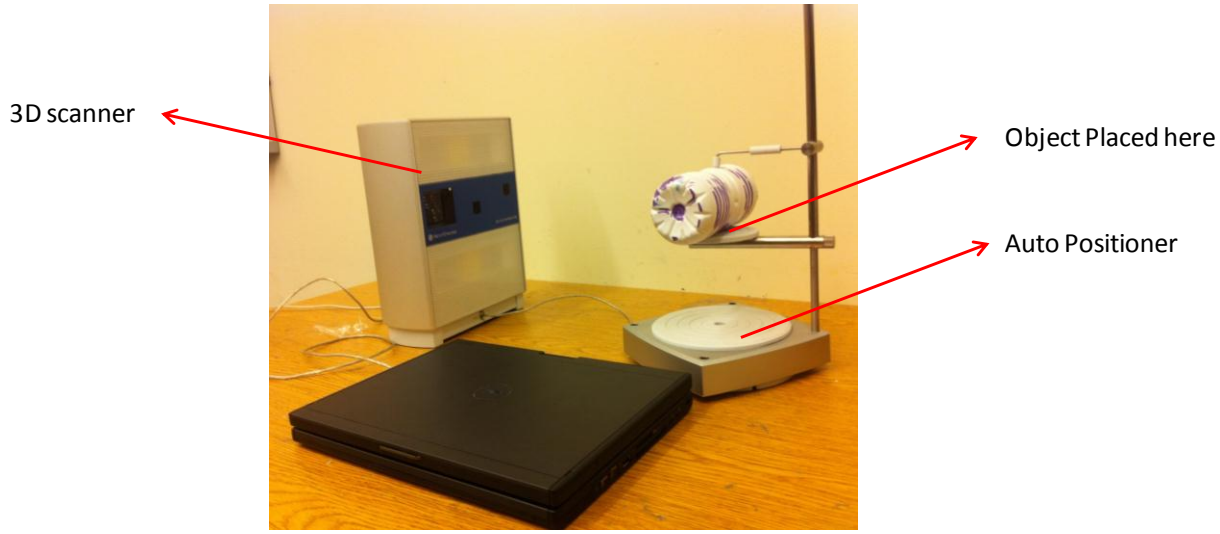

Figure 14: 3D Scanning setup.

3.1.2 3D scanning method

3D scanned images were acquired using the Next Engine 3D scanner. Scanning is of three types first is a single scan where the scan is made at one angle, next is a bracket scan where the scans are made at three consecutive angles, and we get a part of the object and the final one is 360^{o}

scan, where the complete 3D object can be obtained. Figure 15 outlines the scanning procedure. The 360^{o} complete scan was used in this research to obtain complete images of the bottles.

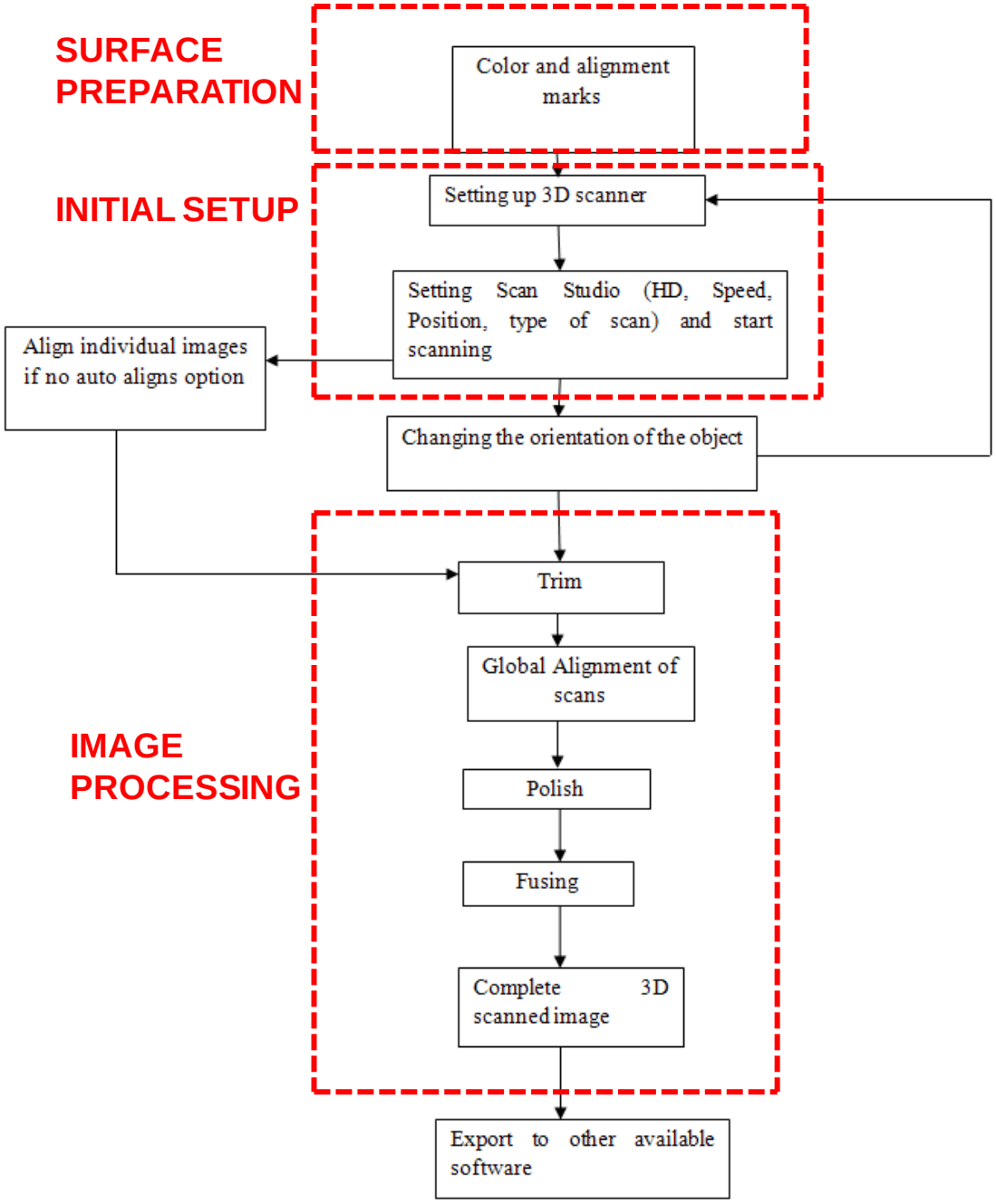

Figure 15: Procedure for scanning.

3.1.2.1 Surface Preparation

The scanner identifies the object using reflection of lasers so, if the object is transparent the rays pass through the object and no reflections are gathered. Hence, the objects were colored. RUST OLEUM paint of white color was used to paint the bottle and different colored markers were used for aligning the multifamily scans. The objects should not be glossy so, magnetic flux, talc powder was usually used to provide the rough finish. In this study the spray paint itself provided the rough finish to the objects. Markings are made on the bottle for alignment purposes. Figure 16 shows how the bottles are pained and typical markings.

Figure 16: Surface preparation of bottles.

3.1.2.2 Scanning Procedure

Scan studio is supporting software to the 3D scanner. Figure 17 shows a snapshot from the software. The Object was placed on the auto positioner and area of interest was selected by

highlighting the area as shown in the Figure 17, next the type of scan was selected, 360 was used in scanning the bottle. Next, selecting the number of divisions indicates the number of rotations the auto positioner takes for a 360 degree scan. 16 was used in our case. Points/inch^2 indicates the quality of the image--more number of points captured greater the accuracy; HD (17K points/inch^2) was used in our case. The target was selected based on the color of the object and environment where the scanning is being done. In this study neutral was selected as the scanning was done in the closed room and at minimal light exposure. Range/ precession is selected based on the size of the object and accuracy of the scans. In our case, "wide" range was selected and the object was placed 17 inches from the scanner. After setting up all the above parameters, scanning was started. The object was oriented differently to capture the missing areas. Hence we obtained different families of scans for different orientations of the object. The next step was to improve the image quality trim, polish, and fuse were a few options provided in the scan studio software to improve the final quality of the image.

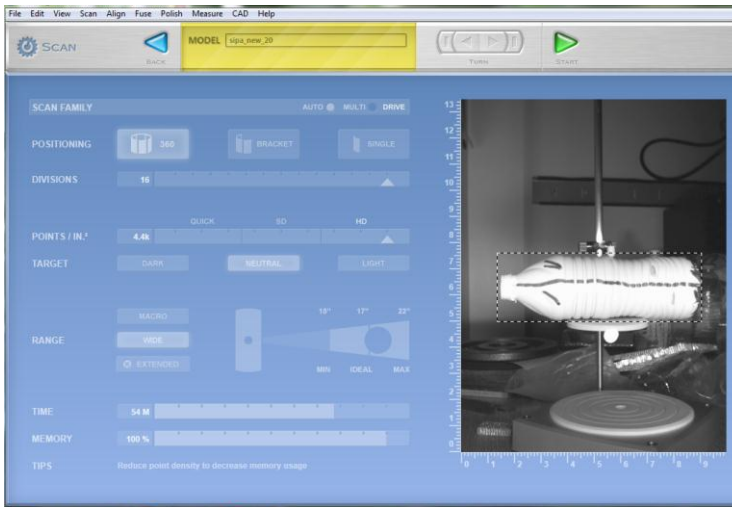

Figure 17: Snapshot of 3D scan software.

Trim:

Trim is an option in the scan studio software. While selecting the area of interest, the part gripper was also often selected; hence we obtain unwanted areas. The unwanted areas were selected using the available tools in the trim option and were deleted. Scan families were trimmed individually before the alignment step. An "auto trim" option was also available, it detects and removes unwanted areas that were captured at a steep angle relative to the line of sight of scanner [80]. In scanning the bottle, the manual trim option was used in order to prevent data loss in auto trim.

Alignment:

The aligning tool not only aligns single images but also aligns multiple families. During the initial stages of research, the individual images were aligned using manual selection of common areas but over a period of time the software was being updated and the individual images were auto aligned. Multiple family scans were aligned identifying the common locations. The alignment screen would split into two parts one part is aligned family and the other part is unaligned as seen in Figure 18. Using the alignment marks made during the surface preparation the two multi families were aligned placing three pins at the common locations.

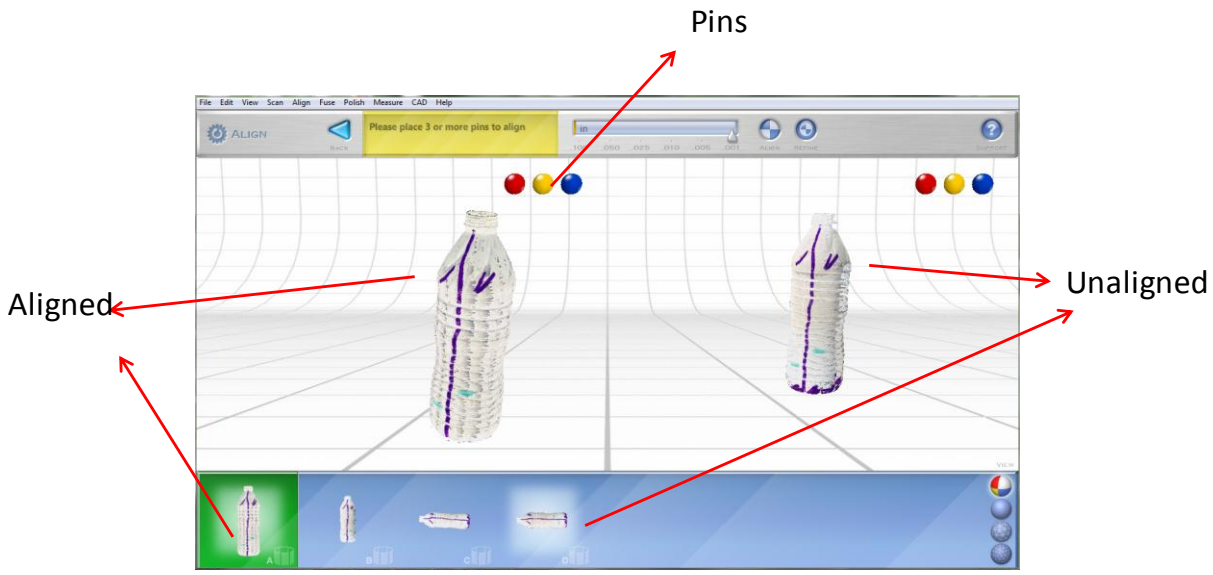

Figure 18: Alignment of multifamily scans.

Fusing:

Fuse is an option in the software which was used to merge, re-mesh, fill holes and simplify the aligned image. The tolerance was selected and it performs simplification at required areas, more data is gathered at complex shapes and it simplifies the data at large planes. The tolerance used in this study was 0.0025".

Polish:

Polish is an option in the software which was used to fill the holes which were left during scanning. The holes are automatically detected once the polish option is selected. The options include flat filling, smooth filling, and curvature filling. After polishing the model, the defects needed to be cleaned; the clean defect option automatically identifies the self-intersecting meshes. Once we follow the steps of aligning, fusing and polishing the 3D scanned image can be exported to other available software.

3.1.4 Converting 3D scanned image to CAD and importing to FE

Extracting a CAD model from a finished product was important due to the absence of the CAD models. Extracting the CAD models from the bottles and importing them to FEM software without loss of data was a part of the project. RapidWorks software which is a comprehensive tool to convert scanned images to CAD software making the models parametric was used. Figure 19 shows the outline of the converting procedure. The initial step would be importing the scanned image to RapidWorks which is a direct step. The saved 3D scanned image will be in ".scn" format and this directly opens in RapidWorks. The scan tools like trim, polish are available even in RapidWorks so, once the image is imported in RapidWorks the defects are cleaned and polished.

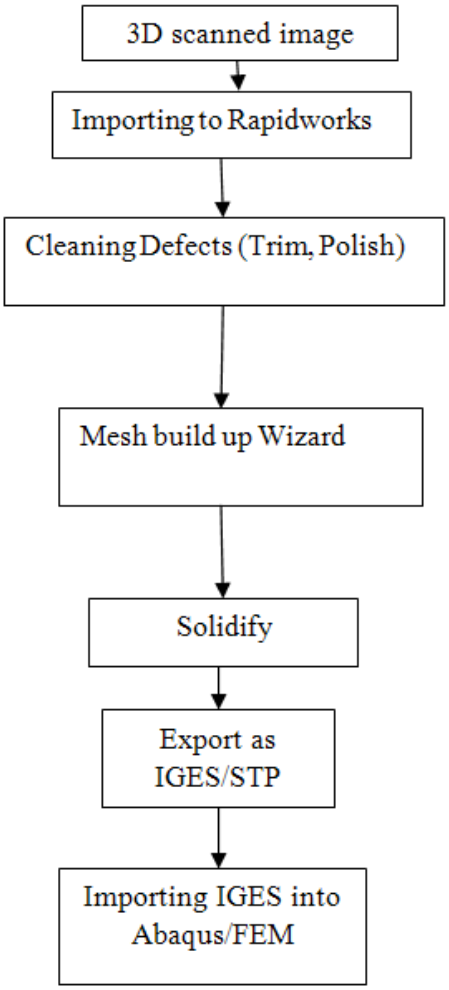

Figure 19: Procedure to import scanned image to CAD.

Mesh Build up Wizard:

This is an option in RapidWorks software. This option is available in scan tools, this command is an interface to create a defect free and water tight mesh model from raw scan data [81]. Initially the unwanted data was deleted by selecting the poly vertices per noisy cluster, 100 in the case of a bottle. The next step was to create triangles and merge them as a single mesh. The density of the mesh is in between dense and sparse. The final step is then finalizing the mesh which enhances the mesh quality. Figure 20 shows the image after the mesh build up wizard tool was used.

Figure 20: Quality of image after mesh build up wizard.

Solidify:

After creating water tight mesh model [no holes], surfaces were created on the model using an auto surfacing option, the number of surfaces depend on the quality of the scan, 2000 surfaces were used for all the models here. Patch size regularity which controls the regularity of a patch was uniform. The relax initial mesh option was selected to get uniform surfaces. The geometry capture accuracy that controls the degree of resemblance of the created surface with original re constructed model was tight [81]. The surfaces must be checked for defects in body tools and the check defect option automatically cleaned defects once they were detected. After creating surfaces, an export option was selected, and files were exported as an IGES or .STP format. Once the model is saved in IGES or .STP format they can be imported as CAD or FEM.

3.2 Hoop Strength measuringTechnique

3.2.1 Fixture Design

The hoop strength of the bottle determines how the bottle undergoes deformation upon holding the bottle, which was initially hard to quantify. Moreover there were no standard procedures available to measure hoop strength. To perform the hoop strength testing of the bottle, the fixture was designed at Oklahoma State University* and a standard test method was developed using that fixture. The principle behind the design was considering the bottle as a thin walled cylindrical structure and the hoop stress and longitudinal stresses were calculated using the equations 3.1 and 3.2 respectively [79].

$$\sigma_h = \frac{pD}{2t} \qquad 3.1$$

$$\sigma_l = \frac{pD}{4t} \qquad 3.2$$

The two considerations for the design were, the materials used for this fixture must be corrosive resistant and the fixture must fit on an INSTRON machine. The final design was developed making improvements to the initial attempts, finite element analysis was performed to the final design in Pro-engineering software to observe the stress concentration areas. Figure 21 shows the final design in Pro-E. However, the mass attached to the rope was eliminated after the

fixture was set up on the Instron. Instead the belt was extended and fixed on the other end

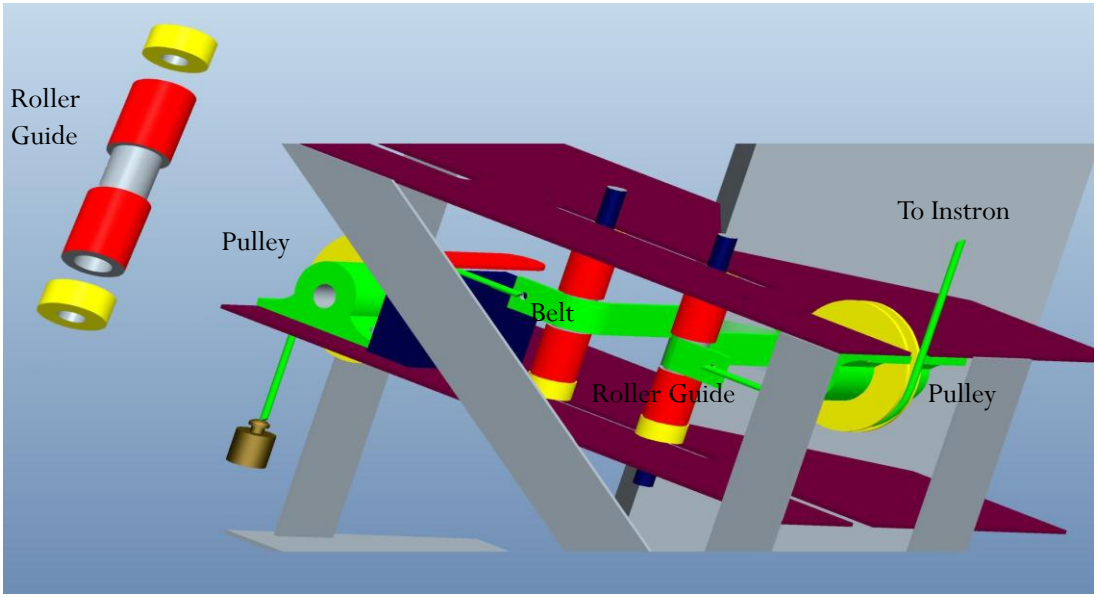

Figure 21: Final design of fixture for testing hoop strength of bottle.

The final set up of the fixture is shown in Figure 22. The fixture was bolted on an INSTRON machine using four 3/8”- 16 bolts; the bottle was placed on a base plate, different plates were made for different sizes of bottle; the Kevlar belt passes around the bottle, through the gaps provided on a wedge. Oone end of the belt is connected to the rope and the other end is fixed between the plates. The rope from the belt goes around the pulley and connects to the nut-bolt which itself is fixed to the top load cell of the Instron machine.

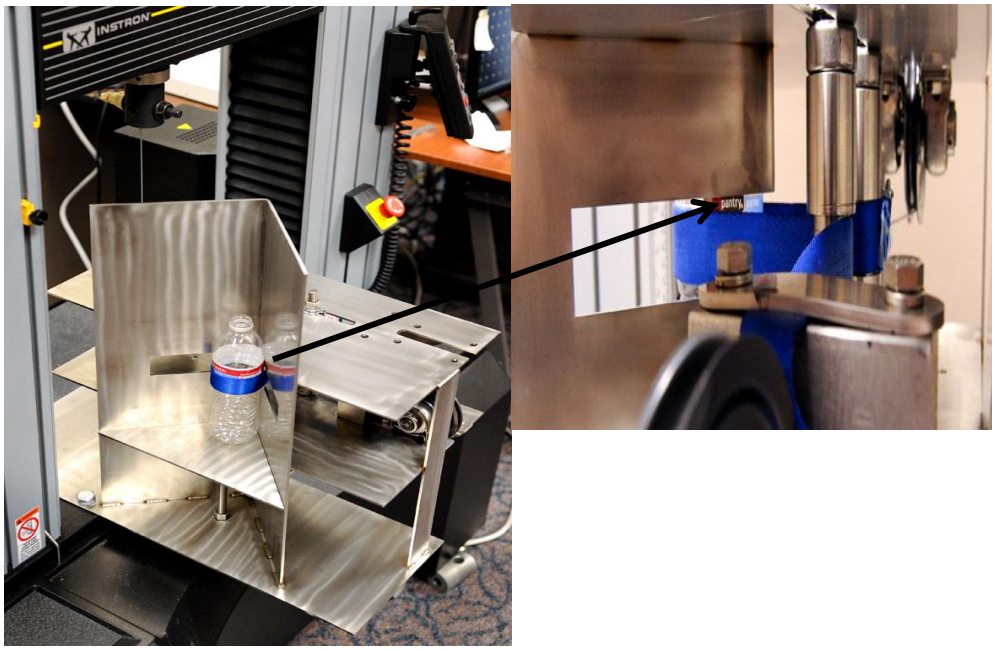

Figure 22: Fixture setup on an Instron.

3.2.2 Test procedure

The primary aim was to develop a standard procedure using the developed fixture, compare the different designs and compare several bottle designs. The bottle samples used in the experiments were of different designs with different processing history. The main difference in designs is the change in shape of the ribs, design (G) is having columns near the waist, designs (A, C, and E) have deep ribs and designs (F, D, and B) have less deep ribs. A test procedure was developed to check the hoop strength and rank the designs based on performance. All the designs were tested at the waist location shown in Figure 23.

Figure 23: Modified fixture with point load application.

The experimental set up is shown in the Figure 22. The load displacement curves for each bottle design were plotted and the slopes in the elastic regions of the curve were measured. Stiffness of the designs was obtained by the slopes. The initial tests were conducted at 2mm/min strain rate till the displacement reached 15mm. It was modified as the bottle did not completely deform, so the procedure was changed to 10mm/min with completion when the load reached 44 .44N (10 lbf) The increase in strain rate showed a difference. The load was applied uniformly all around the waist but in reality upon holding the bottle the load is applied by concentrated forces at discrete locations

The design was again modified as shown in Figure 23 so that the force was applied at two particular locations. Thick walled plastic cylinders (sharpie pen) of diameter 0.4" were cut and two pieces of 1" length were taken out and the edges filed to get a smooth finish. They were attached on the Kevlar band using binding wire. Using the modified set up, the tests was

repeated at 10mm/min strain rate. The tests were repeatable; hence all the designs were ranked using the modified set up and test procedure.

3.3 Top Load testing Procedure

The 1 liter filled bottles were placed on a standard INSTRON set up as shown in Figure 24, and the compression platens were loaded at different strain rates until the bottle was deformed completely.

Figure 24: Top load setup on Instron.

3.4 Stretch Ratio Measurement Technique

As discussed in section 1.5, injection molded preforms are stretched and blow molded to obtain bottles. The ratio of distance between any two points after blowing to the distance between two points before blowing is known as the stretch ratio.

Injection molded preforms were collected from four different plants and markings were made at 5 mm starting from the neck region along its length and blown in the respective plants, the designs of the bottles were different. The distances between the markings on the bottle were measured using the paper scale and the stretch ratios were calculated for the different designs. Figure 25 shows the markings on the preforms and markings on the bottle.

Figure 25: Markings on preform and bottle.

3.5 Wall thickness Measurement techniques

Wall thickness of the bottle changes along the length of the bottle so, uniform thickness cannot be assumed. There is a need to measure the thickness distribution along the length to implement the thickness data in a finite element model. A Magna Mike tool was used to measure the thickness. The Magna Mike works on the principle of Hall Effect. The setup of the equipment is shown in Figure 26. The bottle was marked at every 5 mm along its length and a steel ball was

placed inside the bottle. The Magna Mike wand was placed outside the bottle, the ball gets attracted to the wand once both wand and the ball are aligned. The thickness value (distance to the ball) is displayed on the screen. Three sizes of ball diameters 1/16", 1/8" and 3/16" were available. The ball size is selected according to the geometry of the object. Larger ball size is preferred since accuracy is more, but when the geometry prevents from using larger ball, the smaller balls were used. The thickness was measured at a point and along the length of the bottle; the results are plotted in the graph.

Figure 26: Magna Mike setup for the measurement of wall thickness.

CHAPTER IV

4. FINITE ELEMENT PROCEDURE

Finite element analysis was used to assess the design and evaluate the performance with change in the design; it also provided a supporting method to the experimental methods. ABAQUS 6.9 was used as an FEA tool in this research. The aims of the research were to assess the design on applying the top load to a 1 Liter bottle, develop a procedure to check the bending of the bottle, measure the effect of change in wall thickness on bending, assess variation of bending with change in design, and predict cylindrical hoop strain to evaluate the hoop strength measured from the newly developed fixture. Each problem has different boundary conditions and material distribution, but the procedure followed for simulations would be similar. Figure 27 outlines the procedure.

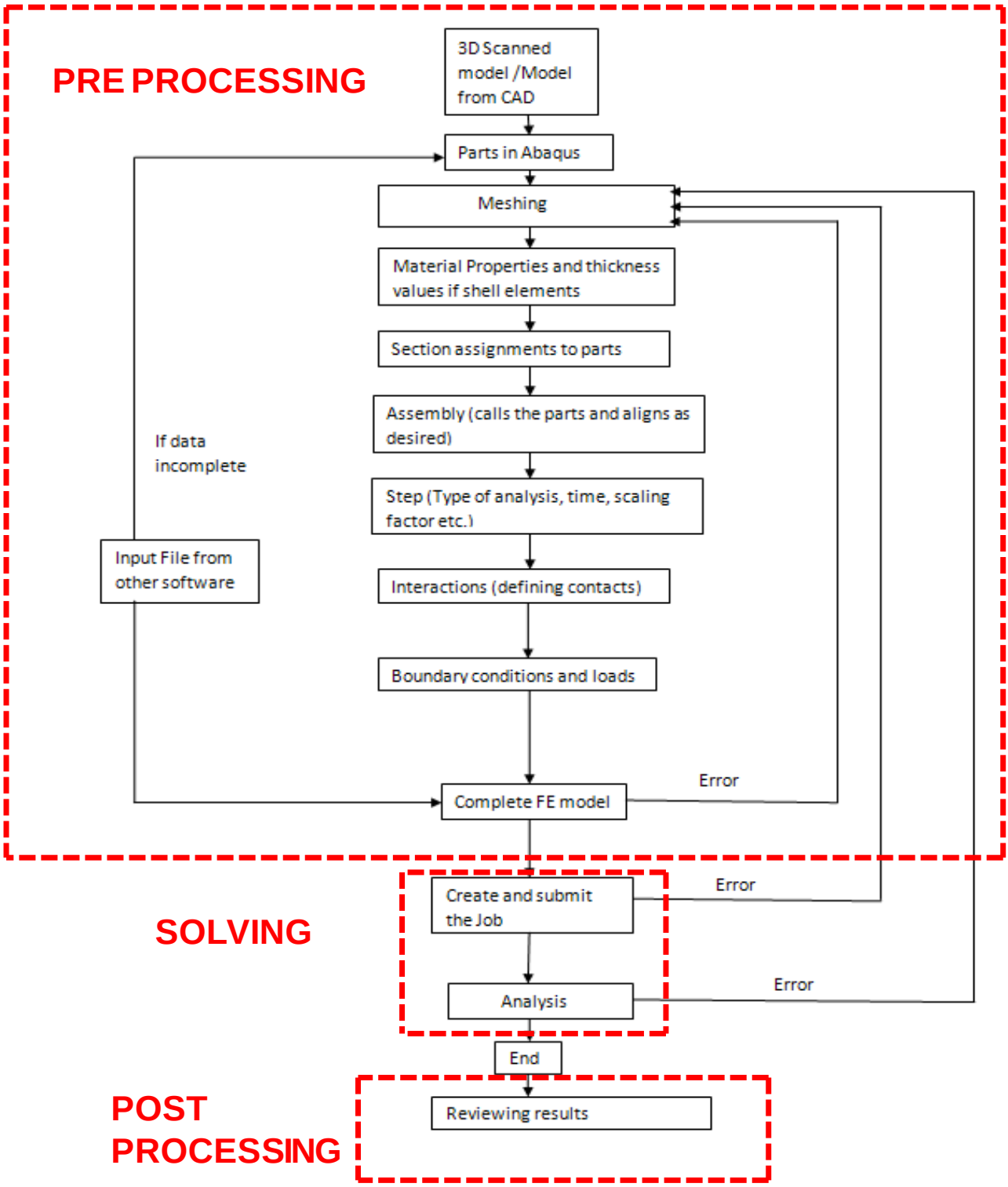

Figure 27: Finite element analysis procedure in ABAQUS

4.1 Part Generation

The modeling of any simulation embarks on creation of parts involved in analysis. Depending on the deformation behavior of the particular part in the analysis, the type of the part is selected. The available form of parts in ABAQUS are deformable, rigid solid; and deformable, rigid shell. Eulerian parts can be used to model liquid elements in Eularian analysis and Legrangian-Eularian analysis. The parts can be of exact size that match its real time objects or scaled depending on the requirement or accuracy needed. They can be created in the part module or can be imported from other supporting software stored in formats such as ".IGES, .SAT, .STP". The entire model containing the part, model data can also be imported into ABAQUS. The 1 liter model was imported as an ".inp" file and the 0.5 liter models were imported from the 3D scanned model developed in Rapid Works and saved as an ".IGES" format. Imported parts cannot be edited.

4.2 Meshing Techniques

Generating meshes on parts was done in the mesh module. The results of the analysis depend on the quality of meshing. Meshing starts with assigning a seed on the parts. This determines the mesh density at particular region of the part. The part is seeded according to the complexity of the geometry, different seeding can be assigned to different regions of the part. After seeding is assigned to the parts, the meshing operation is performed. Structural meshing, swept meshing, bottom up meshing, and free meshing are the common meshing techniques used in ABAQUS 6.9. In all the simulations performed in this research, the free meshing technique was used. Free meshing is unstructured, flexible and has a complex topology. Element shape plays a major role; it determines what shape the meshes are. Quad, tri, tetra and hexa are available mesh shapes in

ABAQUS. Hexa mesh was used for all the simulations because of its accuracy and degrees of freedom.

Assigning element types to the mesh region is a critical step, the type of element depends on type of analysis and the behavior of the part in analysis. Element types can be assigned to part mesh and orphan mesh; it can also be changed once it is created. Wide ranges of element types are available in Abaqus of which the shell element type was used for modeling bottles in all the simulations performed. Shell elements are of two types; continuum and conventional shell elements. Conventional shells are used when thickness is much less than other dimensions and a continuum shell is used when the thickness is in comparison with the other dimensions. Figure 28 explains the difference between the two shell elements. Conventional shell elements were used to model bottles for all the simulations in this research. After creating meshes, a mesh part is created so that the same part can be used for different purposes. The mesh part created acts as an independent part with the same mesh attributes of the original part.

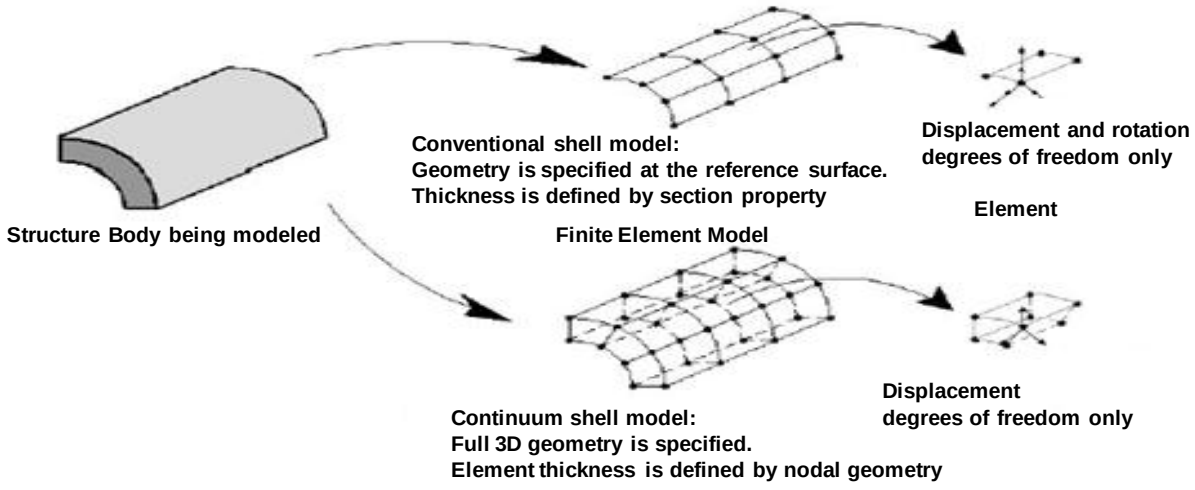

Figure 28: Difference between continuum and conventional shell [21].

4.3 Material Modeling

Creation of material properties and assigning the material properties to the individual parts are discussed in this section. This governs the nature of the final results hence, understanding the material properties and inputting accurate values is of high importance. Properties assigned to the model are divided into four parts (a) General properties, (b) Elastic properties, (c) Plastic properties, and (d) Creep properties

The general properties include density, *depvar,* and other properties from user subroutines. Here only density (1335kg/m^3) was entered, and was constant for the entire model. Elastic properties can be defined as isotropic, orthotropic, anisotropic, and with engineering constants depending on the type of material. This can be determined from stress strain curves or other mechanical testing. In the 1 liter model case, the elasticity data, density were taken from the output of virtual prototyping software [74], this was of "engineering constants" type. For the other 0.5 liter models, elasticity data was calculated from stress strain curves [82] and it was isotropic type. Plastic properties were assigned using a classic plasticity model. The plastic properties for the 1 liter model were taken from the output of the virtual prototyping software, and the same plastic data was used for the other 0.5 liter models. Creep properties can be assigned using sub options in plasticity, POTENTIAL option in ABAQUS replicates a power law model of creep [20], the constants of the POTENTIAL option for the 1 liter model was taken from the virtual prototyping software, the average of same creep data was used for the other 0.5 liter models.

After creating material data, sections have to be created for each material, defining their thickness attributes in the case of shell elements. As the element type was "conventional shell," the thickness of the element was the assigned thickness value. The thickness values can be

assigned while defining the section or it can be assigned as nodal thickness or elemental thickness in a discrete field manager and then call that file while assigning thickness. In the 1 liter model, the thicknesses were defined for each node in a discrete field manager as the thickness values were taken from the output of virtual prototyping software. There were 198 sections with different material properties and different thickness values. For the 0.5 liter models, the thickness values measured using a Magna Mike were used as input for defining sections. There were 10 different sections with the same material properties but different thickness values.

The next step was assigning the sections to the parts. This can be done either by creating element sets in the input file or assigning sections individually to the part. In the creation of element sets or nodal sets, they are created first and the sections are assigned to those nodal or elemental sets. Whereas, in assigning sections individually, the mesh elements were manually selected in the view port and the sections were assigned to those elements. In the 1 liter, model the sections were assigned by creating element sets in an input file, and for the 0.5 liter models, the sections were assigned manually in the view port.

4.4 Step Module

The type of analysis is assigned in this section. In all the FE problems there is at least two steps. One is the initial step, which is the default step. All the initial boundary conditions are defined in the initial step. The second step is the analysis step, which is chosen according to the type and complexity of the problem. In this research, the bottle buckles and a transient response is required; hence dynamic explicit mode was chosen. The total step time, increment [number of time steps/ interval], and mass scaling factor [Reduces the net mass used for simulation. It does

not affect the simulation results. Reducing the mass scaling factor increases the simulation time] were defined in for the dynamic explicit step.

4.5 Contact formulations

The interactions between the multiple parts in an assembly are defined by contact formulation. Considering all available algorithms in ABAQUS, a general contact algorithm was used to define the contact between the rigid plates and bottle in the top load simulation of the 1 liter model. This contact method supports multiple contacts, simple to define, and fewer restrictions on elements. Surfaces are predefined in the part region and the surfaces which are in contact were selected in this region. The interaction properties must also be defined in this section. In this model, the interaction properties were; frictionless contact for tangential behavior and hard contact for normal behavior.

4.6 Boundary Conditions

The boundary condition is one more important factor which governs the output of FEA; a thorough understanding of the boundary conditions is required to get good results. The load and boundary conditions are assigned in this section. The boundary conditions also depend on step; they can be modified in each step. In the case of dynamic explicit analysis, the amplitude must be predefined in assigning displacement boundary conditions in an analysis step, amplitude ramps the load and prevents impact loading [75, 83].

4.7 Constraints of specific Problems

4.7.1 Hoop strength of the cylinder

In this case three designs of cylinders were modeled with shell elements of 1 mm thickness, the first design (a) was only a cylinder, the second design (b) was a cylinder with a 0.2 mm rib at the center, and the third (c) design was a cylinder with 0.3 mm ribs. Elastic, general properties of PET were assigned to the model. Standard simulations were performed. A pressure of 1 MPa was applied to all the designs as shown in Figure 29.

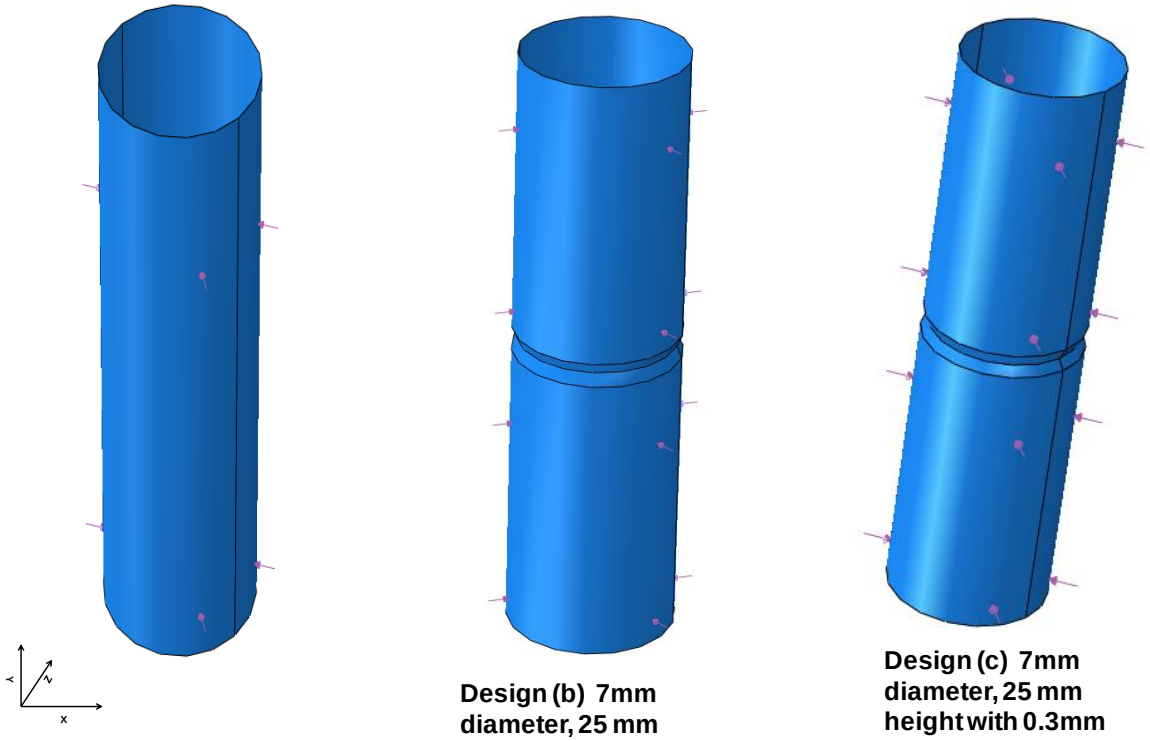

Figure 29: Models of cylinders considered for the hoop strength.

4.7.2 1 liter Model Top load

Part Generation: 1 liter Bottle was imported to ABAQUS in ".inp format" and the plates were modeled in ABAQUS using an analytical rigid model.

Meshing: The model imported was of orphan mesh type so no manual seeding and meshing was required, the mesh was of shell element "S4R" type and the plate was modeled with analytical rigid elements, so no meshing was required, since it does not undergo deformation. Membrane which simulates an intersection layer for air and water in the bottle was meshed with M3D8R membrane elements which can stretch infinitely.

Material Modeling: The material properties include general, elastic, plastic and creep properties, the material properties were changing along the length of the bottle and are of the form shown below.

Properties:

General properties:

Density: 1335 kg/m^3

Elastic properties:

Elastic properties are assigned in the form of engineering constants

E_2 (MPa)	E_1(Mpa)	E_3(MPa)	ν_{11}	ν_{22}	ν_{33}	G_{12}(MPa)	G_{23}(MPa)	G_{13}(MPa)
1254.74	1345.39	1254.74	0.4	0.4	0.4	448.12	480.5	448.12

Table 2: Elastic properties.

Plastic Properties:

Yield stress (MPa)	Plastic Strain
75.49	0
155.26	0.928

Table 3: Plastic properties.

Creep properties:

R_{11}	R_{22}	R_{33}	R_{12}	R_{13}	R_{23}
0.993	1	0.993	1	0.993	1

Table 4: Creep Properties.

Membrane properties: the intersection layer of water and air. The properties of this layer were

Density = 1.189 kg/m^3

Bulk Modulus = 1.42 X10^5 Pa; Poisson's Ratio= 0.5

Plates were considered to be rigid—no mechanical property needs to be assigned.

The thickness distribution was also taken from virtual prototyping. The sections were assigned by creating element sets and assigning the respective properties and thickness data to the sets created.

STEP Module**:** Dynamic explicit analysis was chosen with a time period of 5 and mass scaling factor of 2E5.

Contact formulations: The surfaces were created for the plate, top region of bottle, bottom region of bottle. The general contact algorithm was used to define the contact between the plates and bottle.

Boundary Condition: The boundary conditions were as shown in Figure 30. The bottom plate was fixed in all directions. The top plate was fixed in all directions, except in the Y (vertical) direction. The displacement was given in the Y direction with the amplitude defined such that it

ramps up with load. A pressure of 1 atm was given to the internal section of bottle and the amplitude was defined to control the change in pressure with deformation.

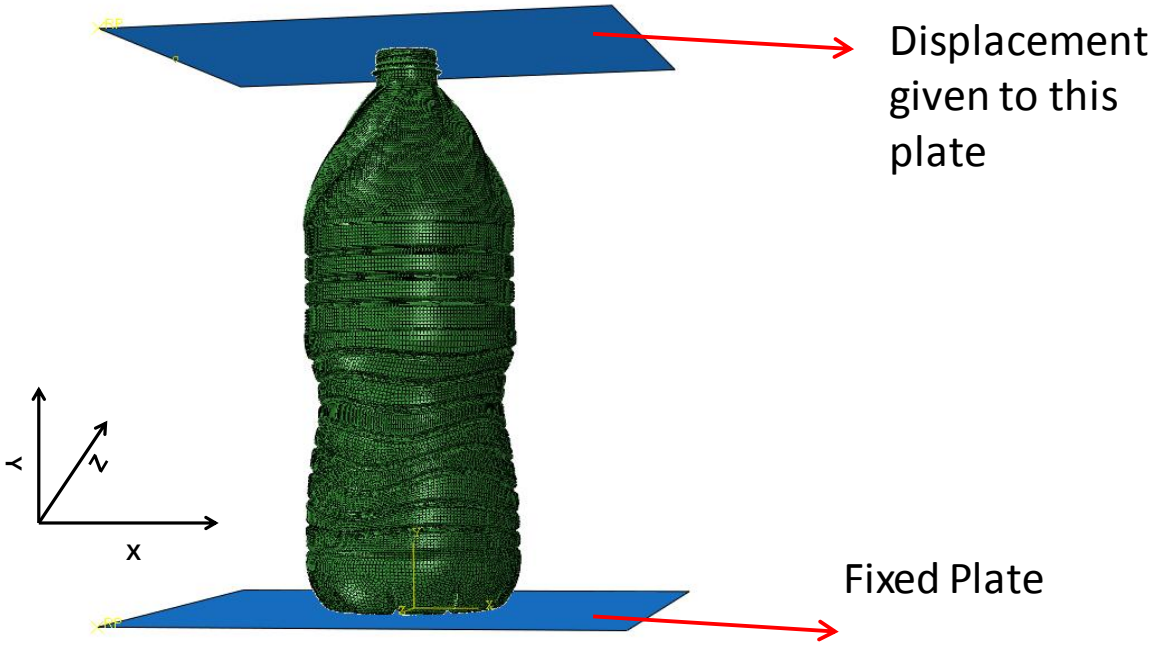

Figure 30: Boundary conditions for top load of 1 liter model.

4.7.3 1 liter Bending model

The model which was used to check the top load performance was also used to check the bending performance so, the part, meshing, material properties were the same. The step and boundary conditions were assigned as follows:

STEP Module: Dynamic explicit analysis was chosen with a time period of 2 and mass scaling factor of 2E5.

Boundary Conditions: The boundary conditions were as shown in the Figure 31. The bottom of the bottle was fixed in both rotational and translational directions. Amplitude was defined to

ramp up the load. The middle node at the top was given a displacement of 11.5 mm (H sin 3 and" H" is height of the bottle), with the defined amplitude in the X direction.

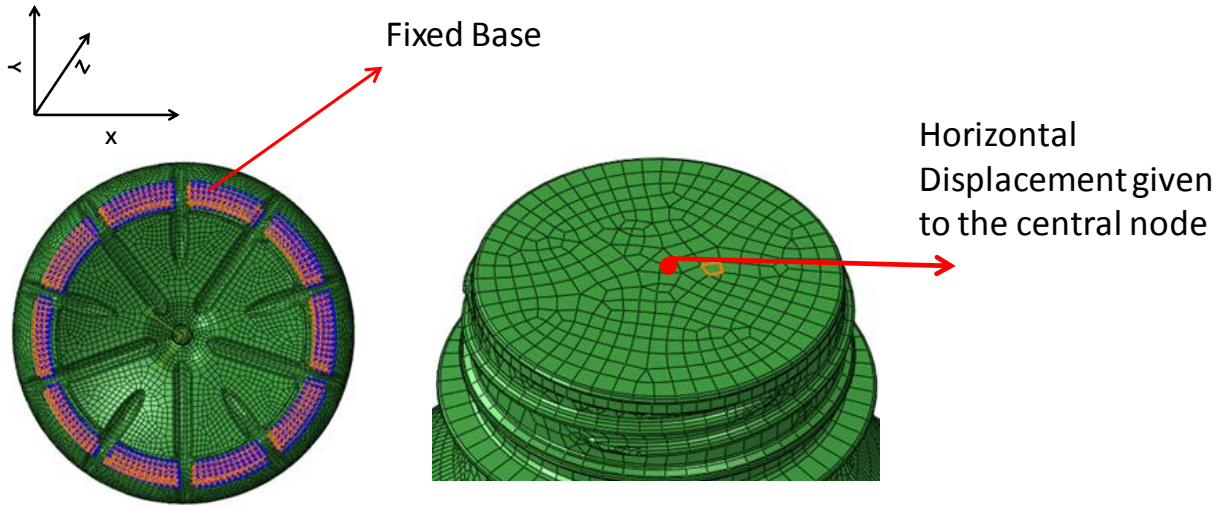

Figure 31: Boundary conditions for bending of 1 liter bottle.

4.7.4 0.5 liter models for Bending

Part generation: The 3D scanned models are imported as ".IGES" to ABAQUS.

Meshing techniques: All the parts were seeded according to their shape and the free meshing technique was used to mesh the parts. Convention shell elements "S4R" were assigned.

Material properties: The material properties include general, elastic, plastic and creep properties, the material creep and plasticity properties are same as the properties defined in 1 liter model the general and elastic properties are taken from *Bandla* [82].

The thickness distribution was taken from data measured using a Magna Mike. The sections were assigned manually by selecting regions. The thickness was assigned to the respective regions.

STEP Module: Dynamic explicit analysis was chosen with a time period of 2 and mass scaling factor of 2E5.

Boundary Conditions: The boundary conditions were as shown in Figure 32. The bottom of the bottle was fixed in both rotational and translational directions. Amplitude was defined the same as for the 1 liter model. The middle node at the top was given a displacement of 9.2 mm (H sin 3 and" H" is height of the bottle), with the amplitude defined in the X direction.

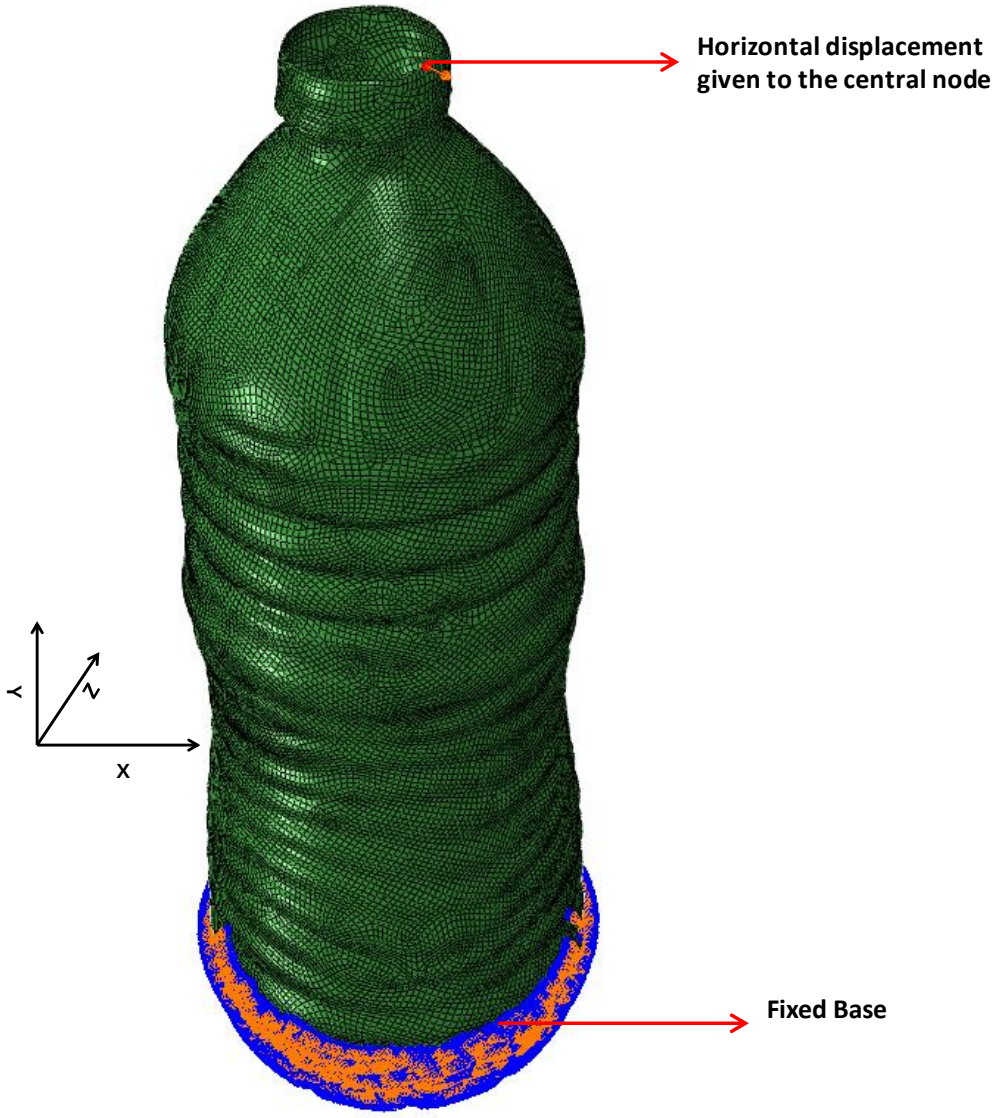

Figure 32: Boundary conditions for 0.5 liter bending.

CHAPTER V

5. RESULTS

5.1 Hoop strength Testing Results

5.1.1 Hoop strength using fixture

The results showed load displacement curves obtained from the experiment (shown in Figure 23). Overall, 8 different designs were considered for testing; design A had two different processing conditions and two different orientations. Each design showed different stiffnesses. Multiple samples were tested for each design of the bottle. The initial results of 2 designs shown in Figure 33 were conducted using the initial fixture design with a 2mm/min strain rate. Later the strain rate was increased to 10mm/min and those results are as shown in Figure 34. Figure 35 shows the results with a 10mm/min strain rate and the modified set up.

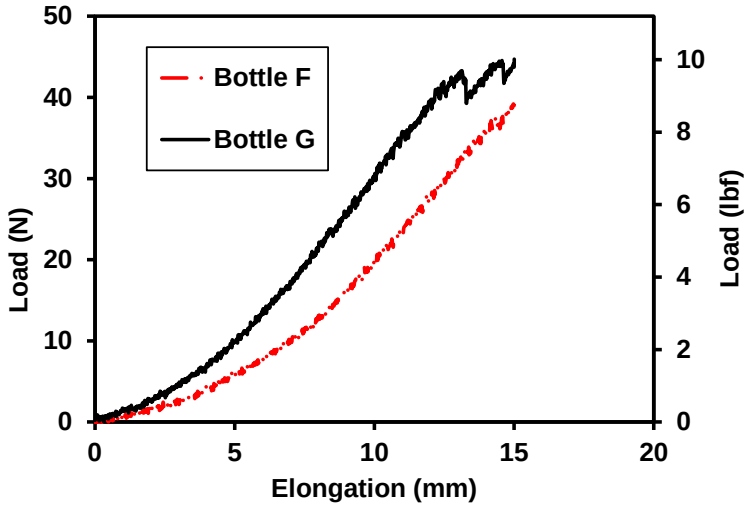

Figure 33: Hoop strength results using 2mm/min strain rate.

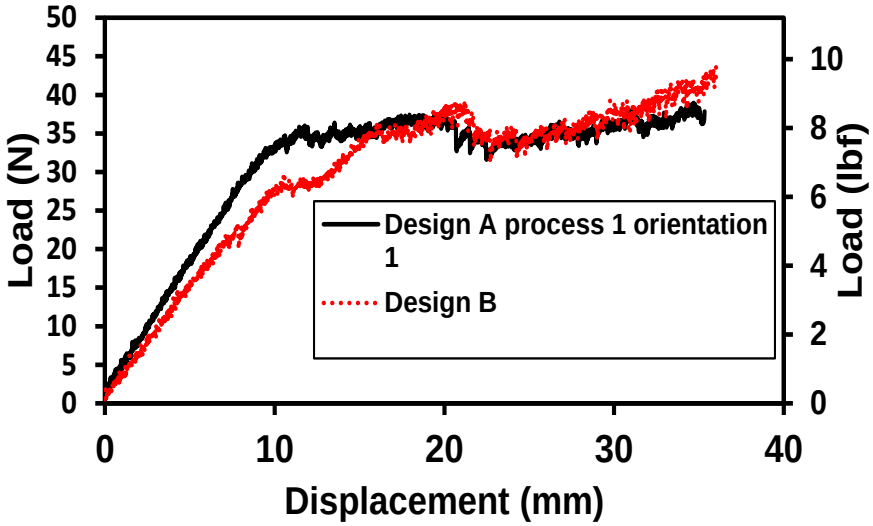

Figure 34: Hoop strength results using 10mm/min strain rate.

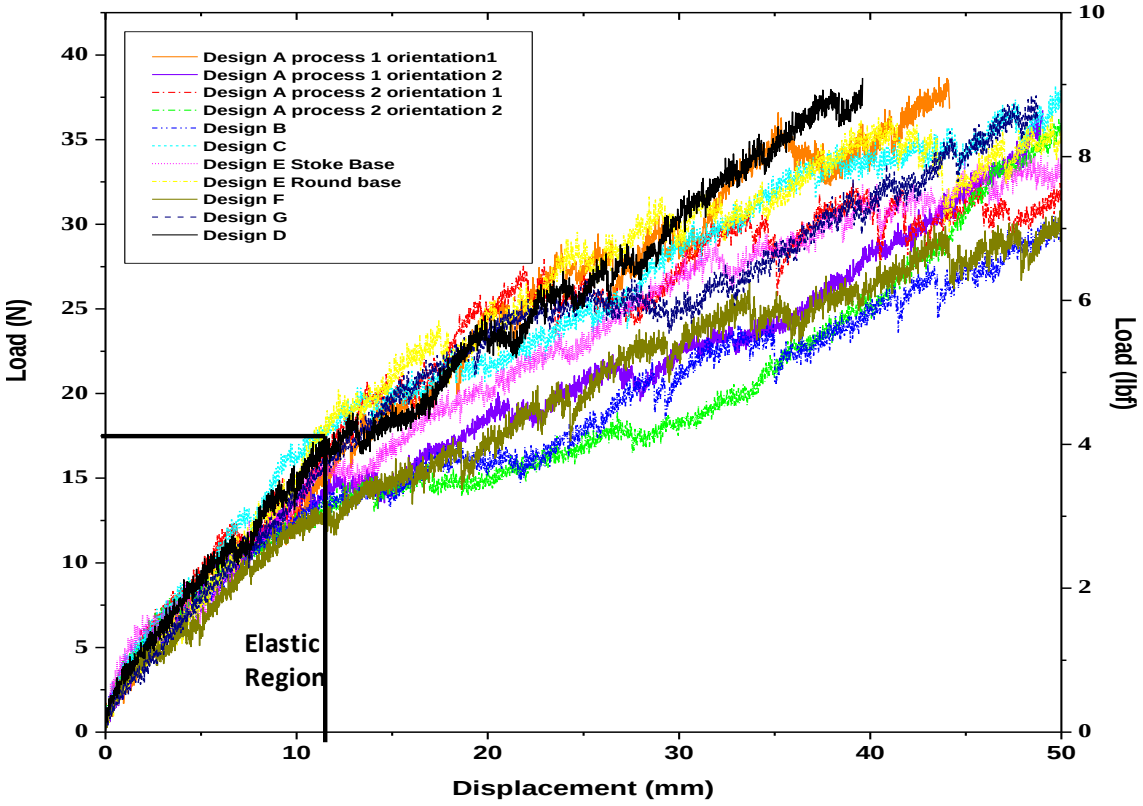

Figure 35: Hoop strength results of all the designs using modified fixture.

After plotting load displacement curves, the slopes are calculated for only elastic regions of each curve. Slope better is proportional to stiffness hence the designs are ranked according to their slope. The slopes are shown in Figure 36 and ranking is shown in table (5).

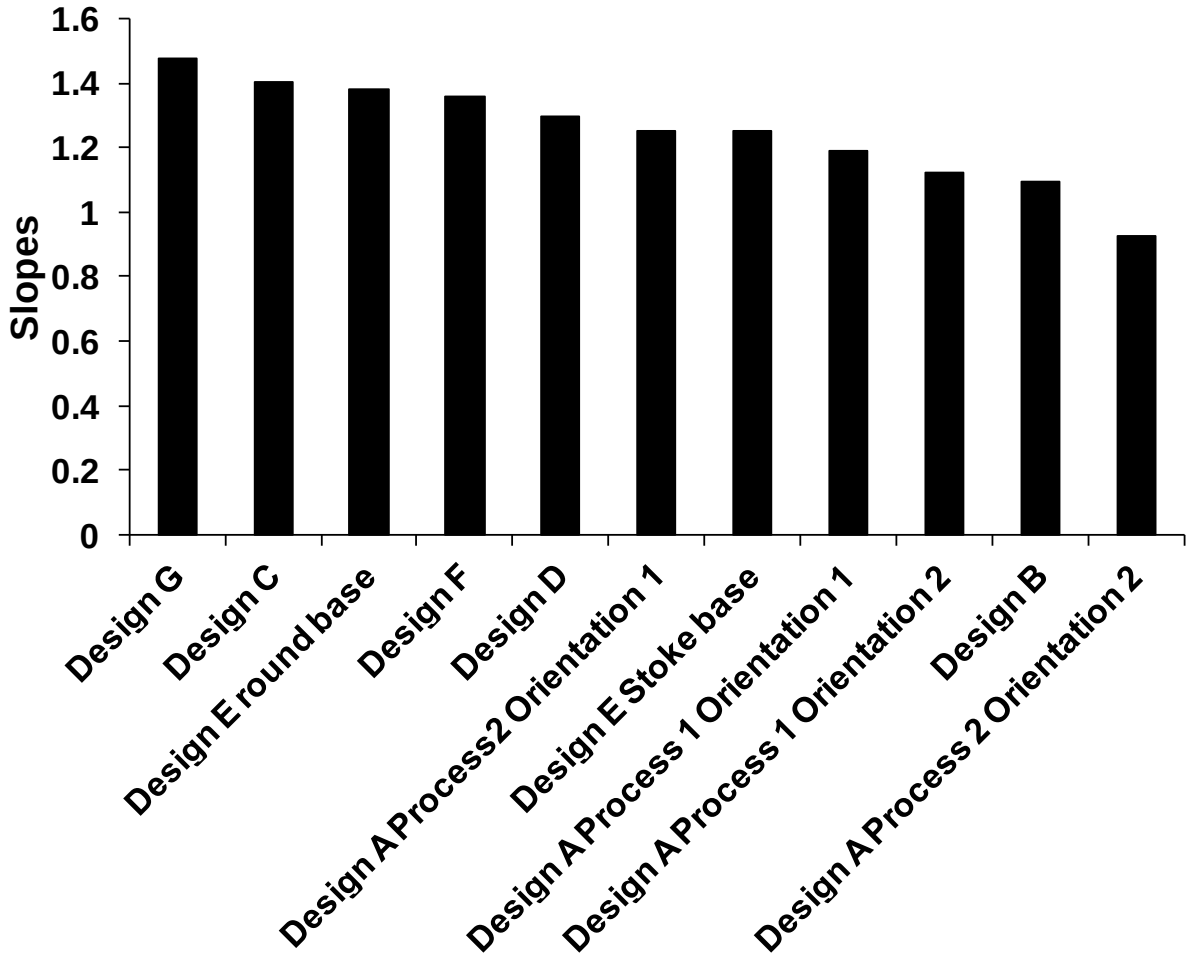

Figure 36: Slopes of the designs based on hoop strength.

Rank	Bottle	Slopes (N/mm)	Weights (gms)
1	Design G	1.4738	8.61
2	Design C	1.404	8.5
3	Design E Round base	1.378	8.54
4	Design F	1.3603	9.17
5	Design D	1.294	9.17
6	Design A Process2 Orientation 1	1.2534	8.5
7	Design E Stoke base	1.253	8.54
8	Design A Process 1 Orientation 1	1.189	8.5
9	Design A Process 1 Orientation 2	1.124	8.5
10	Design B	1.094	8.5
11	Design A Process 2 Orientation 2	0.9285	8.5

Table 5: Ranking and weights of the designs according to the hoops strength of the designs.

5.1.2 Cylindrical hoop results

Figure 37 shows the results of the hoop deformations. The hoop strength of the cylinders is compared in terms of hoop deformations. The results are compared with the results of hoop strength test of the bottles.

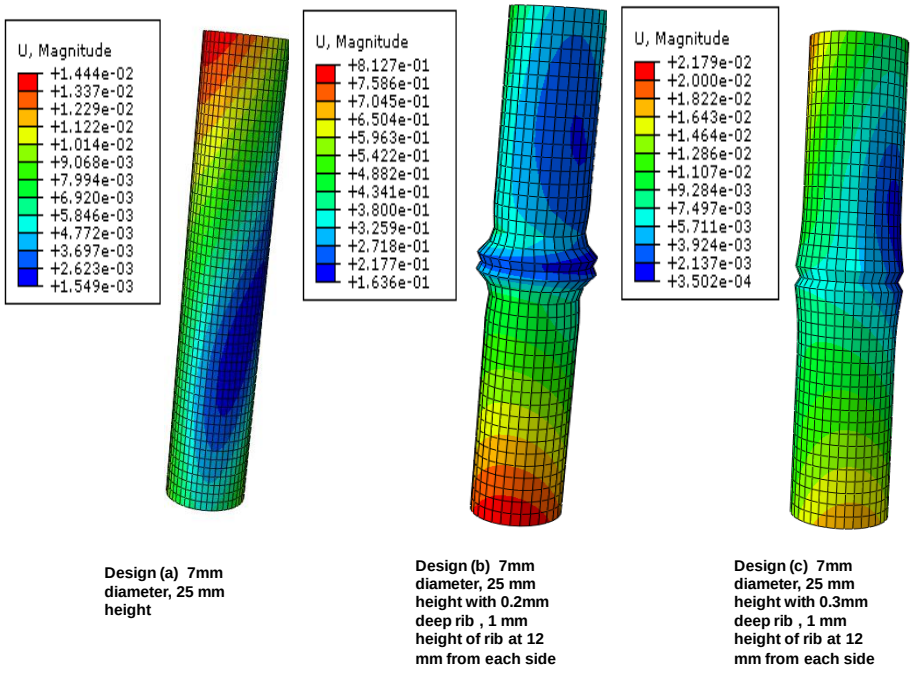

Figure 37: Simulation results of hoop deformations (mm) of three cylinders.

The hoop strength testing results are shown in the Table 5. We see a significant change in the stiffness of the designs, the Figure 33 shows the results with free compression with slow strain rate and Figure 34 shows the results of free compression with high strain rate, if we compare these results with the results on Figure 35 which was conducted using the modified strip that is applying force in concentrated locations, the ranking of the bottle designs does not change.

The main difference in designs is the change in shape of the ribs, design (G) had three columns, designs (A, C, E) had deep ribs and designs (F, D, B) had normal ribs, the design with deep ribs showed better performance compared to the design with less deep ribs; the design with no ribs showed best performance compared to other results.

Simulations were performed by applying pressure to the surfaces as shown in the Figure 37 to the normal cylinder, cylinder with normal ribs, cylinder with deeper ribs. The cylinder with no ribs showed better hoop performance followed by a cylinder with deeper ribs and with narrow ribs respectively.

From the results of simulations and the experiments, if the load is applied at concentrated locations, the hoop strength of the bottle depends on the shape of the ribs. The change in processing history also shows a difference in hoop strength, the orientation of the bottle also has an effect in the hoop strength as shown in Figure 35.

5.2 Stretch ratio measurements

The stretch ratios were measured for four designs using the technique described in section (3.2.3). Five samples were measured for each design and the thickness was measured at the

stretch marks, see section (3.2.4). The plots show the results of stretch ratio and the thickness at those markings. Table 6 shows the weight of the preform.

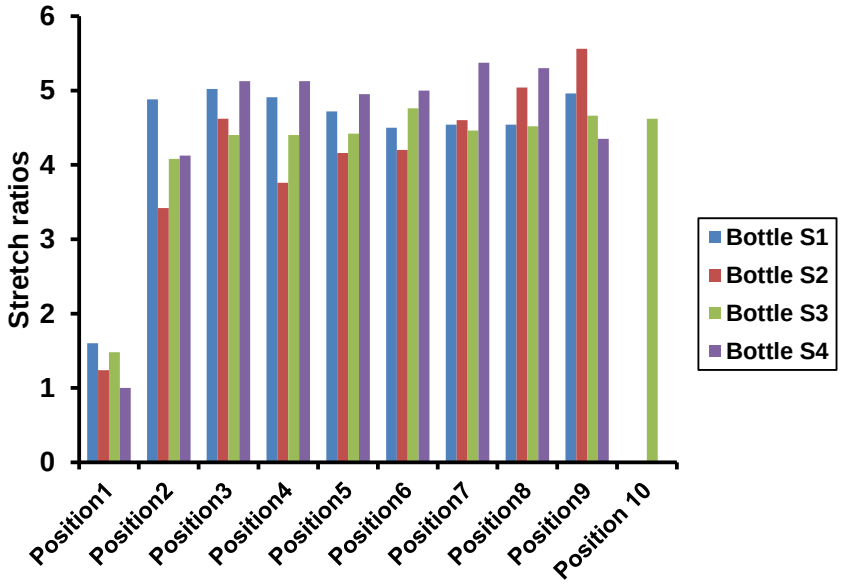

Figure 38: Stretch ratios at different positions of the bottle.

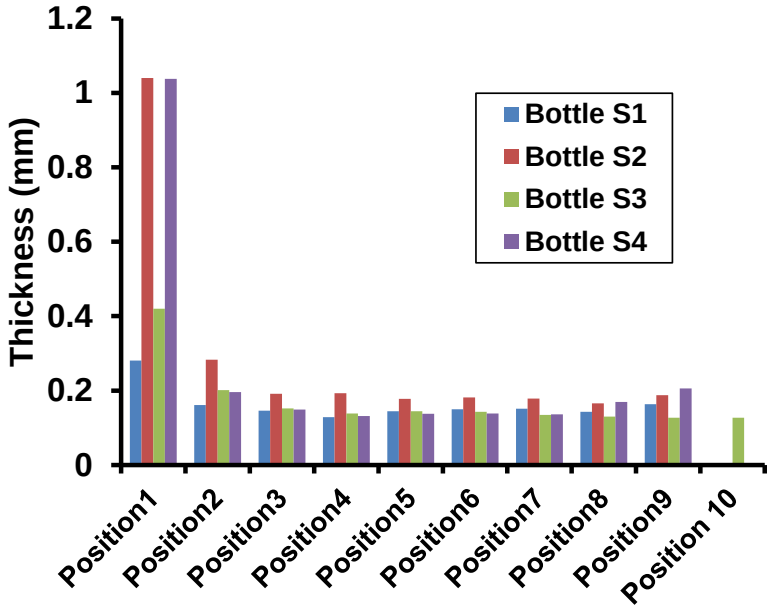

Figure 39: Thickness values at the stretch markings.

Bottle Design	Preform Weight (gms)
S1	9.89
S2	12.45
S3	9.71
S4	9.16

Table 6: Weights of the designs of stretch marked bottles.

Different designs have different stretch ratios. The design S1 (9.89gms) starts with low stretch ratio, increases till the position 3, decreases till position 6 and increases again till position 9. The design S2 (12.45gms) starts with low stretch ratio increases until position 3, decreases at position four and increases until position 9. Design S3 (9.71gms) starts with low stretch ratios and increases till position 3, maintains constant stretch ratios until position 5, increases at position 6, decrease at position 7, and increases till position10. Design S4 (9.16gms) starts with low stretch ratio and increases until position 3, decreases until position 5, increases until position7 and increases until position 9. The thickness changes exactly in the reverse trend of stretch ratios for all the designs. Overall the trend follows starting with low stretch ratios at the beginning and increasing till position 3 and after position 3 different designs follow different trend.

5.3 Wall thickness measurements

The wall thickness of the bottle changes along its length. Figure 40 shows the wall thickness measurements of 1 liter and 0.5 liter bottle.

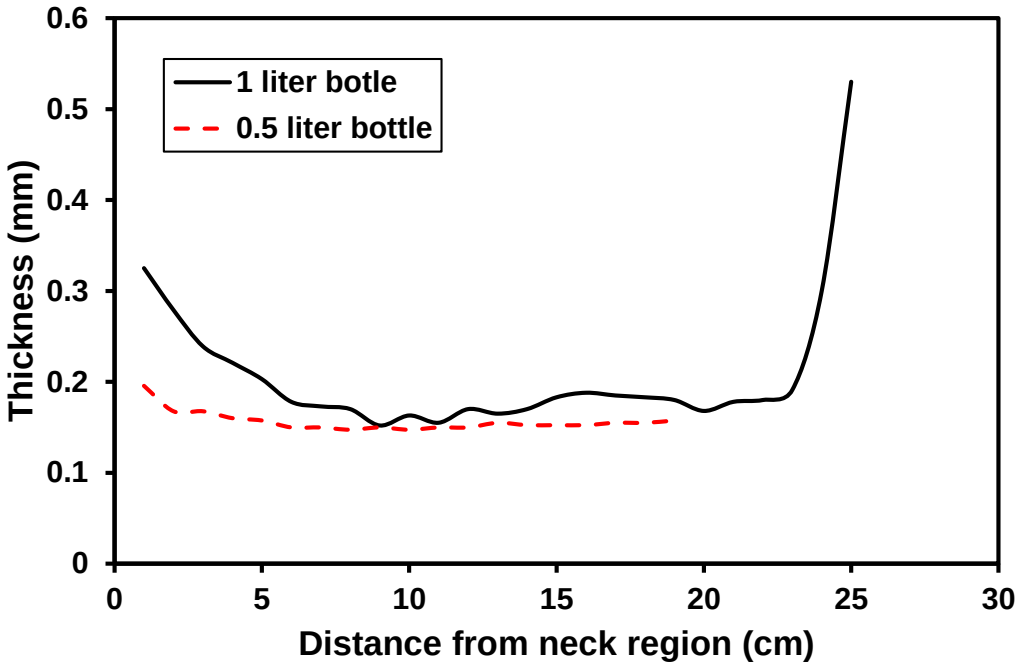

Figure 40: Wall thickness measurements of 1 liter and 0.5 liter bottles.

5.4 Top Load of 1 liter Model

5.4.1 Experimental results of top load

The results shown in Figure 41 show the experimental top load results, the experiments were performed at different strain rates, the bottle undergoes elastic deformation followed by failure and a plastic region with hardening, the main aim to perform in this experiment was to check the results until the initial failure and attempt validation of the simulation.

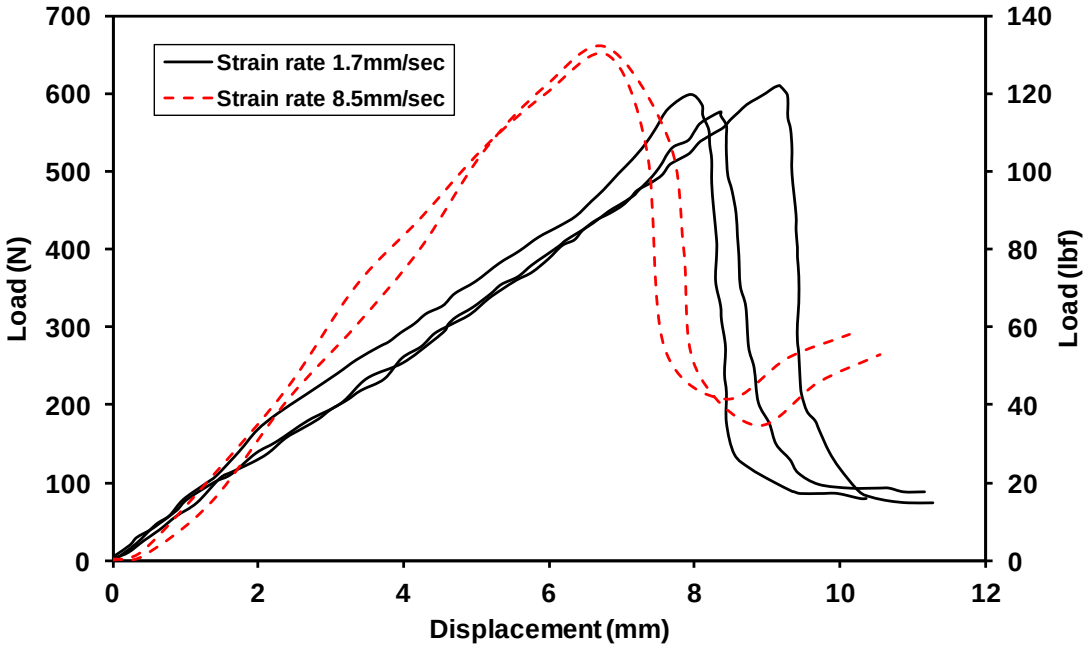

Figure 41: Experimental results of top loading on 1L bottle.

5.4.2 Top load simulation results

The simulation was carried out using the model, material data specified in the section (4.7.1). The top load was done for filled bottle. Figure 42 shows the stress distributions and the load displacement curve.

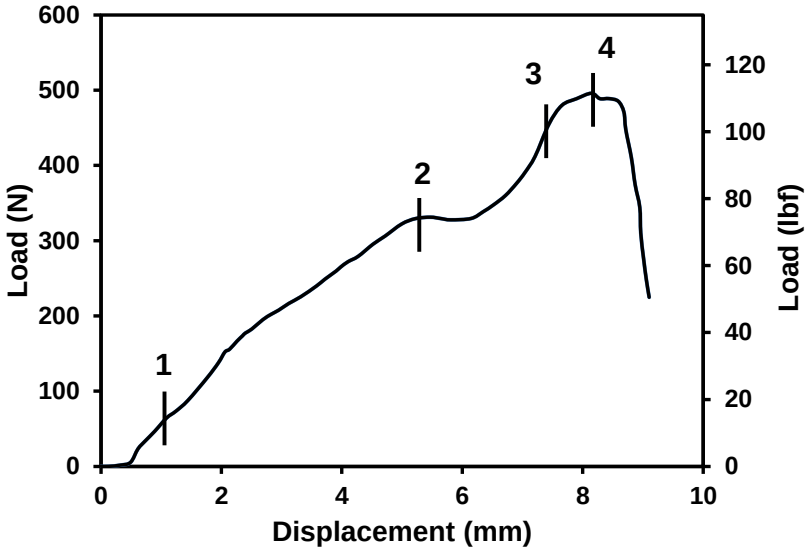

Load Displacement Curve

3. Stresses are focused in waist region

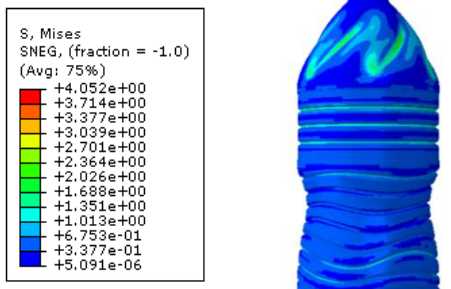

1. Initial step : Stresses focused near shoulder region

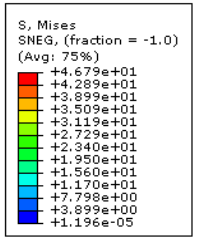

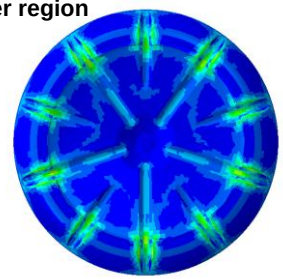

2. Base starts deforming

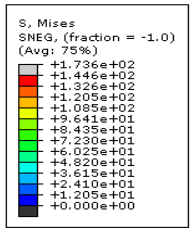

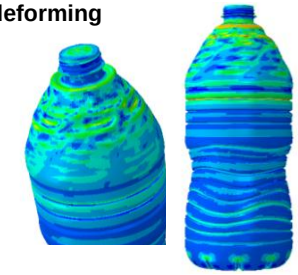

4. Final Buckling below the neck region of the bottle

Stress Distributions[MPa] at 1,2,3,4 locations in graph

Figure 42: Top load results of a full 1 liter bottle.

During top loading of a bottle, the stresses vary in the design during the simulation. As seen in Figure 42, in stage 1 the stresses are focused in the shoulder region, during this stage the stresses immediately shift to the ribs in the label panel; in stage 2 pressure in the bottle increases hence the base starts deforming; in stage 3 the stress concentration shifts to the center of the bottle, this region takes the maximum load before the actual deformation of the bottle. In the final stage, the stress concentration shifts back to the shoulder region, the bottle starts deforming near the neck region and the load starts to fall in this stage.

Overall performance of the bottle depends on strength of all the regions of the bottle as stresses shift over the bottle but, the actual deformation of the bottle starts below the neck region.

5.5 Bending Results of 1 liter model (Bending vs. Wall thickness)

The simulations were performed using the model and procedure stated in section (4.7.2). The wall thickness was changed three times. In the 1st case, the model with the original wall thickness was leaned to 3 degrees. In the second case the wall thickness of entire model was increased by 0.1mm. In third case the wall thickness of the entire model was increased by 0.3 mm. In case 4 the wall thickness of entire model was reduced by 0.05mm. The results show a significant change in performance.

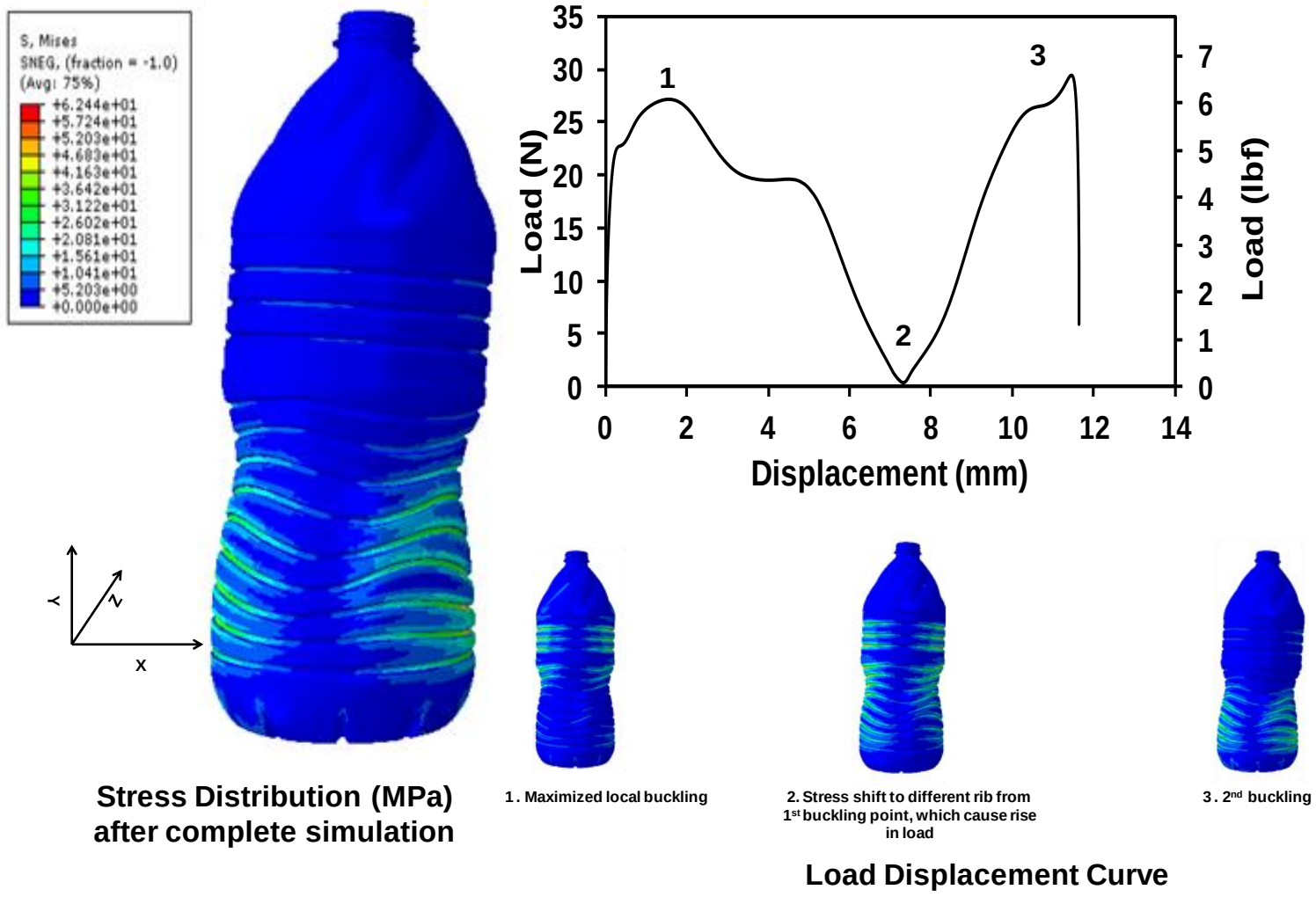

Figure 43: Results of 1 liter original model uponbending.

In this process the stress concentration varies during Bending. Figure 43 shows the results of the original model upon bending.

- In stage 1 the stresses are focused in ribs near label panel.
- Middle region starts buckling and from stage1 to stage 2 the load starts falling.
- In stage 2 the buckling ends and the stress shifts its focus in different region hence the load starts raising until stage 3.
- In stage 3 buckling causes in fall in load.
- After bending, the stresses are distributed in the waist and bottom region of the bottle.

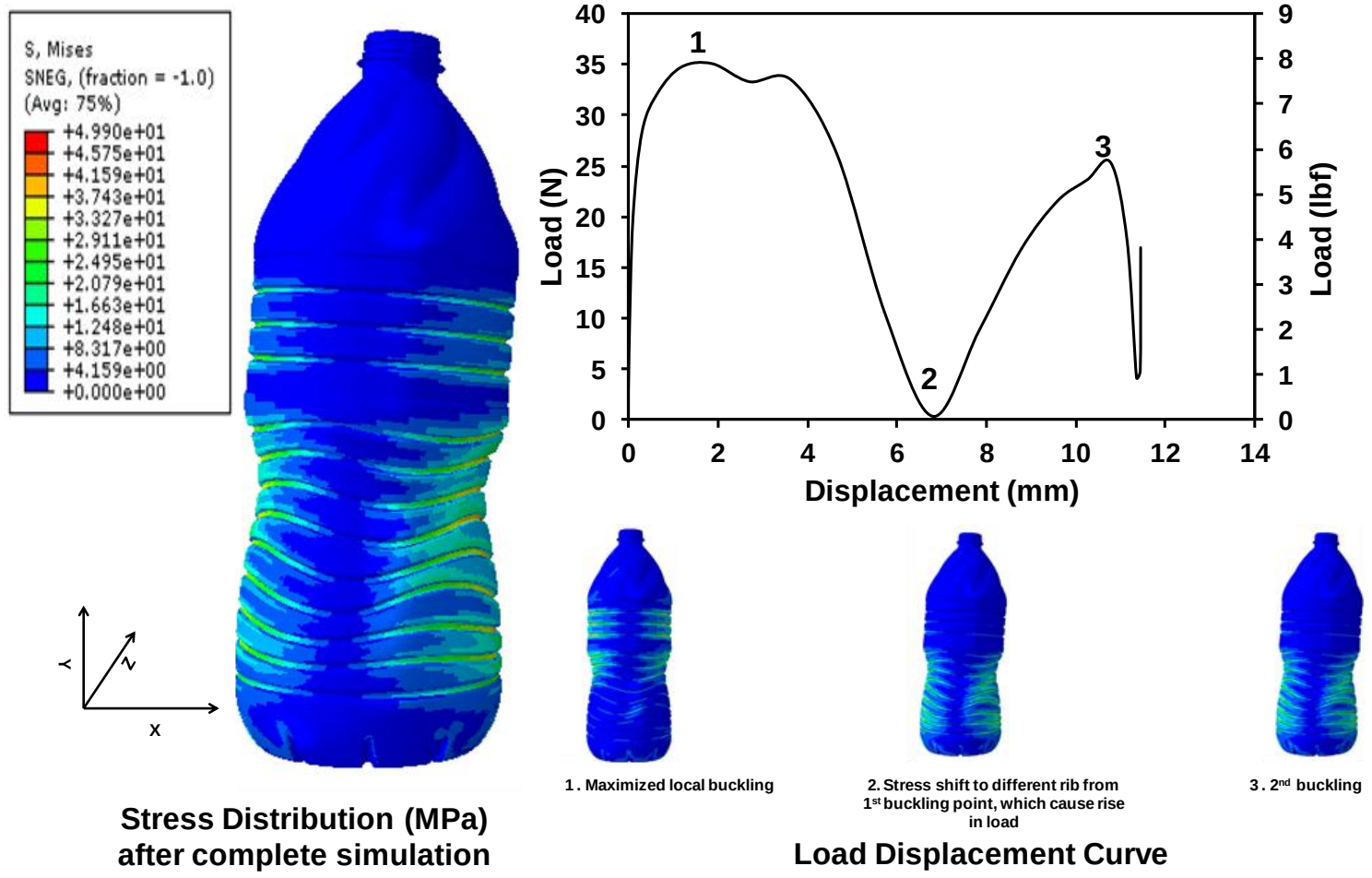

Figure 44: Results 1 liter model with 0.1 mm increase in thickness upon bending.

For model 2 (a 0.1 mm increase in thickness) due to the increase in wall thickness, the critical load before buckling increased compared to model 1, as seen in Figure 44.

- In stage 1 the stress concentration areas were focused at the ribs near label panel and the waist region started buckling; there is a slight rise in the curve due to shifting of stresses in different regions.
- The buckling continues until stage 2, and the load started falling; in stage 2 the buckling ended and the stresses started shifting focus in different regions; hence the load started rising again until stage 3.
- In stage 3, buckling caused the load to fall but, here the peak load before the 1^{st} buckling was less than the peak load before the second buckling.
- After buckling in stage 3 there was again a rise in load due to a shift in stresses to different regions.
- At the end of bending, the stresses were distributed on the ribs near label panel, the middle region, and the bottom of the bottle.

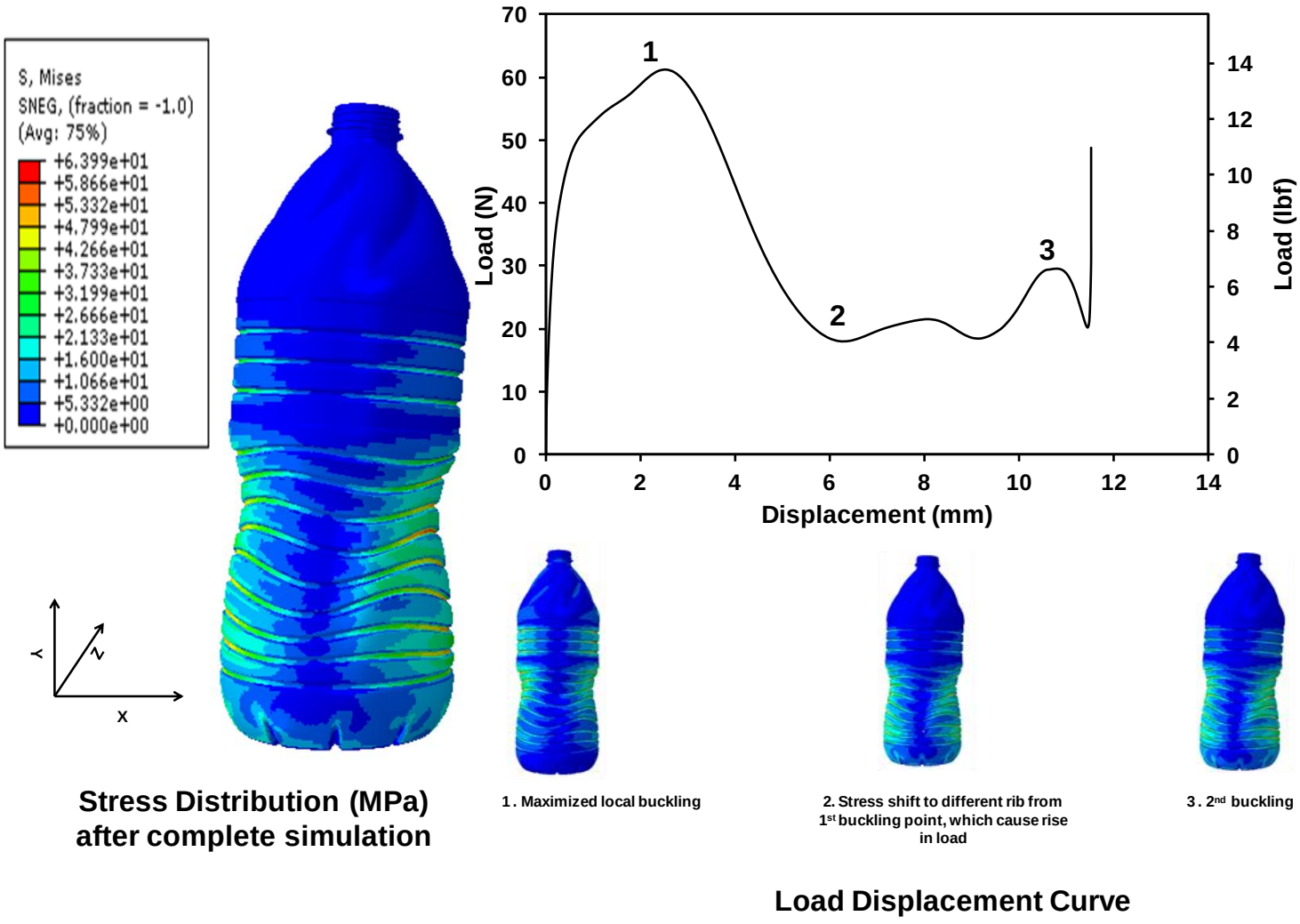

Figure 45: Results 1 liter model with 0.3 mm increase in thickness upon bending.

In model 3 (0.3 mm increase in thickness), due to the increase in wall thickness the critical load before buckling was increased again compared to models 1 and 2, as seen in Figure 45.

- In stage 1 the stresses were focused at the ribs near label panel but, at the same time they were distributed in the rest of the regions of the bottle.
- The waist region started buckling and the load fell until stage 2, but the load did not go to zero as the stress concentration regions shifted before the load reached zero.
- In stage 2, the buckling ended and the stresses started shifting focus to different regions; hence the load started rising until stage 3 as was seen earlier.
- Buckling occurred and there was an immediate shift of stress concentration regions so the load started rising.
- At the end of bending, the stresses were distributed in the ribs near the label panel, the waist region, and the bottom of the bottle.

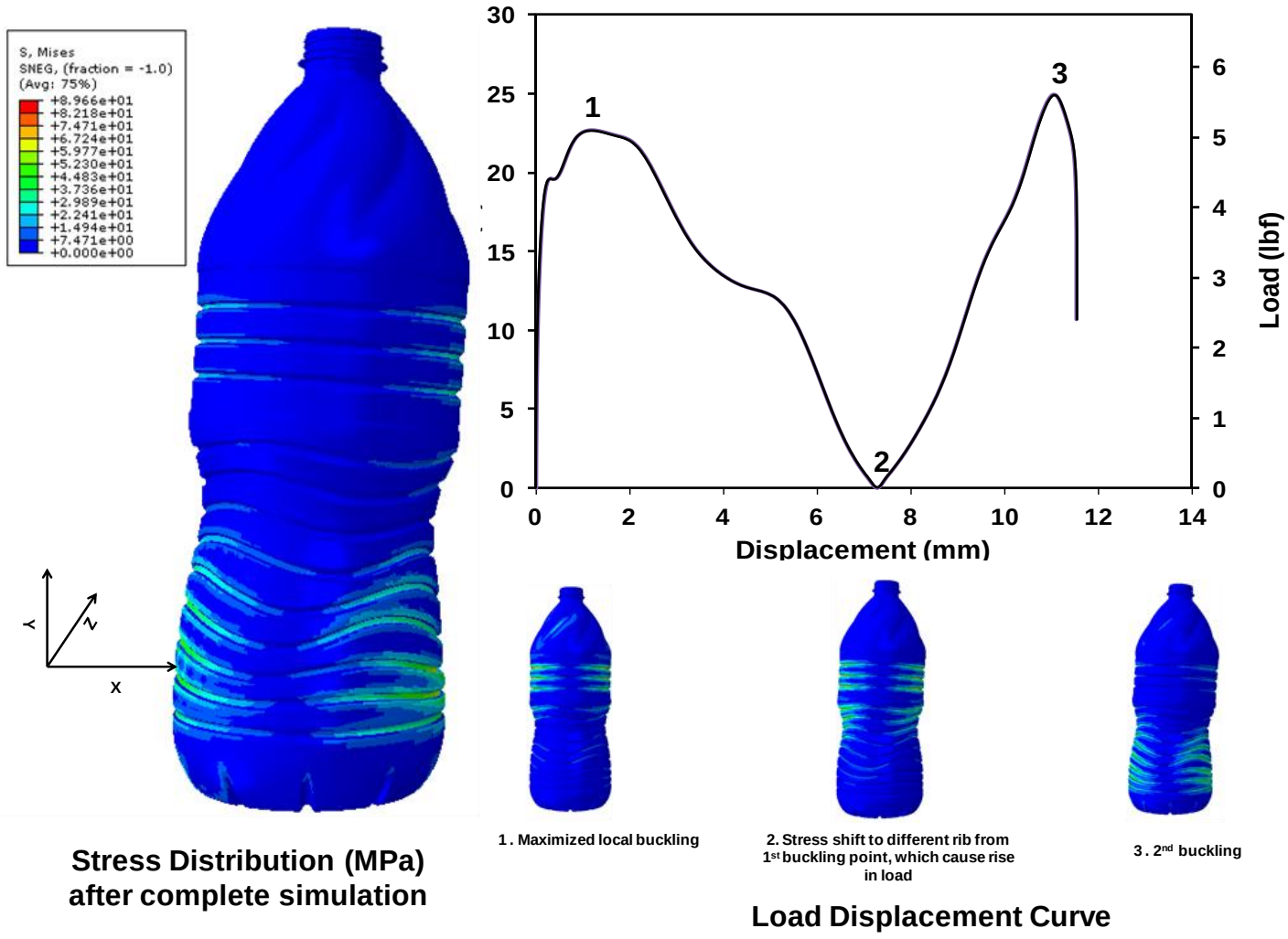

Figure 46: Results 1 liter model with 0.05 mm decrease in thickness upon bending.

In model 4 (0.05 reduction in thickness), due to the decrease in wall thickness, the critical load before buckling was less compared to model 1, 2 and 3 as seen in Figure 46.

- In stage 1, the stresses were focused at the ribs near label panel, buckling occurred.
- From stage 1 to stage 2, the load started falling.
- In stage 2, the buckling ended and the stresses started shifting in different regions; hence the load started rising until stage 3.
- In stage 3, buckling caused a fall in load.
- At the End of Bending, the stresses were distributed in the waist and bottom region of the bottle.

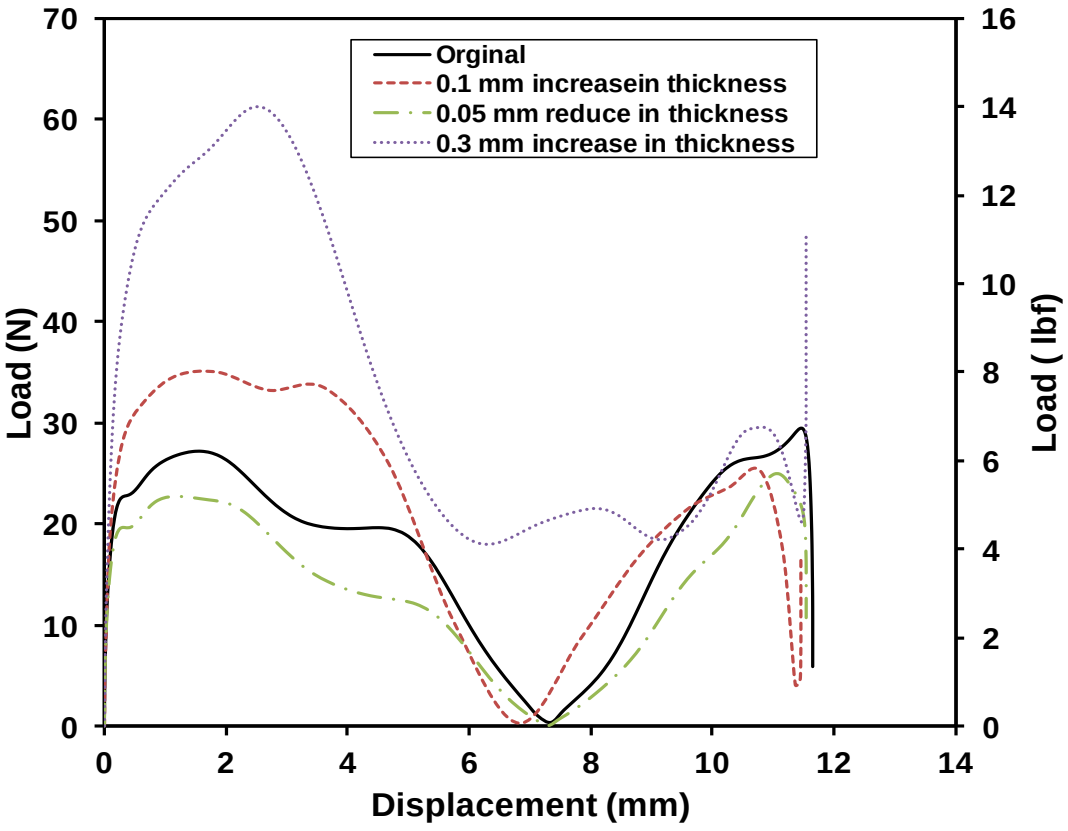

Figure 47: Comparison of load displacement curves of 1 liter models on bending.

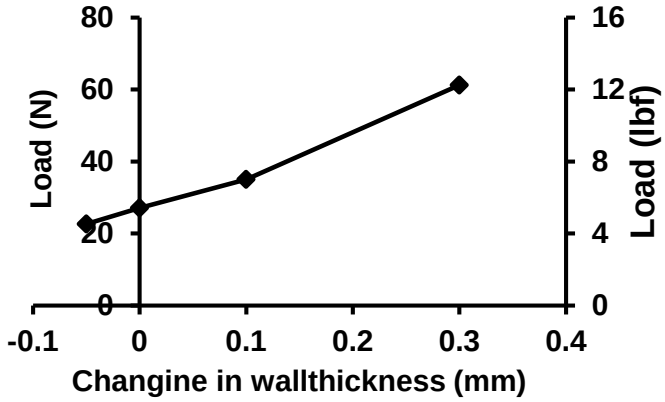

Figure 48: Effect of Change in wall thickness

The final stress distribution in the bottle did not show any trend with change in wall thickness since it depends on how and where the bottle is deforming on all the intermediate stages during

the Bending process. However, in model 1 and model 4 the stresses at the end were more concentrated in one particular region, whereas in model 2 and model 3 the stresses were distributed all over the bottle. If the wall thickness is very less the stresses shift from one region to the other more easily, and at the end, the stress concentration is far away from the region where the load is applied. In contrast, when wall thickness is more, the stresses will not shift from one region to other initially, but at the end, the stresses are distributed all over the bottle. Figure 47 shows the load displacement curves of all the 1 liter models on bending.

The load until the 1st critical buckling increases with an increase in thickness, as seen in Figure 48. The slope of line 1 was 19.36, line 2 was 18.13, and line 3 was 29.45. The slope is not uniform. It gradually decreases with increasing wall thickness.

5.6 Bending vs. change in Design

3D scanning was performed on the bottles as discussed in section (4.7.4) and imported to FEA to study the performance of designs on bending the results show how four different designs undergo deformation during bending.

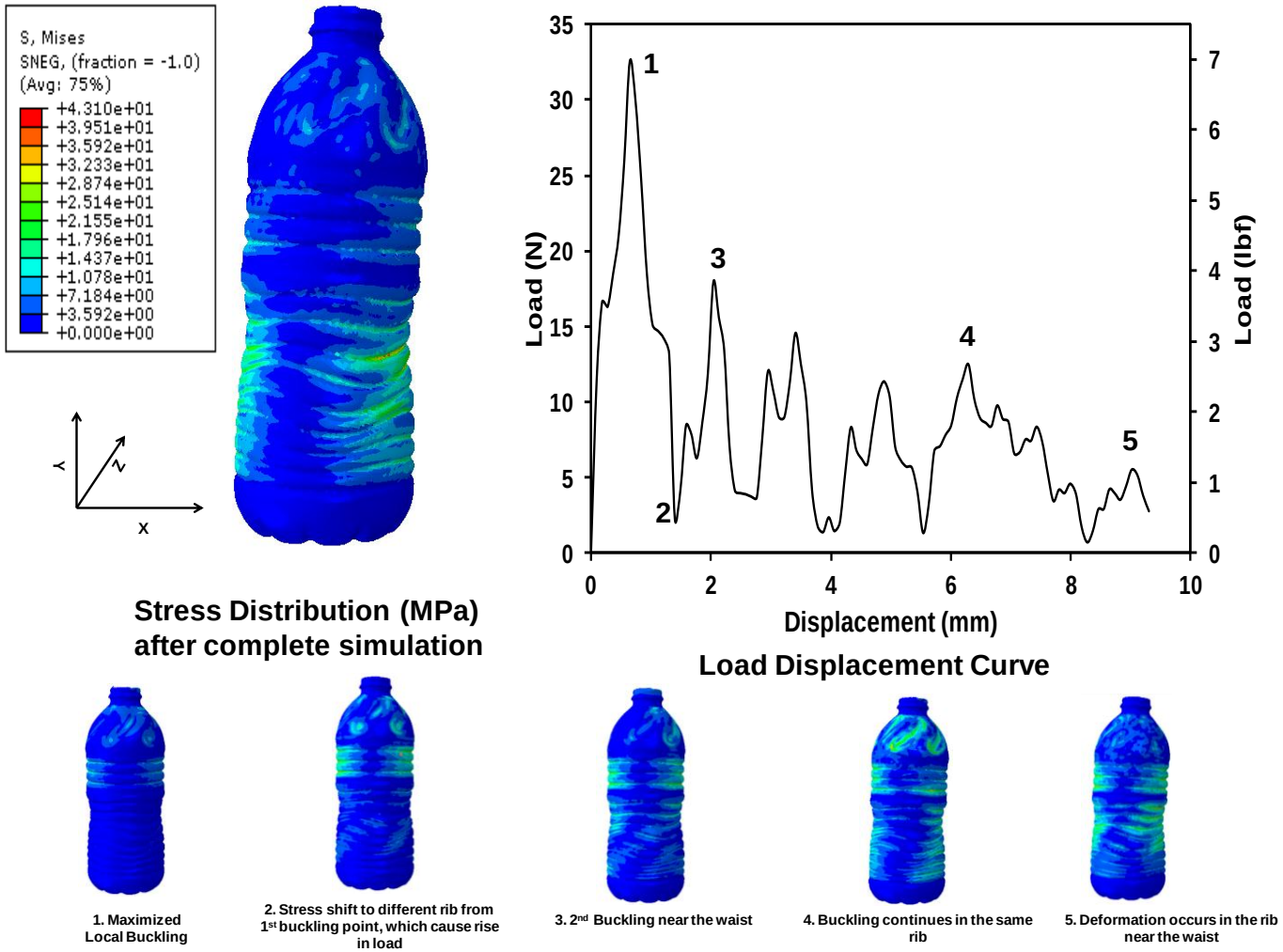

Figure 49: Results of design L1 upon bending.

Results of the design L1 as shown in Figure 49 infers following.

- In stage 1, the stress started acting in the shoulder region, shifted its focus to the ribs in the label panel after some delay; then buckling initiated in one of the ribs.
- In stage 2 buckling ends, the stresses shift focus to a different region and then the load rose till stage 3.
- In stage 3, buckling initiated and load falls; this process follows.
- In the stage 4, the load was constant with increase in displacement.
- In stage 5, the end the buckling initiated and concentrated near the waist region of the bottle.

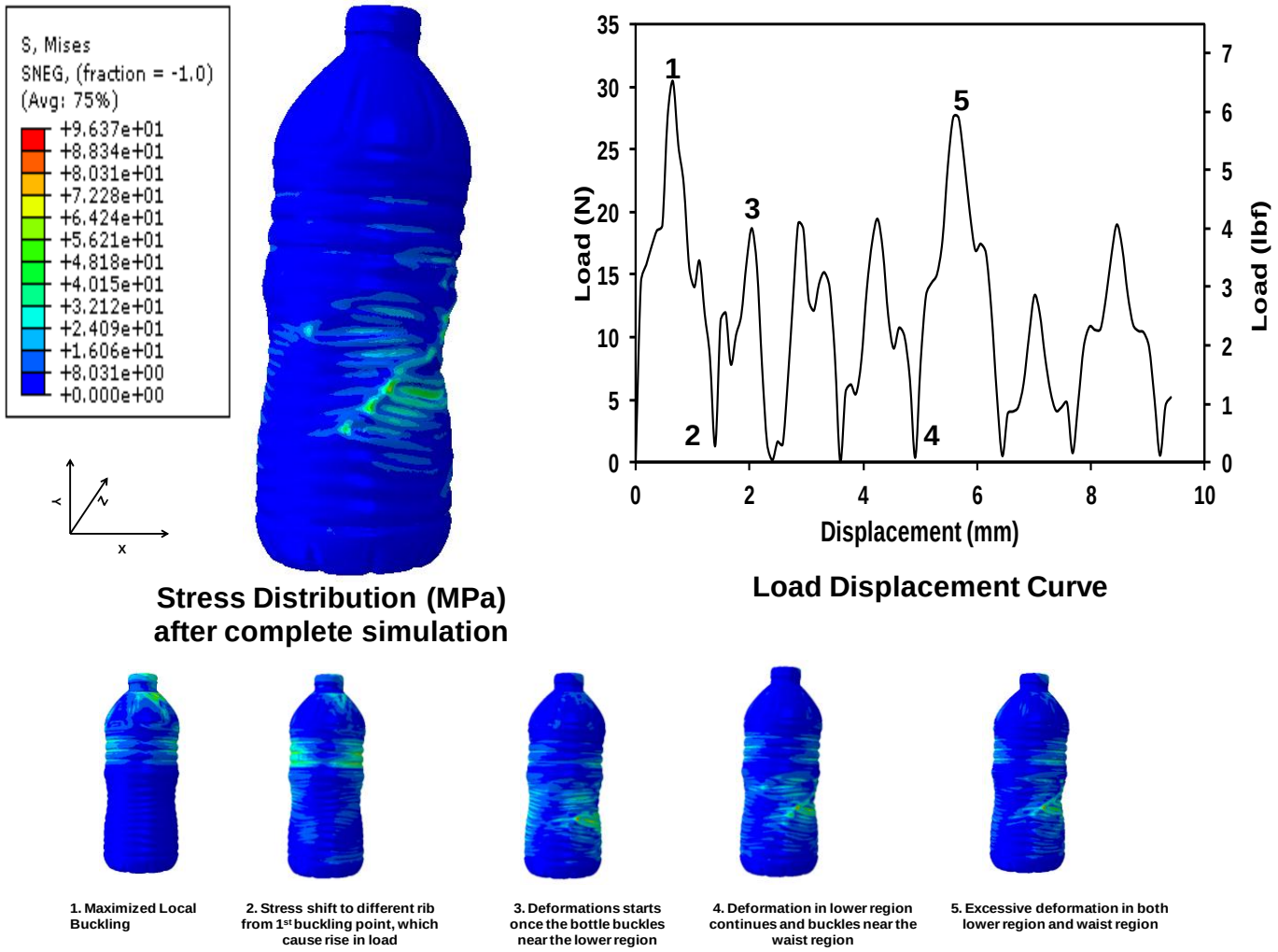

Stress Distribution (MPa) after complete simulation

Load Displacement Curve

1. Maximized Local Buckling

2. Stress shift to different rib from 1st buckling point, which cause rise in load

3. Deformations starts once the bottle buckles near the lower region

4. Deformation in lower region continues and buckles near the waist region

5. Excessive deformation in both lower region and waist region

Figure 50: Results of design L2 upon bending.

Results of design L2 are as shown in Figure 50 and infers following

- In stage 1, the stresses started at the neck region and immediately transfer to the ribs in the label panel and buckling initiated.
- In stage 2, the buckling ended, in this region, stresses shifted to different regions and the load increased.
- In stage 3, the buckling initiated and the bottom portion started deforming. The stresses started shifting focus. Buckling initiated in different regions, and there was a significant deformation near the bottom region.
- In stage 4, the buckling ended and the load was raised.
- In stage 5, the buckling occurred in the same location as the deformation increased. On further bending and at the end, the bottle deformation was focused on the bottom region of bottle.

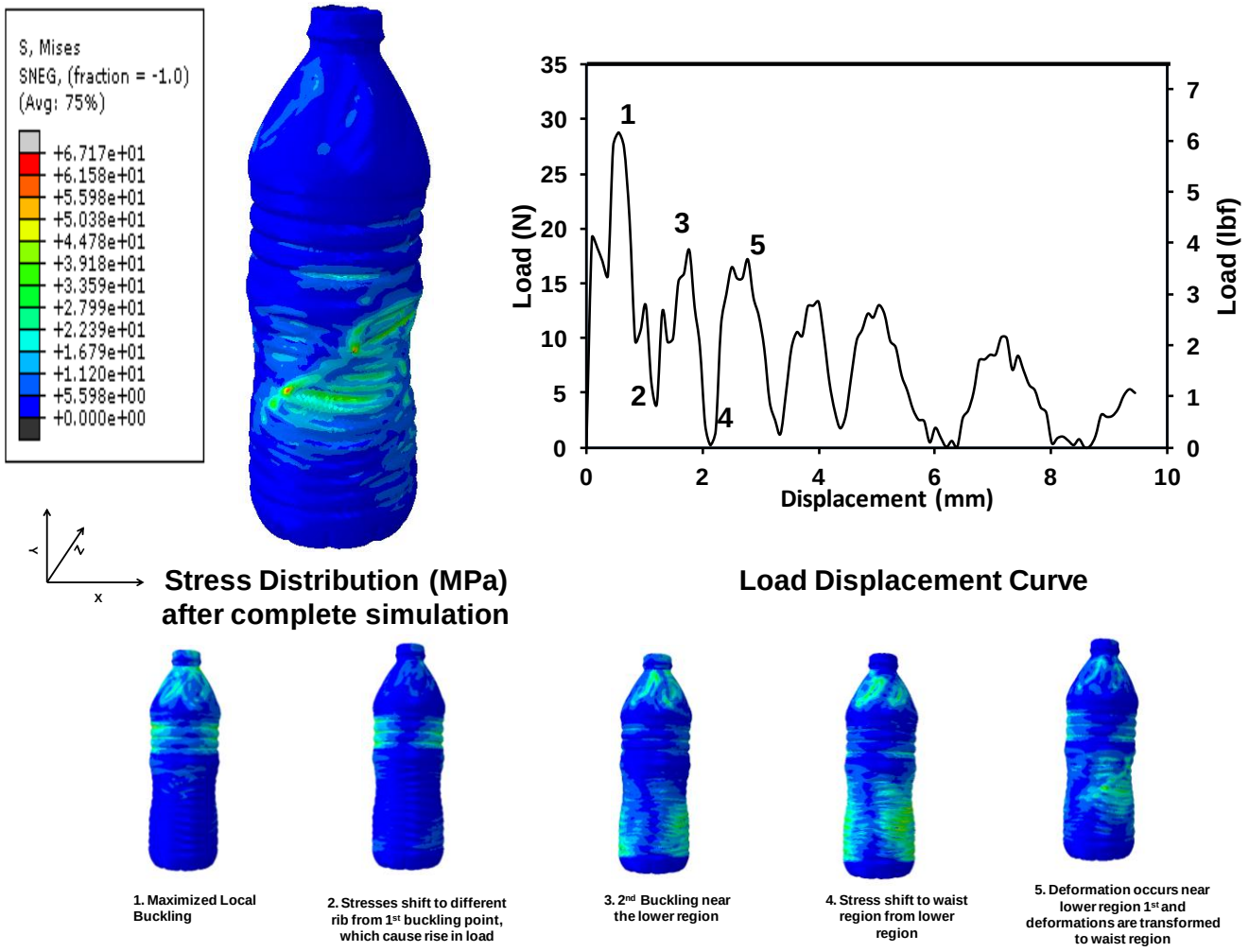

Figure 51: Results of design L3 upon bending.

Results of the design L3 as shown in Figure 51 suggest:

- In stage 1, the stress started acting in the shoulder region and shifted focus to the ribs in the label panel without delay; buckling was initiated in one of the ribs.
- In stage 2, buckling ends, the stresses shifted focus in different regions (both in above and below the initial deformation region) and then the load increased until stage 3.
- In stage 3, buckling initiated and the load fell. This process continued and buckling occurred in the bottom region of bottle.
- In the stage 4, the load was increases as buckling shifted from the lower to the middle region. During this process there was a shift in the stresses.
- In stage 5, the end of buckling initiated and concentrated near the bottom region and the waist region.
- At the end, buckling was focused in both the waist and lower regions.

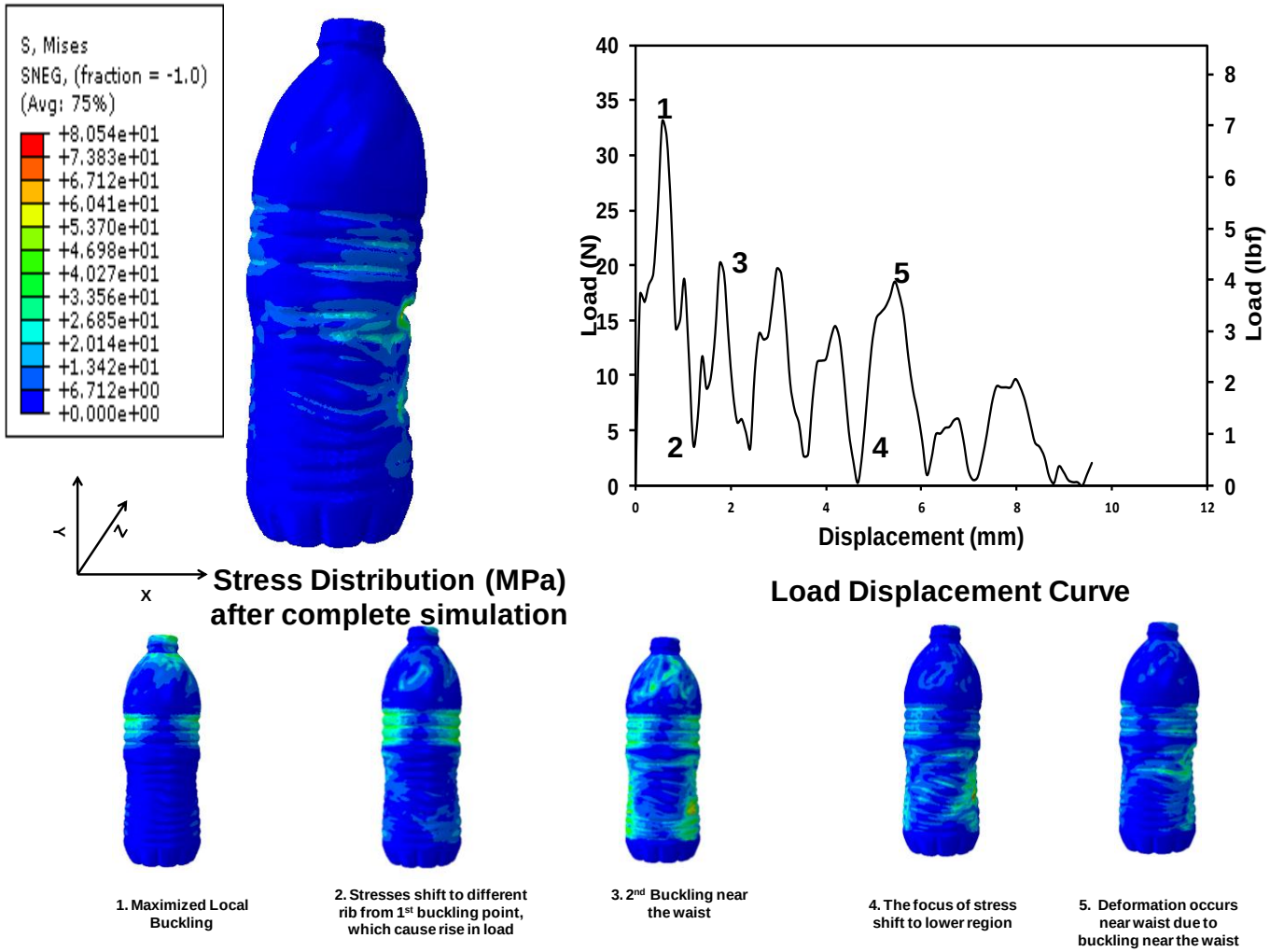

Figure 52: Results of design L4 upon bending.

Figure 52 shows the results of the design L4 and the following was observed from the results:

- The stresses started acting in stage 1 and transferred to the ribs near the label panel region without delay. Buckling started in one of the ribs and then the load started falling.
- In stage 2, the stress started shifting focus to different regions, load increased until stage 3.
- In stage 3, the middle region started buckling, load fell until stage 4.
- In stage 4, load started increasing.
- In stage 5, buckling completed at the end. The significant deformation was near the waist region of the bottle, and slight deformation was observed at the lower region of bottle.

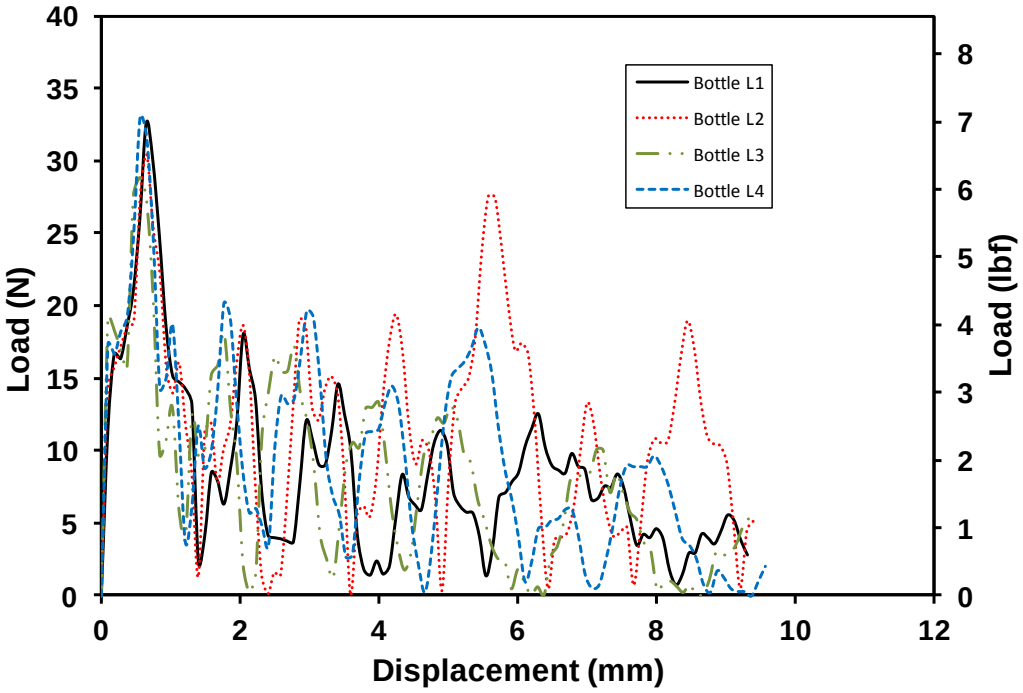

Figure 53: Comparison of load displacement curves of all 0.5 liter models on bending.

Overall, the load deflection curve fluctuates due to constant shifts in stress concentration regions, the 1st critical buckling was more for design L4 followed by L3, L1, and L2 respectively. Figure

53 shows the comparison of load displacement curves for all the designs. The ultimate region of deformation due to bending depends on the shape, angle of the shoulder region, and ribs near label panel.

CHAPTER VI

6. DISCUSSION

Assessing the structural performance of PET bottles and correlating with the process parameters is one of the interests in the beverage packaging industry. Polyethylene Terephthalate is semi crystalline and has the ability to undergo strain induced crystallization. During ISBM, the process used in making bottles, the preform undergoes stretching and blowing simultaneously. Overall, the bottle has non-uniform thickness and material properties along its length. A change in design leads to a change in distribution of properties and hence the structural performance of the bottle.

Top load, bending, and hoop strength tests were performed to check the structural performance of bottles. Top load testing was performed on filled 1 liter bottles to assess the structural design and validate the Finite Element Model with experimental results. Bending analysis was performed on the validated 1 liter model to check the stress along the bottle and the load variation while bending. The wall thickness of the bottle was changed four times to see the response in stress and load displacement curves for the 1 liter model. The same method of bending was implemented for 0.5 liter designs. As a part of this, 3D scanning technology was being to make CAD models from finished parts and import them to FEM, four different designs were imported form CAD, and bending was performed maintaining a constant wall thickness for all the designs. Hoop strength tests were performed on nine different designs to check the

stiffest design. Apart from the structural performance tests, stretch ratios for four different designs and thickness at the stretch markings were being measured as an attempt to correlate stretch ratios, thickness, and structural performance.

6.1 Validation of Top load:

The experiments were performed at different strain rates. With an increase in strain rate there is an increase in apparent stiffness. Some differences between experimental results can be due to a change in wall thickness distribution from bottle to bottle.

When comparing the results of the experiment and simulations, during the initial stage (until load reaches 300 N) the simulation results were in correlation with the experimental results. After 350 N, the base started deforming and bulging occurred, there was a slight deviation here. The peak load before failure in the finite element model was less than the actual case. This might be due to several factors. The simulation was stopped at 9.5 mm, but at that displacement the simulation load was higher than that of the experiment. That is, after buckling the load was dropping slowly. In addition, how accurate the material thicknesses were measured on the bottle, it will contribute some error. This might also be a reason for discrepancies between simulation and experimental results.

Though the model was unable to predict certain phenomena, it predicted the deformation regions and the pattern of the load displacement curve. In addition, if we compare this model to a previous model [Ing and Chittepu], the difference between the simulation and experiment similar. Figure 55 shows the difference between the present work and previous models developed.

The results shown in Figure 54 show the comparison of experimental and simulation results, the results show that the finite element model correlates well with the experimental results.

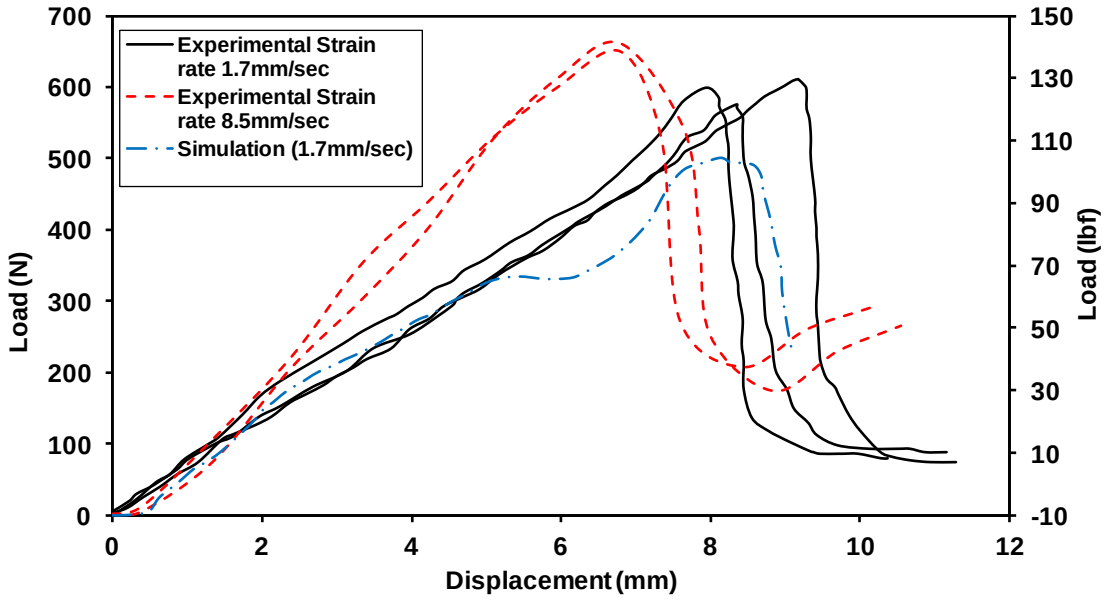

Figure 54: Validation of experimental and simulation of top load.

6.2 Relating Results of top load, bending, hoop strength to Design

From the simulation and experimental results performed in this study, design shows a significant effect in performance of the bottle. The change in design features included the angle between the neck and shoulder, bell curves on shoulder, ribs in the label panel, waist region (symmetric or asymmetric) and change in lower shape. Wall thickness was also a key factor in design, and determined the performance. Increasing the wall thickness leads to an increase in weight of the bottle. Bending and hoop strength have an effect in design, and have been studied in this research.

Bending depends on thickness of the bottle but only until the 1st critical buckling point. The 1st critical buckling load increases with an increase in thickness, but after the 1st critical buckling ends, it depended on where the stress concentration was shifting as the load again increased. Depending on that, for instance, the 2nd peak load of model 4 was less than its 1st peak load. The non-uniform trend of bending vs. thickness can also be due to a change in the material properties and wall thickness along the length of the bottle.

With a change in design, the main difference in bending performance is the change in deformation regions of the bottle. This difference is due to the change in stress distribution during the bending process. If the angle between the neck and shoulder is more, the stresses shift slowly to the next region such as the ribs in the label panel. The deep ribs in the label panel causes stresses to focus for a long period during bending and the final deformation occurs near the waist region. The bell curves in design L1, L3, L4 are of a similar kind and in these designs, after the second stage, the stresses were also distributed in the bell curves of the shoulder region apart from the lower region. Whereas, in design L2, the bell curves were of a different shape. Once the stresses reach the label panel in the second stage, the stresses only transfer to the lower region. They did not shift back to the shoulder region. Overall, the final deformation will occur in the waist the intersection of the waist, and the lower region of the bottle. If the design has deep ribs near the label panel or more neck-shoulder or more shoulder area, the combination of the three may shift the region of deformation at higher locations in the bottle. If the design has less deep ribs, less neck shoulder-region, less shoulder area, then the deformation occurs in the bottom region of the bottle. The bottles are stored in pallets so, if the deformation occurs in the bottom region any additional load would damage the bottle in the lower row and there is a chance of collapse for other bottles since the angle of inclination is more. If the deformation is

in the waist region, the angle of inclination is less and there is less movement to the bottles in the higher rows of the pallet. So the main aim in designing the bottles to withstand bending is the deformation during bending must be as high axially as possible along the bottle.

In hoop strength testing, the deep rib designs show better performance compared to other designs, the design with 3 large columns showed the best results. The symmetric and asymmetric shapes in the waist and lower region were also considered in the performance because the asymmetric design leads to two different orientations of the bottle. The results vary in two different orientations.

6.3 Reliability of FEM results

The finite element analysis results of plastics are often wrong when compared to FEA results of normal metals, since there is a lag in incorporating polymer properties to the codes. Additionally, the strains of normal elastic metals would usually be less than 3-4%. In contrast, polymers have large strains. However, numerous codes and elastic-plastic, viscoelastic material models have been developed in the past three decades, as discussed in chapter 2. The user has to use the respective material model, even if they are dealing with plastics in the elastic region, to avoid errors due to large deformations. Deformations are the primary output of any finite element code from which strain is calculated. Stresses are then calculated depending on contact formulations and the material model. The simulation results on plastic parts are generally evaluated based on deformations, strains, and load-displacement curves; rather than stresses and stress-strain curves to avoid miscalculations due to errors in material models. Overall, thorough

knowledge of material models is necessary before the finite element model is built. This avoids possible errors in the analysis of plastic parts.

In the case of bottles made of PET or any other material, the process dependent parameters also come into account. As discussed in previous sections, the performance of the bottle depends on process parameters. The reliability of the FEM also depends on how the process dependent parameters are considered in the finite element model to analyze the model. Chittepu, *et al.*, performed top load simulations of a PET bottle in LS DYNA software using the piece wise linear plasticity model as a material model. Figure 11 shows the correlation between simulation and experiments. There is an excellent correlation in the elastic region and the correlation decreases after first buckling, since the material behavior of PET is complex after buckling and the material model could not predict post buckling behavior. Overall the results have a good correlation between simulation and experiments. The extreme correlation can also be due to good performance of the software and the geometry of the bottle is simple. Ing, *et al.*, performed simulation on PET bottles. The advantage of considering process dependent parameters was explained. The simulations were performed in ABAQUS software. The initial simulation was performed by considering a uniform modulus and five different thicknesses along the bottle. In a second case an integrative approach was used. The bottles were made with defined stretch ratios and tensile testing was performed in different locations and the correlation between stretch ratio and stretch ratio dependent material properties were plotted, as shown in Figure 57. Polynomial curves were fitted along the points. Hence, the stretch ratio dependent indirectly process dependent material properties were considered for the simulation. Figure 12 shows the comparison of measured and two simulated results. The integrative approach correlated better compared to the conventional model. The geometry here was a simple geometry. Integrative

approaches have a good correlation with measurements. However, including the complex material models for plastic and viscoelastic behavior of PET along with the process dependent properties would give better results. In this research, the material data including elastic, plastic, and creep properties along with varying wall thickness data obtained from virtual prototyping was included. The simulation and the experimental results correlated well with experimental results. However, the geometry of the bottle considered here was complex.

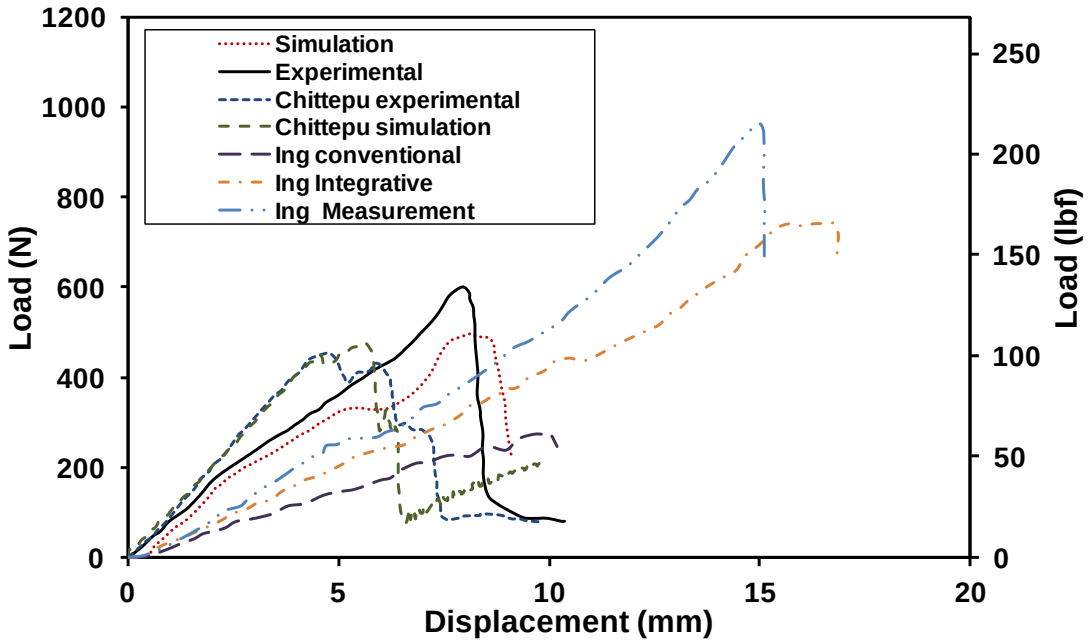

Figure 55: Comparison of validations of present work with chittepu, Ing's results [73 &75].

6.4 Effect of simulation results with increase in time steps

The dynamic simulations work with providing time response of each output. The number of time steps or intervals will decide the detail of the output. So, the number of intervals must be selected according to the details required for the simulations. Figure 56 shows the difference in load displacement curves with three different time steps. The simulations were performed for 2

sec. For 20 time steps, the output was provided every 0.1 sec; for 100 time steps, the output was provided every0.02 sec; and for 1000 time steps, the output was provided every 0.002 sec. An increase in the number of time steps needs more memory though the time required for the simulation is the same.

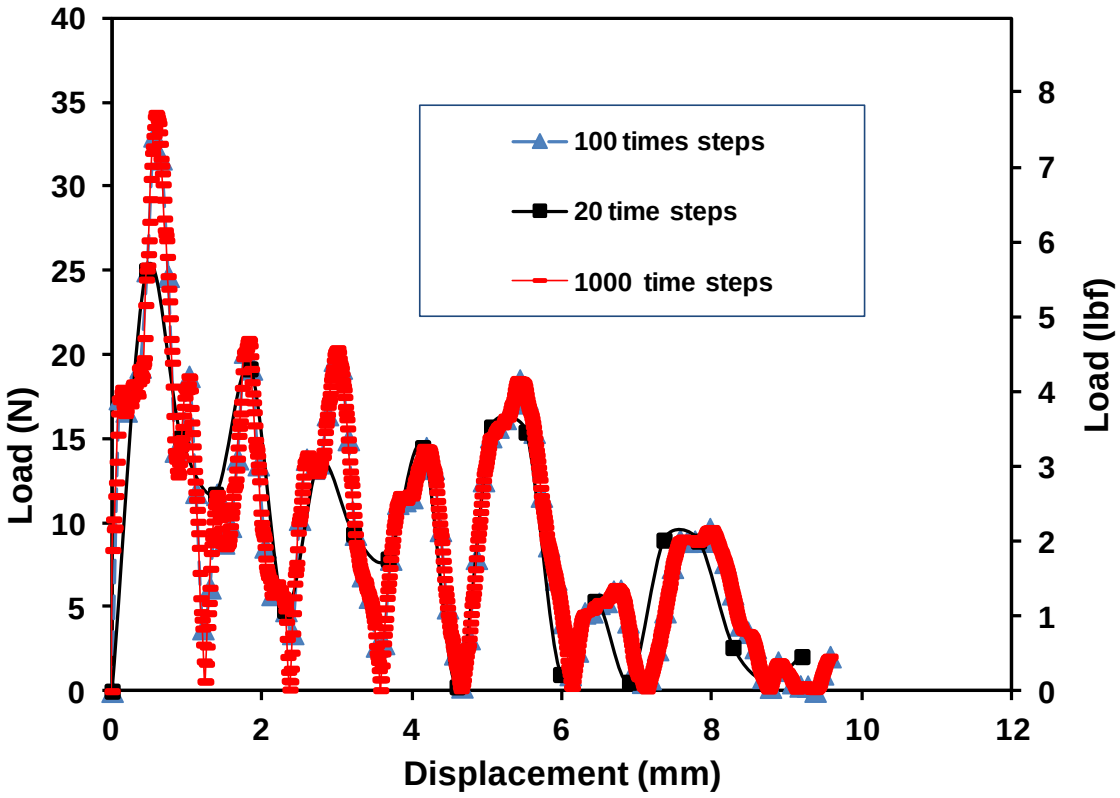

Figure 56: Change in load displacement curve of L4 design on bending with increase in time steps.

6.5 Stretch Ratios and stability of the bottle

By measuring the stretch ratios and the wall thickness at the stretch marks, the relation between the stretch ratio and wall thickness is obtained. Figure 61 shows the dependency of stretch ratios and wall thickness in general, as the stretch ratio increases the wall thickness decreases. Figure 38 shows that the stretching is not uniform along the length of bottle, and there is a dependency

on weights of preform and shape of the bottle design. Stretch ratios are low near the neck region and gradually increase until the middle region. A more constant stretch ratio was observed in the middle region and then it depended on weight of the preform. As one might expect, he average stretch ratios of the light weight preform was more than the heavy weight preform.

The stretch ratios can be correlated to crystalinity and material properties. During stretching PET molecules undergo strain which induces crystallization. Strain induced crystallization leads to an increase in crystalinity, which in turn leads to an increase in material properties, such as the modulus [23-32]. Figures (58, 59) also show that, with an increase in stretch ratio, there is an increase in modulus. Hence, if the thickness is less, the stretch ratios are more along the length, which increases the mechanical properties of the bottle. Hence if light weighting of bottle is the criteria, then the stretch ratios must be increased to make a bottle with better performance.

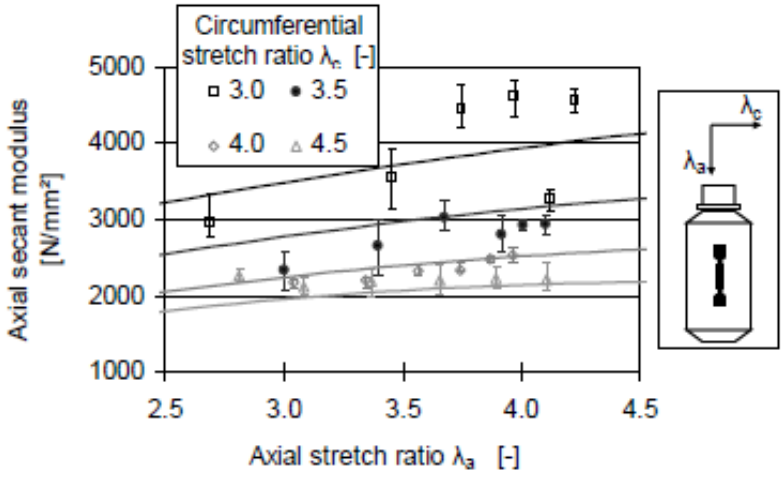

Figure 57: Axial secant modulus vs. stretch ratio[75].

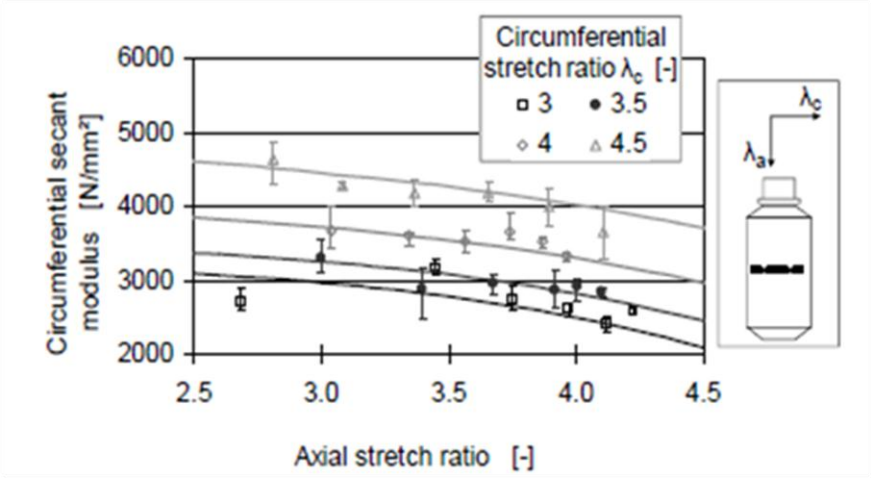

Figure 58: Circumferential secant modulus vs. stretch ratios [75].

Figure 59, shows the standard deviation of the four designs considered for stretch ratio measurement and thickness. The standard deviation increases with increase in weight of preforms. The standard deviation also explains that even if the bottle is of same design there would be the difference in stretching and thickness distribution, deviation is less in position 1 and more near positions 7, 8 and 9.

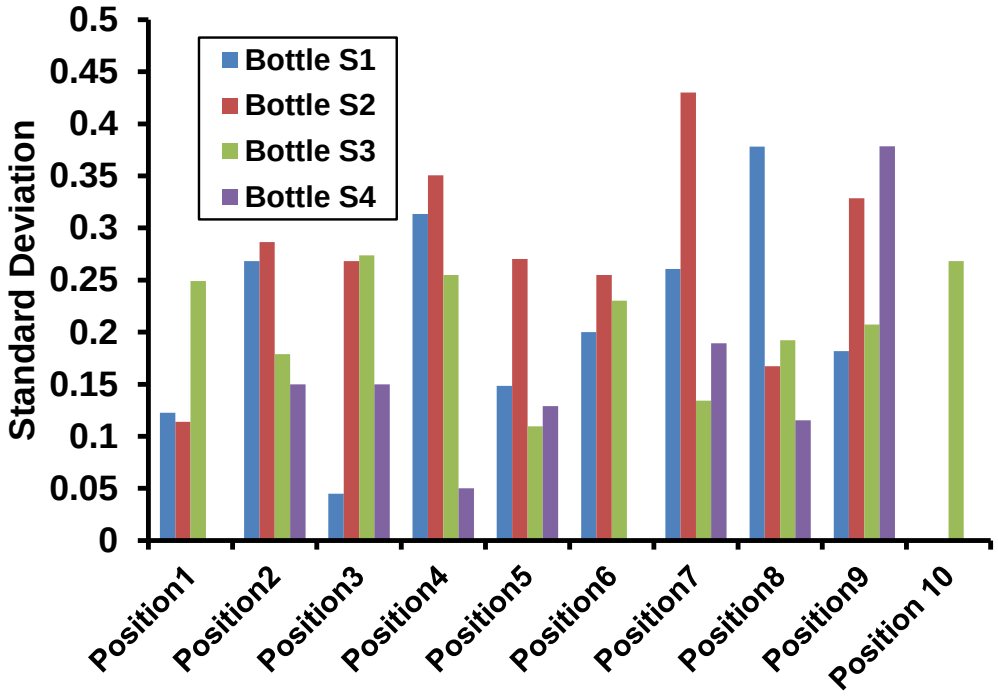

Figure 59: Standard deviation of stretch ratios.

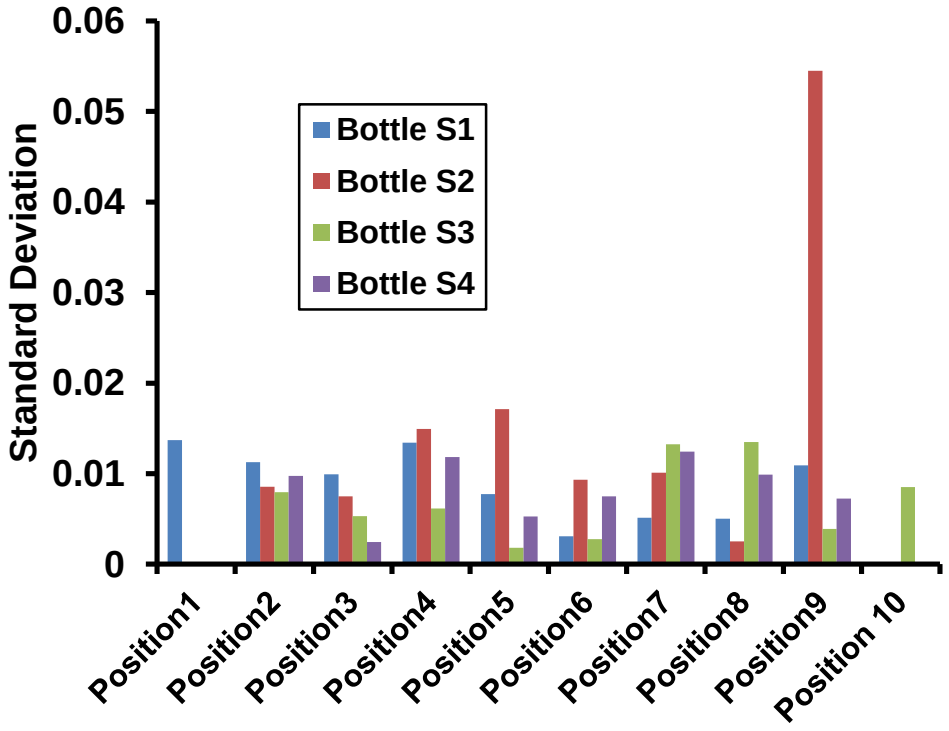

Figure 60: Standard deviation of wall thickness.

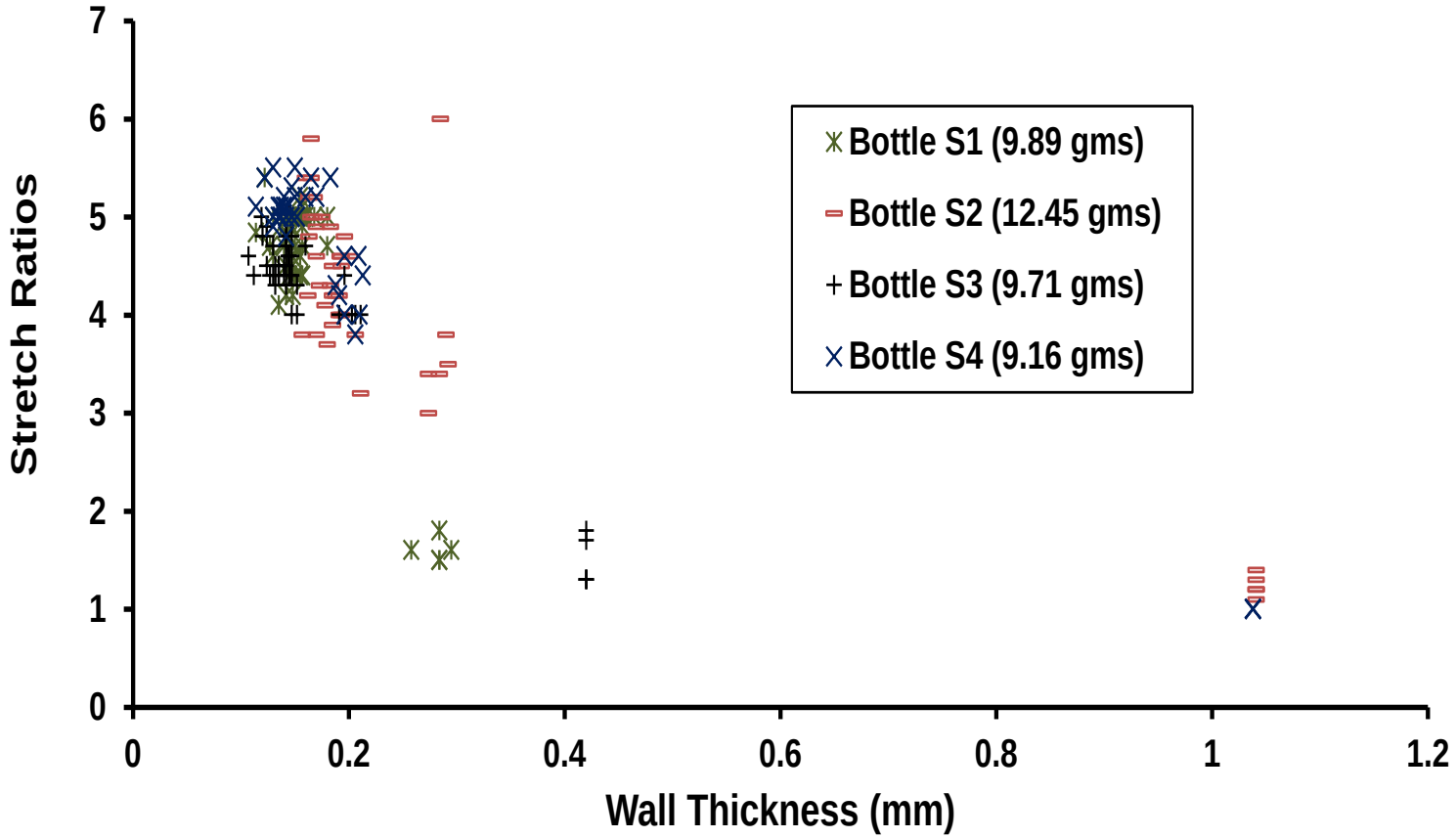

Figure 61: Stretch ratio vs. wall thickness.

6.6 Assigning material properties

From the previous discussions, using good material models and process dependent parameters are the key factors for determining the reliability of FEM results. Apart from that, there are different ways of assigning these material properties and implementing material models which are also important factors.

The conventional way of implementing the material properties is by conducting standard experiments and measuring the modulus. Then considering a constant modulus throughout the model; measuring the wall thickness along the length of bottle and implement around 5 different values in the finite element model.

Assigning can also be done by correlating stretch ratios and stretch ratio dependent material properties. Fitting a polymer curve as performed by Ing *et al.*, even in this case the modulus was initially calculated by the experimental findings. The thickness values and the stretch ratio dependent material properties are assigned to the respective nodes of the model in the input file of the model. A subroutine can also be implemented to assign stretch ratio dependent material properties. However, only an elastic modulus was correlated with stretch ratios. Creep properties, plasticity properties, and other complex behavior of polymers were not yet correlated.

In virtual prototyping, the constitutive models developed to study the polymer behavior is considered, the process parameters effecting the properties of a material are considered and these constitutive models are correlated to the geometry of the body. Hence the geometry is divided into nodes and the material data and thickness data are assigned to nodes. The user has to divide the geometry into the respective nodes, divide the nodes into different sets, and assign the sets with respective material properties and thickness values. This method is the most accurate when

compared to the other methods of assigning material properties, since there is correlation between material models, thickness, process parameters and geometry.

CHAPTER VII

7. CONCLUSIONS

A method for determining structural performance of PET bottles was developed in this research.

Hoop strength testing

Hoop Stiffness testing was done on different designs, the following were inferred conclusions

- The stiffness of the bottles ranged from 0.92875 N/mm to 1.4738N/mm which is a significant variation between the designs.
- The squeze performance does not depend solely on the weight of the bottle; it depends heavily on the shape of the bottle.
- Designs with deeper ribs showed better performance compared to the same designs with less deep ribs, designs with three columns showed the best performance here compared to other designs. The same was observed from the simulation results on cylinders.
- A change in processing history of the same design also affects the squeeze performance.
- Different orientations of the asymmetric bottle showed changes in stiffness.

Top Load Simulation

- The dynamic simulation of the top loading of a bottle gave the step by step response during the deformation.

- The stresses started acting from the shoulder region and went to the middle region. The base started deforming in the second step. The stresses shifted focus to the middle region; later the stresses again shifted below the neck region, and the load started falling once the region in the neck started deforming.
- The Finite element model results were validated with experimental results.
- The correlation between the simulation and experimental work in this research was also comparable with the correlation between simulation and experimental work of other researchers.

Bending vs. Wall thickness

The validated finite element model for top load was considered for bending simulations, the simulation results showed the following conclusions.

- With an increase in wall thickness of the bottle, the bending performance increases, but only until the 1st critical load. After that, the performance depends on how the stresses are distributed in the bottle.
- If the wall thickness is less, then the stress concentration areas are more focused in one area on the bottle. With an increase in wall thickness the stress were distributed more evenly over the bottle.

Bending Vs Change in Design

The bending procedure on the 1 liter model was implemented on the 0.5 liter models. The models which were imported from 3D scanning-rapid works-CAD to FEM were considered for bending the results and showed the following conclusions.

- The bending is different for different designs, the dynamic simulations show step by step response to bending.
- During bending stress distribution starts at the shoulder region, shifts to ribs near the label panel, initial buckling occurs there, and then the final deformation was observed depending on the shape of the bottle.
- If the bottle has more angles between the neck-shoulder region, the stresses were concentrated in shoulder region for more time and there was a lag in shifting stresses from the shoulder to the ribs near the label panel, and if the angle was less there was a faster shift from the shoulder region to the label panel.
- If there are deep ribs in the label panel, the stresses focus here for more time before shifting to regions below the label panel.
- The bell curve on shoulder region for design L2 is different from other designs; this curve prevents the stresses to transfer into this region after stage 2.
- The final deformation region will occur in the waist, intersection of the waist and lower region of bottle. If the design has deep ribs near label panel or more neck-shoulder or more shoulder area, the combination of the three may shift the region of deformation at higher locations in the bottle. If the design has less deep ribs, less neck shoulder-region, less shoulder area, then the deformation occurs in the bottom regions of the bottle.
- The load displacement curve fluctuates for 0.5 liter model because of the shift in stress concentration areas within the bottle.

Stretch ratio-Thickness measurements

- The stretch ratios and the wall thickness are inversely proportional.

- Stretch ratios are more for light weight bottles which can be correlated to the crystalinity, material properties and further form an explanation for the structural stability of light weight bottles.

Overall conclusions

Overall, hoop strength testing procedures were developed and gave a good way to measure the stiffness according the hoop strength, and shows details of the design play a significant role in stiffness. The dynamic simulations of the bottle gave better understanding of the loading and stress distribution in the bottle, rather than relying on the final equilibrium shapes. 3D scanning technology provided a good way of building CAD models from finished parts, which was in turn used to compare designs. There was a significant effect of design and wall thickness change on bottle overall performance. The optimized design of bottle can be pursued from this work.

CHAPTER VIII

8. FUTURE WORK

With the optimized design developed from the results above, a similar method can be scaled up to simulate whole pallet performance, which helps in better understanding of the impact of design features on the performance of designs in pallets. This work would be useful in industry applications. Figure 62 shows a concept for modeling bottles stored in pallets in warehouses or transportation.

In addition, improving material property inputs to the models is important. Crystalinity can be measured on all the designs and correlate with the measured stretch ratios. Crystalinity, wall thickness, geometry of the bottle, and process parameters impact the constitutive models for PET behavior on stretching. A good next step is to develop a numerical model for the optimized design considering these parameters.

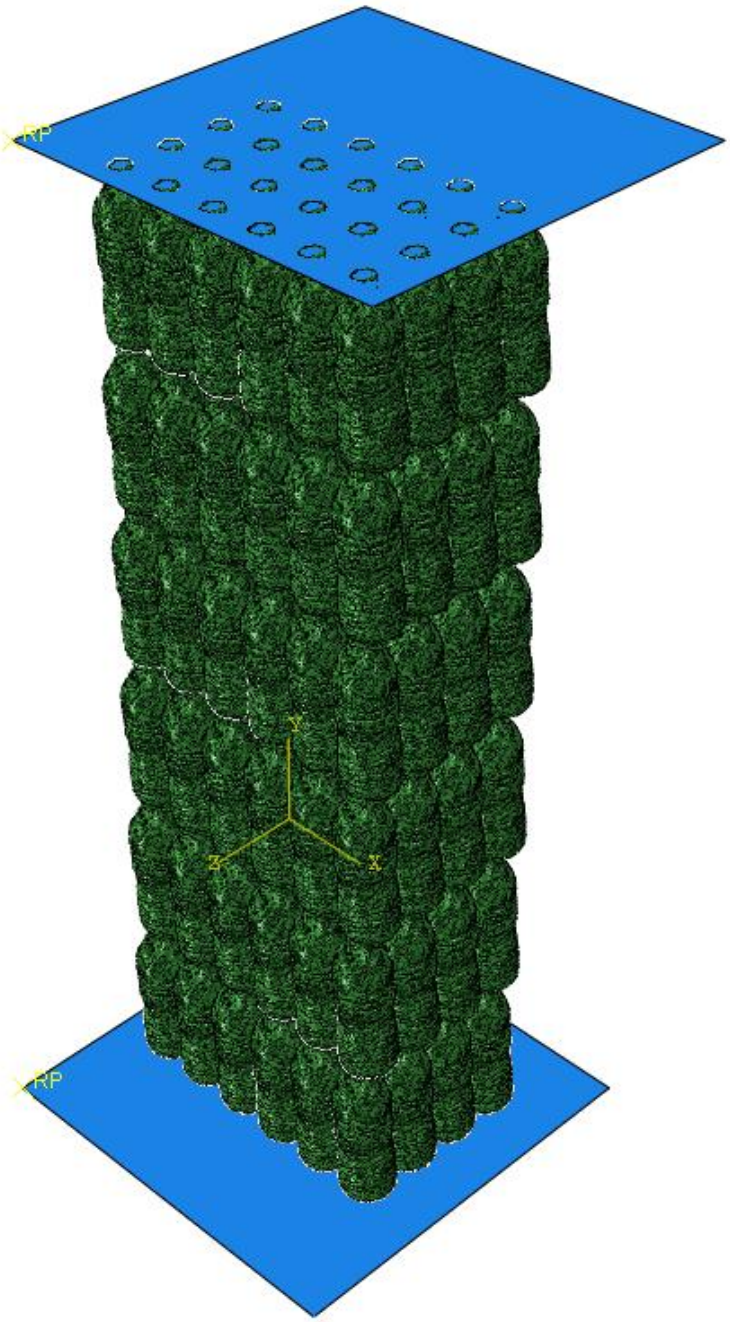

Figure 62: Finite element model of bottles in pallet packaging.

REFERENCES

[1] *Materials and Development of Plastics Packaging for the Consumer Market*: Wiley-Blackwell.

[2] W. E. .Brown, *Plastics in food packaging properties, design and fabrication by william E brown*: Marcel Dekker Inc.

[3] F. D. a. B. D. Pang C. Wei, "Light Weight PET Bottles: A Simulation Study," in *ANTEC*, 2010.

[4] R. G. Raj and B. V. Kokta, "Reinforcing high density polyethylene with cellulosic fibers. I: The effect of additives on fiber dispersion and mechanical properties," *Polymer Engineering & Science*, vol. 31, pp. 1358-1362, 1991.

[5] D. A. J. I. Velasco, M. Sánchez-Soto,A. Gordillo,M. Ll. Maspoch, "Milled Glass Fiber Filled-Poly(Ethylene Terephthalate-co-Isophthalate) Composites - Thermal and Mechanical Properties," *Journal of Thermoplastic Composite Materials*, 2003.

[6] R. U. Ahmed, "Analyzing and Improving Viscoelastic properties of High Density Poly Ethylene," Master of Science, Mechanical and Aerospace Engineering, Oklahoma State University, 2011.

[7] Z. J. Yang, E. Harkin-Jones, G. H. Menary, and C. G. Armstrong, "A non-isothermal finite element model for injection stretch-blow molding of PET bottles with parametric studies," *Polymer Engineering & Science*, vol. 44, pp. 1379-1390, 2004.

[8] "Golbal Packaging Consolidation: Lead, Follow, or Get Out of the Way," in *Packaging Conference*, Las Vegas, 2010.

[9] W. W.Bergmann, Teil1, *Grundlagen*, 3rd ed., 2000.

[10] G. W. Ehrenstein, *Polymer Werstoffe*, 2nd ed., 1999.

[11] H. H. Kausch, "Crazing in polymers," *Advances in POllymer Science*, vol. 1,52/53, 1983.

[12] J.M.Schultz, "Properties of solid polymeric materials," in *Treatise on Materials Science and Technology*. vol. 10, ed: Academic Press, 1977.

[13] H. H. Joachim Rösler, Martin Bäker, *Mechanical behaviour of engineering materials: metals, ceramics, polymers and Composites*: Springer.

[14] G. M. Swallowe, *Viscoelasticity, in Mechanical Properties and Testing of Polymers: An A-Z Reference*: The Netherlands: Kluwer

Academic Publishers, 1999.

[15] H. P. Menard, *An Introduction to Dynamic Mechanical Analysis", in Dynamic Mechanical Analysis: A Practical Introduction*, 2nd ed.: Florida:CRC Press, 2008.

[16] O. U. C. a. N. Dusunceli, "Modeling Viscoelastic and Viscoplastic Behavior

of High Density Polyethylene (HDPE)," *Journal of Engineering Materials andTechnology*, vol. vol. 128, pp. 572-578, 2006.

[17] J. D. Ferry, *Viscoelastic properties of polymers*, 3rd ed.: John Willey & Sons, 1980.

[18] K. Marynowski and T. Kapitaniak, "Kelvin–Voigt versus Bürgers internal damping in modeling of axially moving viscoelastic web," *International Journal of Non-Linear Mechanics*, vol. 37, pp. 1147-1161, 2002.

[19] L. E. Nielsen, "Creep and Stress Relaxation," in *Mechanical Properties of Polymersand Composites*,. vol. 1, ed Newyork: Marcel Dekker, 1974, pp. 65-77.

[20] J. A. o. J. Grönvall, "Analysis of Creep in Paperboard Packages with Plastic tops," Division of Structural Mechanics, LUND university, Sweden, 2004.
[21] "Abaqus Analysis Users Manual," in *Abaqus Online documentation*, ed: Abaqus Inc.
[22] *Handbook of biomaterial propertiesJonathan Black*: Chappman & Hill, 1985.
[23] S. A. Jabarin, "Strain-Induced Crystallization of Poly(Ethylene Terephthalate) " *Polymer Engineering and Science,* vol. vol. 32, p. 9, Septermber 1992
[24] P. C. a. S. Jabarin, "Biaxial orientation of poly(ethylene terephthalate). Part I: Nature of the stress - strain curves " *Advances in Polymer Technology,* vol. vol. 12, pp. 119-132, 1993.
[25] P. C. a. S. Jabarin, "Biaxial orientation of poly(ethylene terephthalate). Part III: Comparative structure and property changes resulting from simultaneous and sequential orientation,"" *Advances in Polymer Technology* . vol. 12, pp. 153-165, 1993.
[26] D. H. M. D. J. Blundell, W. Fuller, A. Mahendrasingam, C. Martin, R. J. Oldman, R. J. Rule, and C. Riekel, "Characterization of strain-induced crystallization of poly(ethylene terephthalate) at fast draw rates using synchrotron radiation," *Polymer* vol. 37, pp. 3303-3311, 1996.
[27] P. Chandran and S. Jabarin, "Biaxial orientation of poly (ethylene terephthalate). Part II: The strain–hardening parameter," *Advances in Polymer Technology,* vol. 12, pp. 133-151, 1993.
[28] C. M. A. Mahendrasingam, W. Fuller, D. J. Blundell, R. J. Oldman, J. L. Harvie, D. H. MacKerron, C. Riekel, and P. Engstrom, "Effect of draw ratio and temperature on the strain-induced crystallization of poly (ethylene terephthalate) at fast draw rates " *Polymer,* vol. 40, pp. 5553-5565, 1999.
[29] C. M. A. Mahendrasingam, W. Fuller, D.J.Blundell, R. J. Oldman, D. H. MacKerron, J. L. Harvie, and C. Riekel, "Observation of a transient structure prior to strain-induced crystallization in poly(ethylene terephthalate)," *Polymer,* vol. 41, pp. 1217-1221, 2000.
[30] A. A. R. Matthews, K. C. Cole, and M. M. Dumoulin, "Roll and Tensile Drawing of PET: Effect of Process Conditions on Structure and Properties," presented at the ANTEC, Atlanta, Georgia, 1998.
[31] E. R. D. a. J. B. Jackson, "The Inter-Relation of Some Mechanical Properties with Molecular Weight and Crystallinity in Poly(ethylene terephthalate)." *Journal of Materials Science,* vol. 3, pp. 464-470, 1968.
[32] M. B. d. R. R. Guzatto, E. L. Gasparotto Denardin, and D. Samios,, "Dynamical, morphological and mechanical properties of poly(ethylene terephthalate) deformed by plane strain compression," *Polymer Testing,* vol. 28, pp. 24-29, 2009.
[33] S. CCI, "Strategic Consulting and Supply Demand Modeling for the PET Raw Material, Resin and Packaging Industry," in *Packaging Conference*, LasVegas, 2011.
[34] S. J. C. M. R. Smith, D. J. Winter, and N. Everall, "Detailed mapping of biaxial orientation in polyethylene terephthalate bottles using polarised attenuated total reflection FTIR spectroscopy," *Polymer,* vol. 47, pp. 5691-5700, 2006.
[35] "Recycling Symbols (US)," ed, 2010.
[36] M. Wortley, "Injection blow molding," in *Practical guide to blow molding*, ed: Smithey Rapra Technology, 2006.
[37] B. Blakeborough, "One-stage injection stretch blow moulding," in *Practical Guide to Blow Blow molding*, ed, 2006.

[38] M. Koch, "Two-stage injection stretch blow moulding," in *Practical Guide to Blow molding*, ed: Smithers Rapra Technology, 2006.
[39] M. Stones. (2009) "Nestle launches lightweight PET bottle. *AP-Food Technology*.
[40] D. Karalekas, D. Rapti, G. Papakaliatakis, and E. Tsartolia, "Numerical and experimental investigation of the deformational behaviour of plastic containers," *Packaging Technology and Science,* vol. 14, pp. 185-191, 2001.
[41] E. Béchet, H. Minnebo, N. Moës, and B. Burgardt, "Improved implementation and robustness study of the X-FEM for stress analysis around cracks," *International Journal for Numerical Methods in Engineering,* vol. 64, pp. 1033-1056, 2005.
[42] J. N. Reddy, *Introduction to the finite element method*, 3rd ed.: McGraw-Hill 2005.
[43] A. D. B. Tirupathi R. Chandrupatla, *introduction to finite elements in engineering*: Prentice Hall, 2002.
[44] Q. C. Pham, F. Vincent, P. Clarysse, P. Croisille, and I. E. Magnin, "A FEM-based deformable model for the 3D segmentation and tracking of the heart in cardiac MRI," in *Image and Signal Processing and Analysis, 2001. ISPA 2001. Proceedings of the 2nd International Symposium on,* 2001, pp. 250-254.
[45] P. A. Du Bois, S. Kolling, and W. Fassnacht, "Modelling of safety glass for crash simulation," *Computational Materials Science,* vol. 28, pp. 675-683, 2003.
[46] A. B. Pifko and R. Winter, "Theory and application of finite element analysis to structural crash simulation," *Computers & Structures,* vol. 13, pp. 277-285, 1981.
[47] K. Tanne, M. Sakuda, and C. J. Burstone, "Three-dimensional finite element analysis for stress in the periodontal tissue by orthodontic forces," *American Journal of Orthodontics and Dentofacial Orthopedics,* vol. 92, pp. 499-505, 1987.
[48] D. T. Chen and D. Zeltzer, "Pump it up: computer animation of a biomechanically based model of muscle using the finite element method," presented at the Proceedings of the 19th annual conference on Computer graphics and interactive techniques, 1992.
[49] J. Amoedo and D. Lee, "Modeling the uniaxial rate and temperature dependent behavior of amorphous and semicrystalline polymers," *Polymer Engineering & Science,* vol. 32, pp. 1055-1065, 1992.
[50] E. M. Arruda and M. C. Boyce, "Evolution of plastic anisotropy in amorphous polymers during finite straining," *International Journal of Plasticity,* vol. 9, pp. 697-720, 1993.
[51] J. A. W. van Dommelen, D. M. Parks, M. C. Boyce, W. A. M. Brekelmans, and F. P. T. Baaijens, "Micromechanical modeling of the elasto-viscoplastic behavior of semi-crystalline polymers," *Journal of the Mechanics and Physics of Solids,* vol. 51, pp. 519-541, 2003.
[52] K. H. S. Ziaei-Rad, "Finite element simulation of polymer behaviour using a three-dimensional, finite deformation constitutive model," *Computers and Structures,* pp. 1643-1655, 2008.
[53] J. Ren and R. Krishnamoorti, "Nonlinear Viscoelastic Properties of Layered-Silicate-Based Intercalated Nanocomposites," *Macromolecules,* vol. 36, pp. 4443-4451, 2003/06/01 2003.
[54] N. Sheng, M. C. Boyce, D. M. Parks, G. C. Rutledge, J. I. Abes, and R. E. Cohen, "Multiscale micromechanical modeling of polymer/clay nanocomposites and the effective clay particle," *Polymer,* vol. 45, pp. 487-506, 2004.
[55] P. K. Valavala and G. M. Odegard, "Modeling Techniques For Determination Of Mechanical Properties Of Polymer Nanocomposites," *Advanced Material science,* 2005.

[56] P. Haupt, A. Lion, and E. Backhaus, "On the dynamic behaviour of polymers under finite strains: constitutive modelling and identification of parameters," *International Journal of Solids and Structures,* vol. 37, pp. 3633-3646, 2000.
[57] N. J. Inkson, T. C. B. McLeish, and D. J. Groves, "Predicting low density polyethylene melt rheology in elongational and shear flows with “pom-pom” constitutive equations " *Journal of Rheology,* vol. 43, 1999.
[58] J. S. Bergström, C. M. Rimnac, and S. M. Kurtz, "Prediction of multiaxial mechanical behavior for conventional and highly crosslinked UHMWPE using a hybrid constitutive model," *Biomaterials,* vol. 24, pp. 1365-1380, 2003.
[59] J. Mackerle, "Finite element analysis and simulation of polymers—an addendum: a bibliography (1996–2002)," *Modelling and Simulation in Materials Science And Engineering,* vol. 11, 2003.
[60] D. K. Lee and S. K. Soh, "Prediction of optimal preform thickness distribution in blow molding," *Polymer Engineering & Science,* vol. 36, pp. 1513-1520, 1996.
[61] F. Thibault, A. Malo, B. Lanctot, and R. Diraddo, "Preform Shape and Operating Condition Optimization for the Stretch Blow Molding Process F.," *Polymer Engineering and Science,* 2007.
[62] C. G. A. J.P.McEvoy, and R.J.Crawford,, "Simulation of the Stretch Blow Molding Process of PET Bottles," *Advances in Polymer Technology,* vol. 17, pp. 339-352, 1998.
[63] K. C. Y. Germain , R.H Wagoner., "A Rigid-Viscoplastic Finite Element Program for Sheet Metal Forming Analysis," *International Journal of Mechanical Sciences,* vol. 31, pp. 1-24, 1989.
[64] G. Venkateswaran, M. R. Cameron, and S. A. Jabarin, "Prediction of PET container properties using film data," *Advances in Polymer Technology,* vol. 17, pp. 217-235, 1998.
[65] S. a. M. Wang, A, "Contact search strategies for FEM simulation of the blow molding process," *Int. J. Numer. Meth. Engng,* vol. 48, 2000.
[66] G. Marckmann, E. Verron, and B. Peseux, "Finite Element Analysis of Blow Molding and Thermoforming Using a Dynamic Explicit Procedure," *Polymer Engineering and Science,* vol. 41, 2001.
[67] C. P. Buckley and D. C. Jones, "Glass-rubber constitutive model for amorphous polymers near the glass transition," *Polymer,* vol. 36, pp. 3301-3312, 1995.
[68] S. Srinath, "Mechanical Behavior Of Polyethylene Terephthalate and its Application To The Reheat Stretch Blow Molding Process," Masters, Mechanical Engineering, Ohio State University, Ohio, 2010.
[69] B. D. Rebecca and K. Dwarak, "A constitutive model for strain-induced crystallization in poly(ethylene terephthalate) (PET) during finite strain load-hold simulations," vol. 128, p. 6, 2006.
[70] R. van Dijk, J. C. Sterk, D. Sgorbani, and F. van Keulen, "Lateral deformation of plastic bottles: experiments, simulations and prevention," *Packaging Technology and Science,* vol. 11, pp. 91-117, 1998.
[71] V. S. a. U. E. S.H. Masood, "Design and Development of Large Collapsible PET Water Cooler Bottles," presented at the Conference on Computer Graphics, Imaging and Visualisation (IEEE), 2006.
[72] B. Demirel and F. Daver, "Optimization of poly(ethylene terephthalate) bottles via numerical modeling: A statistical design of experiment approach," *Journal of Applied Polymer Science,* vol. 114, pp. 1126-1132, 2009.

[73] B. Chittepu, M. Horman, U. Stelzmen, H. Wels, and T. Albrecht, "Deformation Behavior of Filled and Collapsable PET bottles in High Speed Labelling Machines," in *LS DYNA* Europe, 2010.
[74] S. Mukherjee, "Virtual Simulation of Top Load Performance of Plastic Bottles," in *ANTEC*, 2010.
[75] Dr.-Ing. Dr.-Ing. E.h.,Walter Michaeli, "Modelling The Structural Performance Of Stretch-Blow Moulded PET Bottles," presented at the ANTEC, 2010.
[76] R. Tsai, "A versatile camera calibration technique for high-accuracy 3D machine vision metrology using off-the-shelf TV cameras and lenses," *Robotics and Automation, IEEE Journal of*, vol. 3, pp. 323-344, 1987.
[77] A. Karasik and U. Smilansky, "3D scanning technology as a standard archaeological tool for pottery analysis: practice and theory," *Journal of Archaeological Science*, vol. 35, pp. 1148-1168, 2008.
[78] Gustafsson, Agard, and Sedat, "I5M: 3D widefield light microscopy with better than 100 nm axial resolution," *Journal of Microscopy*, vol. 195, pp. 10-16, 1999.
[79] J. A. Collins, H. R. Busby, and G. H. Staab, *Mechanical Design of Machine Elements and Machines*, 2nd ed.: John Wiley and Sons, 2009.
[80] *User Manual*: Next Engine, 2009.
[81] *Rapid works reference manual*: Next Engine.
[82] S. Bandla, "Evaluation And Stability Of Pet Resin Mechanical Properties " Master of Science, MAE, Oklahoma State University, May 2010.
[83] K. Yamazaki, R. Itoh, M. Watanabe, J. Han, and S. Nishiyama, "Applications of structural optimization techniques in light weighting of aluminum beverage can ends," *Journal of Food Engineering*, vol. 81, pp. 341-346, 2007.
[84] Jay Hanan" PET injection and Blow Molding :An Introduction" *Design team presentaiton* March 2011

..

.

VITA

ROHIT VAIDYA

Candidate for the Degree of

Master of Science

Thesis :STRUCTURAL ANALYSIS OF POLY ETHYLENE TEREPHTHALATE BOTTLES USING THE FINITE ELEMENT METHOD

Major Field: Mechanical Engineering

Biographical:

Education:

Completed the requirements for the Master of Science in Mechanical Engineering at Oklahoma State University, Stillwater, Oklahoma in May, 2012.

Received the Bachelor of Technology degree in Aeronautical Engineering at Jawahar Lal Nehru Technological University, Hyderabad, Andhra Pradesh, India in 2009

Experience:
Graduate Research Assistant in Department of Mechanical and Aerospace Engineering, Oklahoma State University, Stillwater, Oklahoma- January, 2010-December 2011.
Graduate Teaching Assistant in Mechanical and Aerospace Engineering at Oklahoma State University, Still water, Oklahoma- August 2009 to December 2010.

Engineering Intern at Advanced Systems Laboratory, Hyderabad, Andhra Pradesh, India- December 2008-June 2009.

Professional Memberships: American Society of Mechanical Engineers, Society of Plastic Engineers.

Name:Rohit Vaidya Date of Degree: May 2012
Institution: Oklahoma State University Location: Stillwater, Oklahoma

Title of Study: STRUCTURAL ANALYSIS OF POLY ETHYLENE TEREPHTHALATE BOTTLES USING THE FINITE ELEMENT METHOD

Pages in Study: 112 Candidate for the Degree of Master of Science

Major Field: Mechanical Engineering

Scope and Methodology:

Light weighting of PET bottles not only reduces material usage but also minimizes the impact on the environment. This has been a driving force behind optimization of designs. In the process of optimization, it is critical to evaluate the structural performance of bottles under different loading conditions. During the manufacturing process, bottles undergo different kinds of loading. FEM was implemented to study the structural performance of PET bottle designs manufactured using ISBM under the conditions of bending and hoop strength. The behavior of a PET bottle under top loading was analyzed using FE modeling and validated experimentally. The validated FE model was used to simulate bending under side load conditions. Further, the effect of changes in wall thickness on bending was studied. In order to understand the role of different structural features in reducing bending, CAD models of four different finished parts were obtained using 3D scanning technology and were imported for FE analysis. Hoop strength tests were also performed on eight different designs with different processing histories using a specialized fixture.

Findings and Conclusions:

Outcomes of this work include a procedure to study the mechanical behavior of PET bottles under conditions of bending and hoop strength, the effect of wall thickness and design on the bottle behavior under bending, and a 3D scanning method leading to a new way of CAD modeling. The imported designs were subjected to FE analysis. The procedures can be generalized to many related engineering problems. The study showed a significant change in bottle behavior with change in wall thickness and design.

ADVISER'S APPROVAL: Dr.Jay. C. Hanan